RAPID PYROLYSIS OF SWEET GUM XYLAN
WITH APPLICATIONS IN MODELLING WOOD

by

Jayant Ghosh

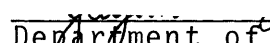B.S., Chemical Engineering
Cornell University (1981)

Submitted in Partial Fulfillment
of the Requirements for the
Degree of

Master of Science in
Chemical Engineering
at the

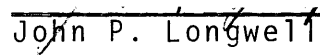Massachusetts Institute of Technology
January 1983

© Massachusetts Institute of Technology, 1983

Signature of Author _____

Department of Chemical Engineering
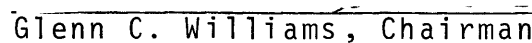January, 1983

Certified by _____

Jack B. Howard, Thesis Supervisor

_____

John P. Longwell, Thesis Supervisor

_____

William A. Peters, Thesis Supervisor

Accepted by _____

Glenn C. Williams, Chairman
Departmental Graduate Committee

RAPID PYROLYSIS OF SWEET GUM XYLAN

WITH APPLICATIONS IN MODELLING WOOD

by

Jayant Ghosh

ABSTRACT

Data were obtained on the yields of tars and chars and on yields,
rates of evolution and compositions of individual gases from the
rapid pyrolysis of sweet gum xylan.

Fifty mg samples of powdered xylan (45-90 microns) were pyrolyzed
at 1000 K/s to peak temperatures between 600 and 1400K in a 3×10^5 Pa
helium atmosphere. Samples were cooled at approximately 200 K/s after
zero residence time at the peak temperature. Gas chromatography was
used to characterize individual gaseous and light tar products. The
char and heavy tars were determined gravimetrically and analyzed by
elemental analysis.

On an ash-free basis, the overall weight loss from xylan was
84 wt%, while the ultimate yield of gases (at 1400K) was 35.8 wt%.
Tar (a heavy liquid product) accounted for the remaining volatiles.
Secondary reactions of tar contributed to increased gaseous product
yields at temperatures above 800K. At temperatures above 1150K
secondary reactions of light gaseous volatiles with char (char gasifi-
cation), resulted in greater overall sample weight loss. Carbon
monoxide and carbon dioxide comprised the largest fraction of the
gaseous products reaching ultimate yields of >17 wt% and 15.2 wt%
respectively. Yields of chemical water reached 5.2 wt%, and the rem-
ainder of the hydrocarbons and heavy oxygenated compounds together
amounted to only 5.1 wt% of the original sample.

A kinetic model based on a single-step first-order reaction was
fit to the experimental data. This procedure gave three rate
parameters for each of the individual gaseous products: (1) V* - the
ultimate yield in wt%; (2) E - the activation energy; and (3) $\log_{10} k$,
where k is the Arrhenius frequency factor. The kinetics of
wood pyrolysis were modelled as the weighted sum of the pyrolysis
behaviors of its three major constituents by taking filter paper

1

cellulose, milled wood lignin and sweet gum xylan as their surrogates. The results were compared with experimental data on sweet gum hardwood pyrolysis and were found to give reasonable agreement for both total gas yields and individual gaseous product yields. However, due to the high char yield from xylan (16.4 wt%), the simulation for overall weight loss consistently underestimated experimental data. Some discrepancies between the simulation and experimental observations arose; these may be attributed to secondary interactions between the decomposition products of the individual wood components, and to possible catalytic effects of the 5 wt% potassium in the xylan samples used.

Thesis supervisors: Jack B. Howard, Professor of Chemical Engineering

John P. Longwell, Edwin R. Gilliland Professor of Chemical Engineering

William A. Peters, Principal Research Engineer Energy Laboratory

January 1983

Professor Jack P. Ruina
Secretary of the Faculty
Massachusetts Institute of Technology

Dear Professor Ruina:

In accordance with the regulations of the faculty, I submit herewith a
thesis entitled "Rapid Pyrolysis of Sweet Gum Xylan with Applications
in Modelling Wood," in partial fulfillment of the requirements for the
degree of Master of Science in Chemical Engineering at the Massachusetts
Institute of Technology.

Respectfully submitted,

Jayant Ghosh

To my mother and father

TABLE OF CONTENTS

LIST OF FIGURES

LIST OF TABLES

ACKNOWLEDGEMENTS

Finally, it is to my family that I must give credit for having brought out the best in me, and in having provided moral support, albeit by long distance.

1. INTRODUCTION

The survival of any technologically advanced civilization will
ultimately depend upon the energy alternatives at its disposal. Since
the industrial revolution of the 1700's, the per capita energy util-
ization has increased and is still increasing today. It has there-
fore become imperative to determine on a detailed basis not only
what methods of fuel use are the most efficient, but also what
alternate as yet unused reserves may make a sizeable contribution to
our energy pool.

To date, synthetic fuels research has been mainly in the area
of exhaustible fuel resources. While crude oil, oil shale, tar
sands and other fossil fuel depletable compounds exist in relative
abundance in various parts of the world, it is clear that the renew-
able energy sources such as biomass deserve increasing attention.

The ratio of time required for the regeneration of the "exhaust-
ible" resources to that needed for the regeneration of "renewable"
resources is approximately four to five orders of magnitude. Our study
is concerned with the pyrolysis of wood and its constituents, but
also with the mathematical modelling of the pyrolysis. A model, if
it proves successful, gives quantitative guidance on how to vary
pyrolysis conditions to make the production of a particularly desirable
fuel component efficient. These are the motivations for the study on
the pyrolysis of biomass.

A summary of the conversion schemes for biomass into fuels is
shown in Fig. 1-1. As of this writing, thermal processes have proven

14
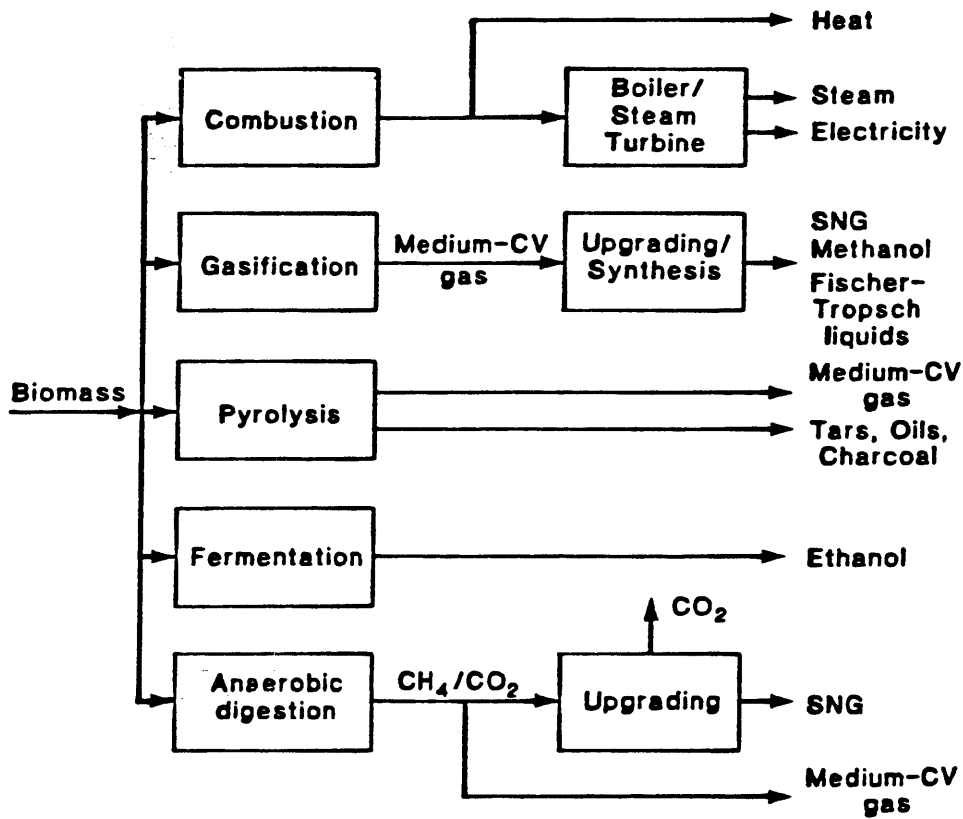
Fig. 1-1 Biomass conversion processes
(Probstein and Hicks, 1981)
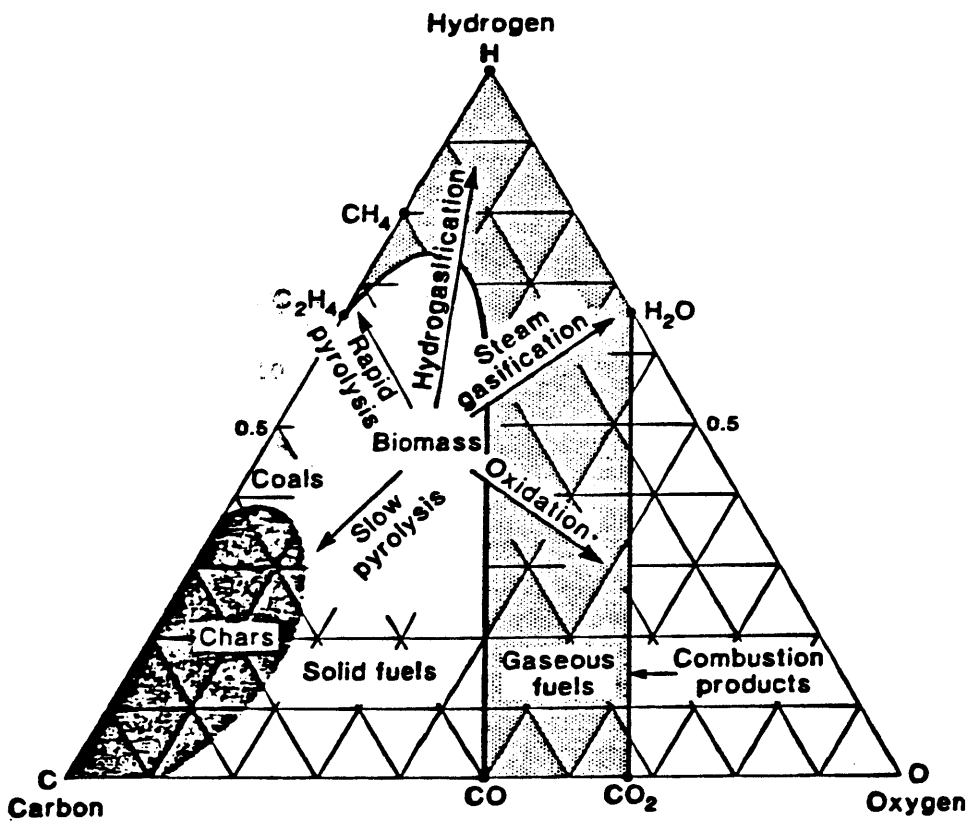
Fig. 1-2 Thermal Conversion of Biomass
(Probstein and Hicks, 1981)

15

to be the most economically viable, and of the three shown in the

figure, we are interested in pyrolysis. A comparison of the thermal

processing of biomass with fossil fuels reveals the following:

- Biomass is a cleaner fuel due to its low sulfur and
  nitrogen content

- It has a larger H/C ratio which favors the production of
  volatiles and decreases the formation of char residues

- It has a lower caloric value than fossil fuels

- It may have a greater moisture content which detracts
  from optimal thermal conversion

Figure 1-2 illustrates reaction pathways in the thermal processing

of biomass.

Biomass is not the solution to all the energy needs of the

United States. Once implemented, a program which makes best use of

the available resources without depleting forests and farmlands

could contribute up to ten percent of total US energy requirements

(Probstein and Hicks, 1981). However, in the face of rapid depletion

of fossil fuels, which today account for almost ninety percent of

our energy, a steady ten percent contribution from biomass would be

of ever increasing importance in the mix of national energy sources

over the next thirty years.

2. BACKGROUND

2.1 The Nature of Xylan

There are many references in the chemical polymer and wood related literature on the nature of the constituents of wood. One of the most authoritative monographs on the topic is by Wenzl (1970), but many other researchers have contributed to the field and are too numerous to be listed here.

For the specific component of interest, the hemicelluloses, the largest body of work relating to their isolation and determination comes from Timell (1964, 1965). Browning (1967) gives an excellent summary of the isolation procedures for wood constituents as well as the separation methods which have been standardized by organizations such as TAPPI. The hemicellulose used in this study, 0-acetyl-4-0-methylglucurono-β-D-xylan (xylan) was prepared by Prof. H. M. Chang of the Department of Wood and Paper Science, North Carolina State University. A flowsheet of his isolation procedure is given in Fig. 2.1-1. The glucomannan obtained in the isolation is also a hemicellulose species but was not investigated in this research. Xylan constitutes 30.6 wt% of extractive-free hardwood (Andrews, 1980); glucomannan comprises only 3 to 5 wt% of it.

While the repeating cellobiose units which form the linear backbone of the cellulose molecule have been well characterized, the same has not been done for hemicelluloses. Though both are found side by side in the cell walls of plants and are natural polymers of repeating

17

Holocellulose

Extract with 24% KOH
(50 cc/g. for 2 hours on shaker under N_2)

Soluble

Add 100% Acetic Acid
to pH 6, then Methanol
to precipitate.

Soluble

Discard

Precipitate

Centrifuge, wash with
65% MeOH, suspend in
water, and freeze dry
Xylan.

Insoluble

18% NaOH + Boric Acid (4%)
(50 cc/g. for 1 hour on shaker under N_2)

Soluble

Add saturated
Ba(OH)$_2$ until
precipitation
is complete.

Insoluble

Filter, wash with water,
add to soluble portion,
wash with 100% Acetic Acid,
then water, discard wash,
and air dry alpha-cellulose.

Soluble

Discard

Precipitate

Centrifuge, wash with
100% Acetic Acid,then
water, suspend in water
and freeze dry glucomannan.

Fig. 2.1-1   Isolation procedure for xylan (Chang, 1982(a))

18

sugar units, their chemical structures are sufficiently different to warrant separate studies of each. Fig. 2.1-2 lists the sugar units which make up hemicelluloses. The main differences between cellulose and hemicellulose are their crystallinity and degree of polymerization (D.P.): native cellulose is linear (D.P. $\sim$ 10,000) and is highly crystalline (i.e., is resilient and rigidly structured); hemicelluloses are more crosslinked (100 < D.P. < 400) and are more amorphous (i.e., less rigidly structured). In comparison, lignin, the remaining major wood component, is highly crosslinked in a complex 3-D structure and is completely amorphous. Figure 2.1-3 compares structures of cellulose, xylan and lignin.

Joseleau and Barnoud (1976) have studied the local ultrastructure of xylans in cell walls of plants via enzymatic degradation. Their findings indicate that young plants produce cellulose and xylan concomitantly in building the primary cell wall. As the plant ages, xylan layers adjacent to cellulose layers reach a maximum thickness. The younger xylan is not structurally different from older xylan, but has a lower D.P.. With increasing maturation, the side groups such as the acetyl or 4-0-methyl groups in xylan are modified. The xylan backbone, however, still untouched at this stage, progressively undergoes chemical restructuring by dehydration reactions to a polymeric compound with OH side groups (Wenzl, 1970). Gradually, xylan assumes a more amorphous structure, and, according to Joseleau et al. (1976) is transformed into lignin which is deposited in middle lamellae of the cell wall. Cellulose too seems to undergo a similar

19
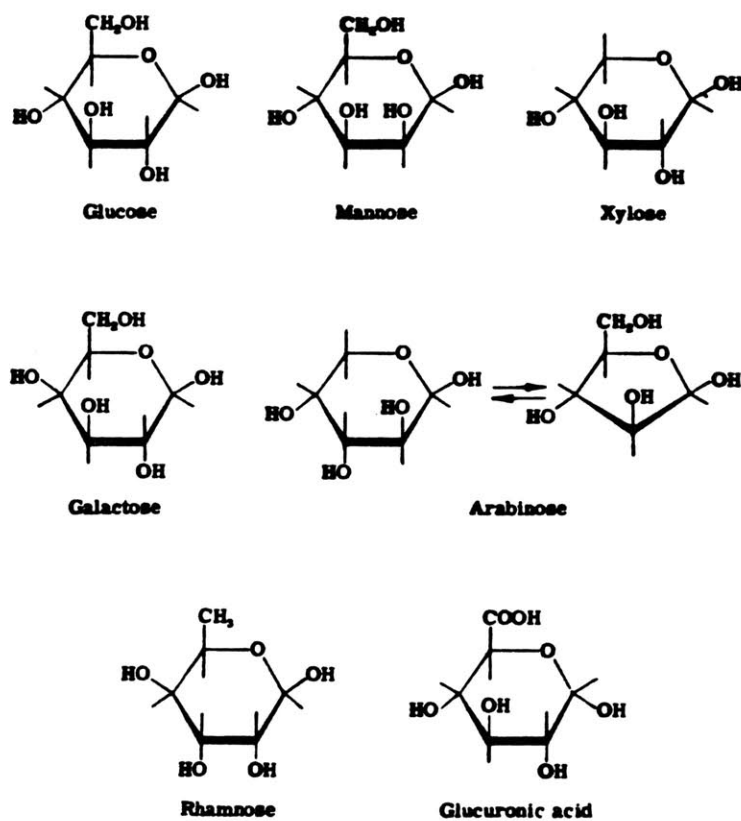
Fig. 2.1-2   Common sugar moities in hemicelluloses
(Wenzl, 1970)
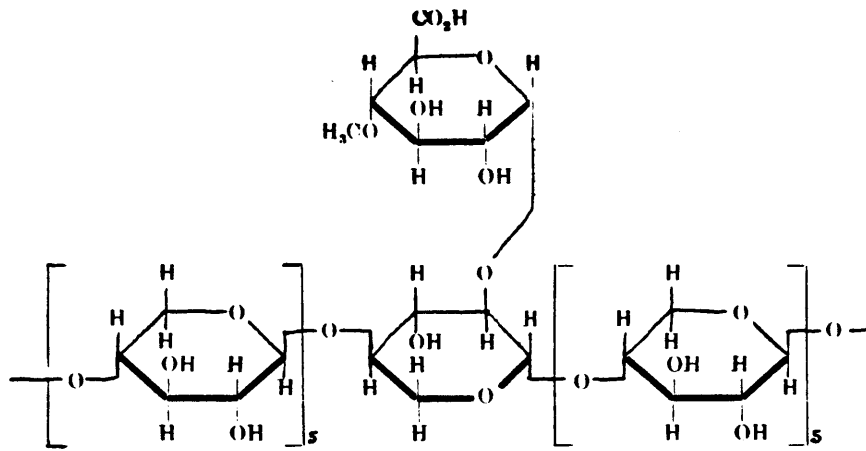
(a) Xylan
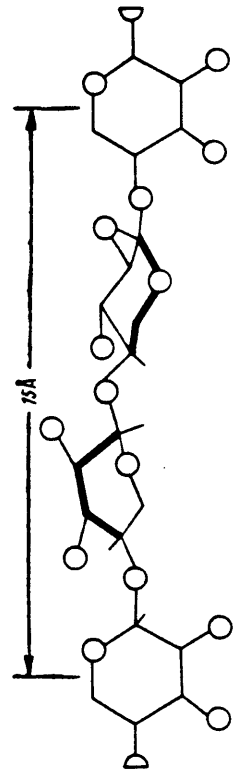
(b) Xylan
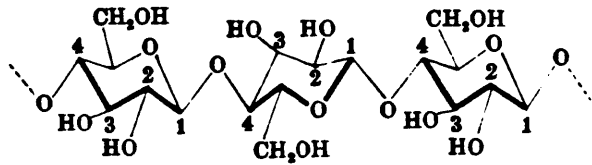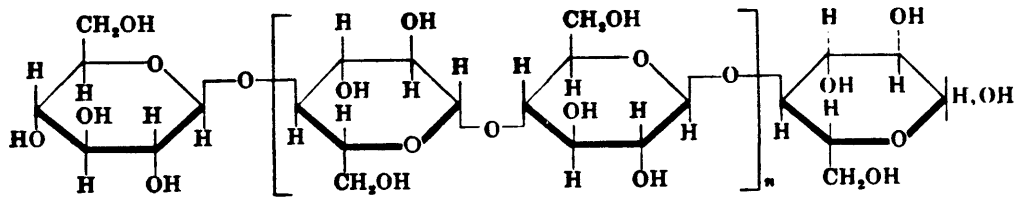
(c) Cellulose

Fig. 2.1-3 Comparison of xylan's structure [(a) and (b)] to cellulose's structure [(c)] from Kollmann and Côté, to lignin's structure [(d)] from SERI.
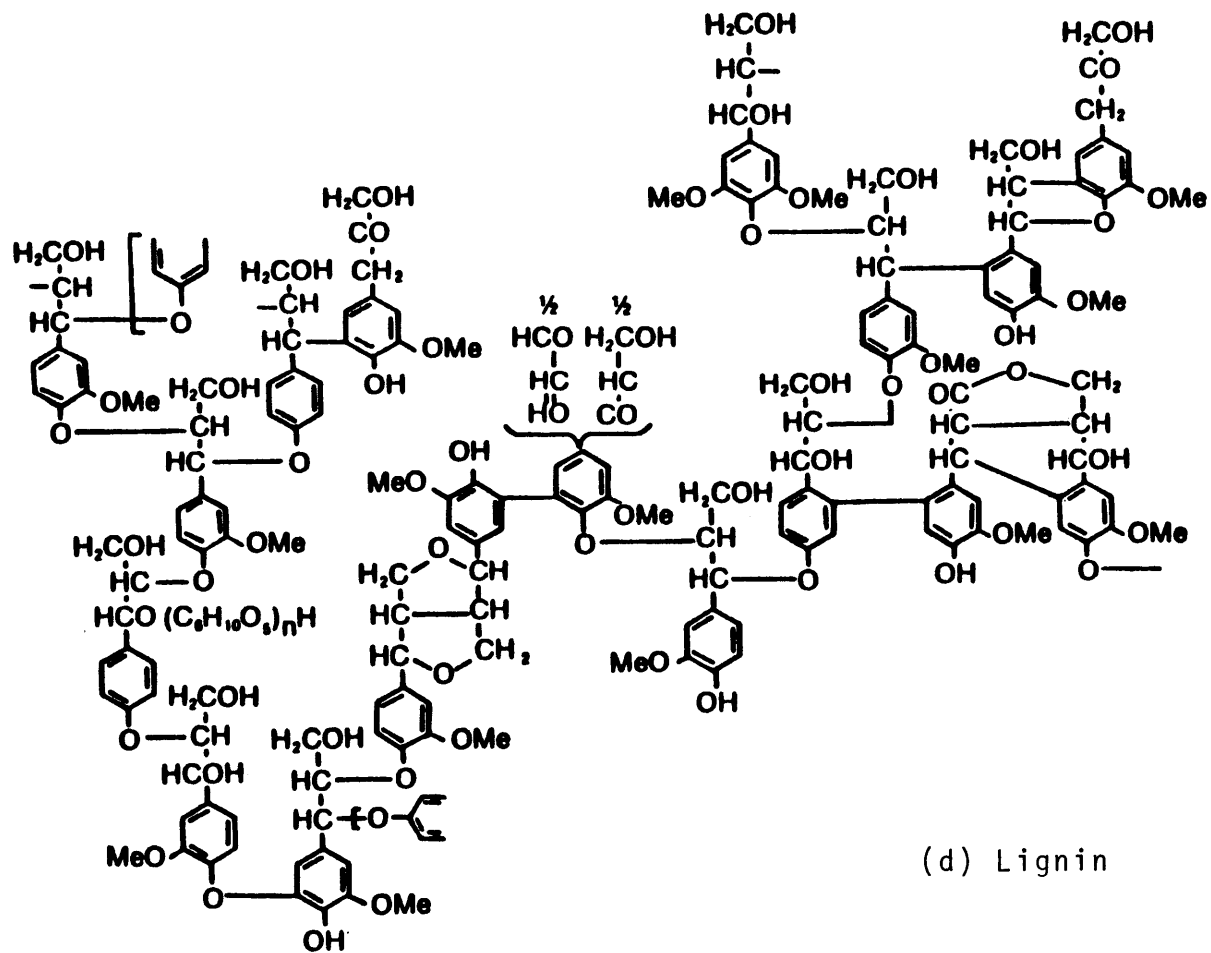
Fig. 2.1-3 (d) Lignin structural formula, SERI (1979)

transformation.

The ash content of wood is generally less than 0.5 wt% (Kollmann and Côté, 1968). Ashing experiments performed on the present xylan showed a surprisingly high ash content of 9.0 wt%. Table 2.1-1 outlines these ashing results and Table 2.1-2 gives the calcium and potassium content of each of the ashes. According to Kollmann and Côté (1968) common mineral constituents in wood ash are calcium, potassium, magnesium, carbonates, phosphates, silicates and sulfates.

2.2 Pyrolysis of Biomass

Good literature reviews of biomass pyrolysis and gasification are given in the compendium published by the Solar Energy Research Institute (SERI 1979). A count of the references for cellulose, xylan and lignin indicates that a clear majority of the published work so far has been on cellulose, while work with lignin is in second place. There appear to be only a few papers on xylan pyrolysis, and this author is unaware of any studies of its rapid pyrolysis.

This research on the pyrolysis of xylan is a continuing effort on a project in which M. R. Hajaligol (1980) studied the rapid pyrolysis of cellulose and T. R. Nunn (1981) investigated milled wood lignin and sweet gum pyrolysis. The present work focuses on the rapid pyrolysis of xylan, and on assessing whether the rapid pyrolysis

Table 2.1-1 Ash from wood and its constituents[*]

SAMPLE	Ash (weight % sample)
No. 507 filter paper (cellulose)	0.07
Sweet gum xylan	9.0
Milled wood lignin	0.15
Sweet gum hardwood	0.23

[*]Samples heated from 298K to 1023K at 5 K/min.

Table 2.1-2 Calcium and potassium content of ash from wood and its constituents[*]

Ashed sample	Calcium		Potassium	
	wt. % of ash	wt. % of sample	wt. % of ash	wt. % of sample
No. 507 filter paper (cellulose)	0.43	3×10^{-4}	4.5	3×10^{-3}
Sweet gum xylan	3×10^{-3}	3×10^{-4}	49.0	4.5
Milled wood lignin	0.33	5×10^{-4}	2.9	4×10^{-3}
Sweet gum hardwood	7.8	1.8×10^{-2}	72.0	0.17

[*]Determined by atomic absorption of aqueous solutions of ash.

behavior of whole biomass (sweet gum) may be predicted from similar information on its three major constituents.

Most of the work to date on the pyrolysis of xylan has been done by Shafizadeh (1972, 1977). Fang and McGinnis (1975) have pyrolyzed holocellulose (delignified extractives-free wood), which thus contains the unsegregated cellulose and hemicellulose fractions. Each study was also supplemented with a discussion of the effects of inorganic additives (mainly $ZnCl_2$ and NaOH) on the pyrolysis products spectrum. Table 2.2-1 and Table 2.2-2 show the product yields from the pyrolysis of xylan; Table 2.2-3 shows the yields from holocellulose pyrolysis.

In addition to these results, work has been done by the same scientists and also by Stamm (1956) on elucidating the chemical structure of tars and chars from pyrolysis. Further investigations into the kinetic mechanisms of xylan pyrolysis have been made by Shafizadeh (1977), but no one seems to have determined kinetic parameters for xylan pyrolysis. From an analysis of rates of free radical formation and of weight loss from cellulose, xylan, lignin and wood, Shafizadeh (1977) concludes that "the free radical formation in wood is roughly the summation of that for its three major constituents". This provides incentive for determining whether pyrolysis behavior of whole wood may indeed be simulated from pyrolysis of its individual components.

Care must nevertheless be taken in comparing different sets of such published data due to the variety of conditions under which biomass pyrolysis has been studied.

25

Table 2.2-1   Pyrolysis products of xylan and treated xylan at 573K.

(Shafizadeh and Chin, 1977)

Product	Neat	+10% $ZnCl_2$
Liquid condensate	30.6[a]	45.3
Carbon dioxide	7.9	7.5
Char	31.1	42.2
Tar	15.7	3.2
High mol. wt. component	(17)[b]	
D-xylose from hydrolysis	(54)[c]	

[a]Percentage, yield based on the weight of the sample.

[b]Based on the weight of the tar

[c]Based on the weight of oligosaccharides.

Table 2.2-2   Pyrolysis of 4-0-methylglucuronoxylan and
0-acetyl-4-0-methylglucuronoxylan at 773K.
(Shafizadeh, McGinnis and Philpot, 1972)

Peak number	Pyrolysis product	Xylan			O-Acetylxylan			Method of identification[b]
		Neat	+ $ZnCl_2$	+ NaOH	Heat	+ $ZnCl_2$	+ NaOH	
1,2[e]	Fixed gases							c
3	Acetaldehyde	2.4[e]	0.1	1.6	1.0	1.9	1.6	c,d,e,f
4	Furan	T	2.0	0.3	2.2	3.5	0.4	c
5	Acetone	} 0.3	T	3.3	} 1.4	T	} 5.8	c
6	Propionaldehyde		T	0.7		T		c,d,e,f
7	Methanol	1.3	1.0	2.1	1.0	1.0	1.8	c
11	2,3-Butanedione	T	T	T	T	T	T	c,d,e,f
12	Ethanol	T		0.6	T		0.6	c
13	2-Butenal	T		1.2	T		1.4	c
14	1-Hydroxy-2-propanone	0.4	T	} 2.0	0.5	T	0.8	c,d,e,f,g
15	3-Hydroxy-2-butanone	0.6	T		0.6	T	0.6	c
16	Acetic Acid	1.5	T	3.1	10.3	9.3	3.4	a,c
17	2-Furaldehyde	4.5	10.4	1.6	2.2	5.0	0.6	a,b,c,d,e,f
	Char	10	26	21	10	23	23	
	Carbon dioxide	8	7	14	8	6	22	
	Water	7	21	26	14	15	19	c

b- Refers to identification methods described in experimental part of paper.
e- Percentage, yield based on sample weight; T=trace amounts.

26

Table 2.2-3 Pyrolysis products of holocellulose from
Loblolly Pine bark.
(Fang and McGinnis, 1976)

| No. | Compound | Total yield (%) | | | Identification methoda |
		Neat	5% ZnCl$_2$	5% NaOH	
1-4	Small molecular weight hydrocarbons	0.40	0.43	1.80	a,b
5	Methanol	1.12	1.72	0.65	a,b
6	Acetaldehyde	0.21	0.15	0.34	a,b,c
7	Acrylaldehyde	0.07	0.05	0.09	a,b,c
8	Furan	0.52	0.64	0.47	a,b
9	Acetic Acid	1.39	0.54	1.04	a,b
10	Diacetyl	0.23	0.24	0.31	a,b,c
11	1-Hydroxy-2-propanone	0.06	0.02	0.22	a,b,c
12	2-Furaldehyde	0.51	0.77	0.06	a,b,c
	Carbon monoxide	5.28	5.80	8.98	b
	Carbon dioxide	11.04	11.81	20.42	b
	Water	37.25	42.51	37.22	b
	Char	20.17	34.83	28.04	--

a. Identification method: (a) Comparison of retention time and addition of known compound; (b) vapor phase fragmentation; and (c) formation of a 2,4-dinitrophenylhydrazone derivative

27

3. APPARATUS AND PROCEDURE

3.1 Reactor

A batch reactor used previously by Hajaligol (1980) for cellulose pyrolysis and by Nunn (1981) for lignin and sweet gum wood pyrolyses was used in this research. The reactor was designed to allow study of a large range of heating rates, residence times and pressures as indicated in Table 3.1-1.

The captive sample reactor is a 22.9 cm by 22.9 cm I.D. Corning pyrex cylinder flanged at both ends by circular stainless steel plates. Feedthroughs were made in the top plate for the electrodes, thermocouple leads and a sampling/injection port for gases. The bottom plate only has an exit port for purging the volatiles into the gas collection system.

The screen which holds the wood samples is a 14 cm by 15 cm piece of 325 mesh stainless steel cloth which is folded twice in its largest dimension. The final result is a piece 4.5 cm by 14.5 cm which fits between the electrodes. The sample is placed in the inner fold, and the thermocouple in the outer fold when the screen is ready to be used in the reactor. The 1 cm diameter brass electrodes spaced 13 cm apart descend 12.5 cm into the middle of the reactor and terminate in 1.8 cm by 2.7 cm by 6 cm solid brass clamps which hold the screen in place.

Table 3.1-1   Variability of Pyrolysis Reaction Conditions

Operating Parameter	Range of Control
Heating Rate	50 to 100,000 K/s
Peak Temperature	400 to 1500 K
Holding Time at the Peak Temperature	0 to infinity sec
Pressure	1.3 to 4.1 X 10^6 Pa

*A separate reactor is available for experiments up to 1 X 10^8 Pa.
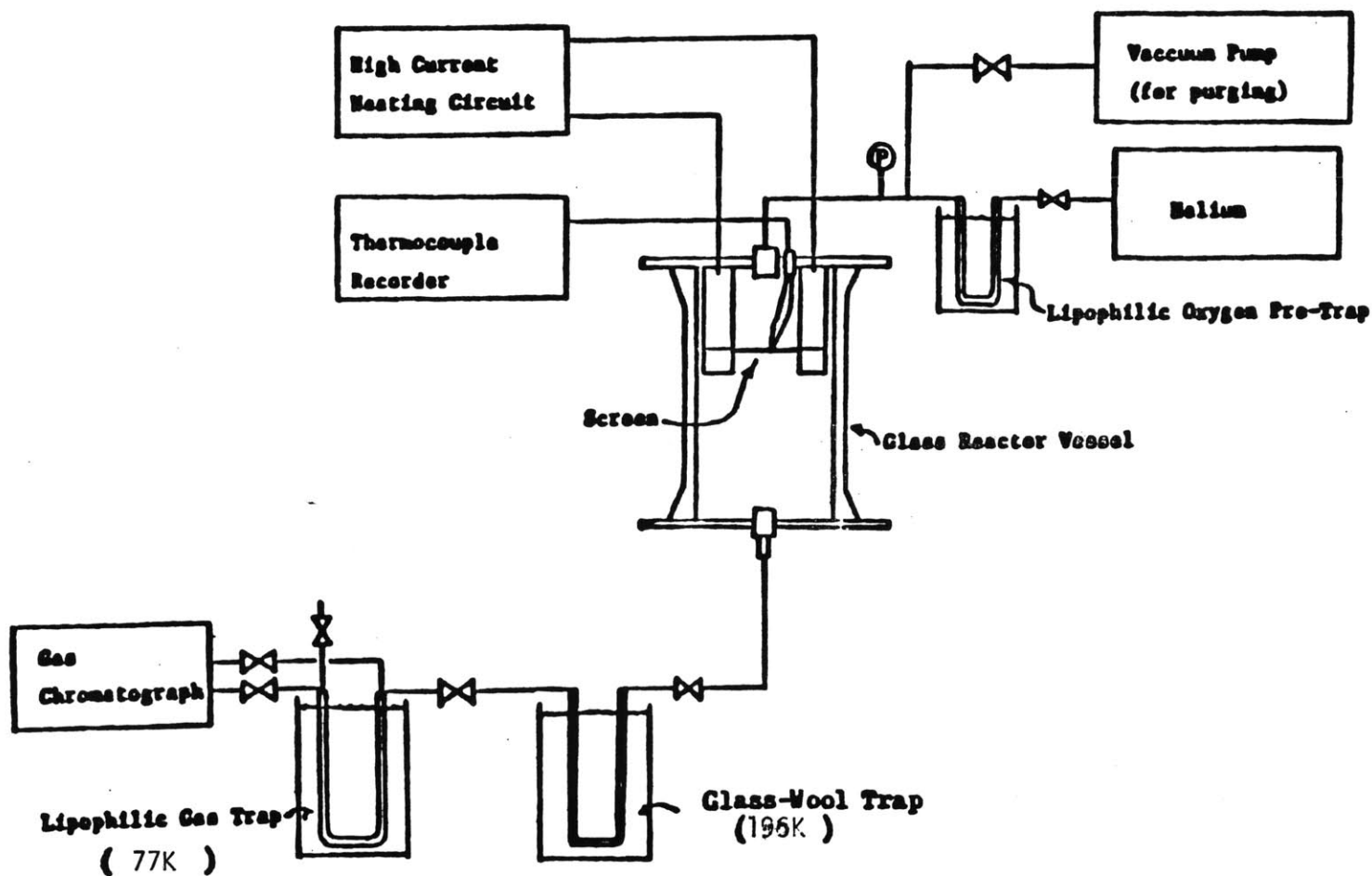
Figure   3.2-1   Schematic of Captive Sample Apparatus (Hajaligol,1980)

3.2 Reactor Accessories

The gas collection system consists of two traps in series. The first U-shaped trap (glass wool trap) is made of a 39.6 cm long, 0.95 cm I.D. stainless steel tube, is packed with glass wool made by Alltech Associates, and is immersed in a methanol/dry ice bath at 195K. The second trap (lipophilic trap) is of the same dimensions but is immersed in a dewar of liquid nitrogen (75K) and is packed with 50/80 mesh Porapak QS chromatographic packing made by Waters Associates.

The rapid response Chromel-Alumel thermocouple manufactured by Omega Engineering Inc. has a wire diameter of 0.00254 cm with a 0.00763 cm bead. The electrical response of the thermocouple is measured on a Hewlett Packard 680M strip chart recorder. A schematic diagram of the reactor is shown in Fig. 3.2-1.

The electrical heating system for the apparatus designed by Caron (1978) is shown by Nunn (1981).

3.3 Gas Analysis

The gases are analyzed on a Perkin Elmer Sigma 2B gas chromatograph with an associated Sigma 10B data integration station. Two stainless steel columns in series are used in the chromatograph: the first is a 45.7 cm long 0.635 cm I.D. column packed with 80/90 mesh 5A molecular sieves manufactured by Analabs Inc.; the second is a

3.66 m long, 0.635 cm I.D. column packed with 50/80 mesh Porapak QS.

Prior to this work, product gas yields from biomass pyrolysis
were determined on a Perkin Elmer Model 3920B chromatograph with a
Porapak QS column only. The switch over to the Sigma 2B was made
not only to get better separation between air and product gases but
also to obtain a superior separation between the carbon monoxide
and carbon dioxide peaks. Furthermore, the new temperature program
for the analysis does not require the subambient temperature program-
ming needed by the Model 3920B (starting at 203K), rather, all
analyses were done above 300K, which resulted in a substantial
savings of cryogenic coolant.

The dual flame ionization (FI)/thermal conductivity (TC) detect-
ors provided consistency checks for certain hydrocarbon yields.
Nevertheless, each detector has its own indispensible role: the FI
detector has better sensitivity than the TC detector for hydrocarbons
while the TC detector is crucial in quantifying those components which
are not recognized by the FI detector. The detailed procedure for gas
chromatography in the Sigma 2B is given in Appendix A.

3.4 Sample Preparation

Hajaligol's (1980) studies of cellulose pyrolysis were performed
with Whatman #507 filter paper in the form of strips 1 cm by 4 cm by
0.0101 cm in dimension; Nunn (1981) used wood powder and pressed flakes

of lignin for his work. The xylan powder used in this study was isolated by H. M. Chang's laboratory (North Carolina State University), from the same wood sample that provided Nunn with sweet gum hardwood and milled wood lignin. It was subsequently sieved in the 45-90 micron range as was the wood powder, to eliminate heat transfer limitations and to ensure that none of the xylan was lost through openings in the screen heater mesh. This powder was kept in a dessicator, over silica gel, for at least one month before use.

In contrast to the earlier biomass studies, the sample weight was reduced from 0.1 g to 0.05 g to ensure no mass transfer limitations existed during reaction. (At one time it was believed that mass transfer limitations were hindering complete reaction; this was later found not to be true. Nunn (1981) presents calculations of an upper limit on powdered sample size for which heat transfer limitations would be unimportant for our reaction conditions.) Halving the sample weight did not adversely affect the material balances for the experiments. The powder was spread uniformly over as large an area of the screen as possible, without coming near the electrode clamps.

3.5 Run Procedure

Prior to their use in experimental runs, the 325 mesh screens were prefired in a helium atmosphere. The helium, from Middlesex Supply Co., is 95.5% pure and contains nitrogen and oxygen gases as

impurities. During the prefiring to a peak temperature of 1300K, the oxygen reacts with the chromium in the stainless steel to give the screen a coating of chromia (Yurek, 1977). The screens, upon cooling, exhibit a more dulled luster than they posessed originally. This procedure is believed to deactivate catalytic sites on the screens and thus retard their ability to influence secondary cracking of pyrolysis products. Hajaligol (1980) discusses experiments which indicated the screen had little effect on the observed pyrolysis behavior of cellulose.

The 50 mg of powdered xylan is then spread as a thin layer on a preweighed screen, which was first dried over silica gel; the screen and sample are left to dry overnight in covered petri dishes containing silica gel. Just before use in the reactor, the screen and sample are weighed until a dry equilibrium weight is established within 0.1 mg.

A circular piece of aluminum foil 21 cm in diameter, with a 4.5 cm diameter opening at its center is placed on the bottom of the reactor around the gas exit port, for tar collection. To further prevent tars from escaping with the gases, a 3.7 cm diameter circular piece of Whatman EPM 1000 glass filter paper is placed over the exit port. The foil, filter and hex-nut (to hold the filter in place) are also dried overnight in covered petri dishes containing silica gel. All parts are weighed until consecutive weighings differ by less than 0.1 mg, and are then properly positioned into the reactor.

After the screen containing the sample is firmly installed between

the electrodes, the thermocouple bead, mounted on a moveable holder in the reactor, is carefully inserted into the top fold of the screen, and is positioned near its center. The top flange of the reactor is lowered to the pyrex cylinder and bolted shut; next, the reactor volume is evacuated to 1.3 Pa. The reactor is pressurized with helium (prepurified by being passed through a lipophilic trap at 75K) to 1.3×10^5 Pa and then evacuated again. This procedure is repeated three or four times. Upon final pressurization, the helium is allowed to reach room temperature (< 5 min.).

The temperature recorder is adjusted to read 298K and motion of the strip chart is initiated; the heating switch is thrown, and the sample is pyrolyzed at 1000 K/s to the desired peak temperature according to the setting on the heating timer. Once the peak temperature is reached, the current across the electrodes is automatically shut off, and the screen cools by convection and radiation starting at an average cooling rate of 200 K/s. After ten seconds of cooling, the temperature recorder is turned off.

The particulates in the reaction gases are allowed to settle and the gases are allowed to reach room temperature (< 15 min.). The vessel is slowly pressurized to 3×10^5 Pa with prepurified helium, and the product gases are purged through the traps for one hour, at a helium flow rate of 0.25 l/min. Hence, 1.6 reactor volumes are passed through the traps.

The captive sample reactor is opened; the screen (containing char), the filter, nut and foil (containing tars) are placed in covered petri

34

dishes containing silica gel, and are weighed until an equilibrium weight is reached. The tars on the sides of the reactor and on the top flange are recovered by wiping these areas with two preweighed, predried Kimwipe tissues which are wetted with a 2:1 volume/volume mixture of nanograde methanol:acetone. A third tissue serves as a control for residual solvent. All three tissues are allowed to evaporate solvent for one half hour in a fume hood, and are then placed in a covered petri dish over silica gel to dry. The tar containing tissues are weighed to a final equilibrium value, and their tar content is obtained by difference from their initial dry weight minus the correction for residual solvent calculated from the weight increase of the control tissue.

The gases are quantified by heating each trap in a boiling water bath (373K) for a half hour during which its contents are desorbed and purged by helium flowing at 0.07 1/min (75 trap volumes total) into the gas chromatograph. In addition, the glass wool trap is extracted with two 10 ml aliquots of a 2:1 volume/volume solution of nanograde methanol:acetone to recover any light tars and liquids which pass through the filter on the reactor's outlet. The resulting tar solution is collected in a preweighed aluminum cup, and the solvent is allowed to evaporate overnight. The total tar yield is thus operationally defined as the sum of the tars on the aluminum foil, the Kimwipe tissues, the aluminum cup, and the filter and nut. The char yield is determined gravimetrically from weight loss of the screen plus sample.

3.6 Error Analysis

Nunn (1981) and Hajaligol (1980) discuss the errors associated with the experimental methods outlined above. The only new sources of error in this work are from the response factors determined for the Sigma 2B gas chromatograph, and are presented in Appendix A.

4. RESULTS AND DISCUSSION

4.1 Global Pyrolysis Results for Xylan

The first section on experimental results presents the yields of char, tar and total gases evolved from the pyrolysis of as-received xylan containing 9 wt% inorganic matter as a function of peak temperature. Figs. 4.1-1 to 4.1-3 show weight loss, gas yield and tar yield respectively. The curves drawn through the data are free drawn trendlines, and show similarities with those observed for the pyrolysis of filter paper cellulose, milled wood lignin and sweet gum hardwood (Hajaligol, 1980; Nunn, 1981).

The char yield decreases dramatically between 550-750K after which it levels off to 32 wt%. The yield stays level until 1100K when it starts to drop again. At a temperature of 1400K the yield is lowered to 27 wt% and is still decreasing.

Gas production commences at 600K and rises continuously to 35 wt% when the temperature is about 850K. The yield is constant at 35 wt% in the temperature interval 850-1300K; past 1300K there is a slow increase in gas production again. At 1400K, the yield is 37 wt% and is still increasing.

Tars are generated before gases and are evolved at about 500K. Their yield peaks at 37 wt% between 750-800K, declines to a plateau of 33 wt% at 1000K, and remains constant with further increase in temperature.

37
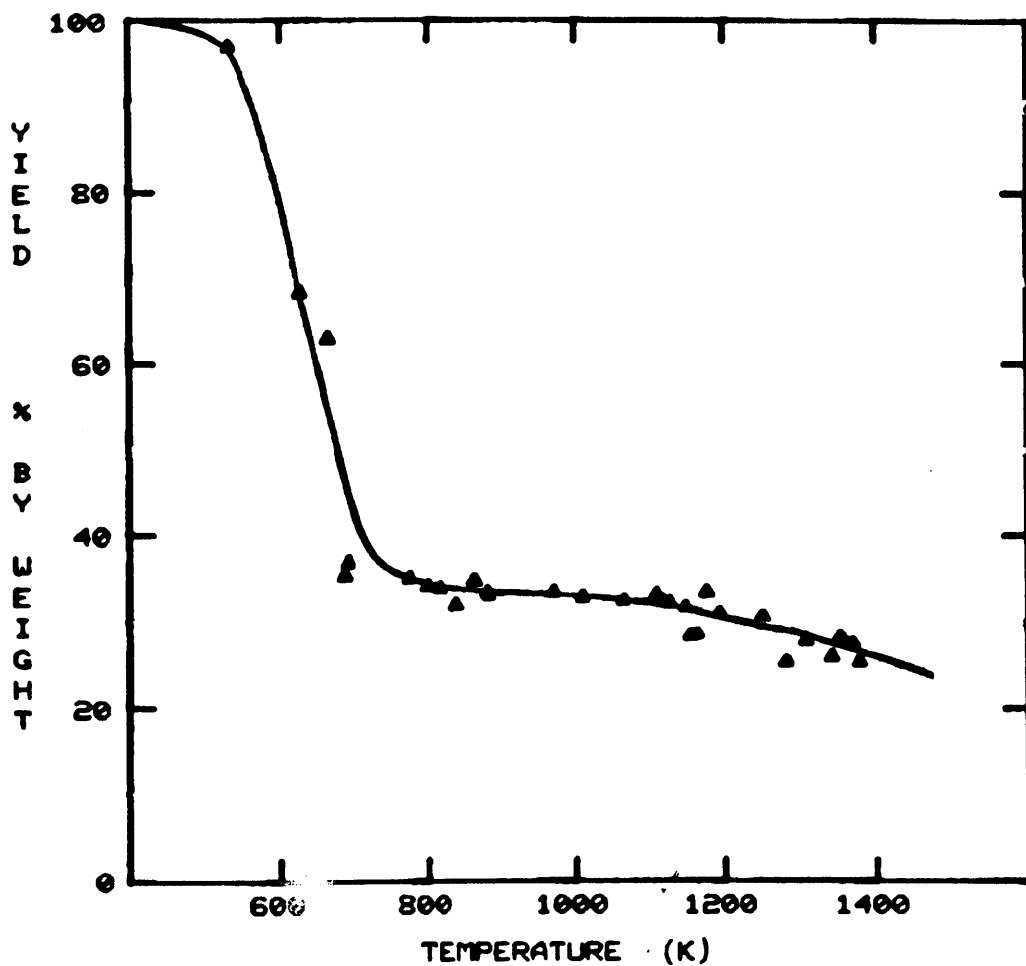
Fig. 4.1-1 Char yield from pyrolysis of sweet gum xylan.
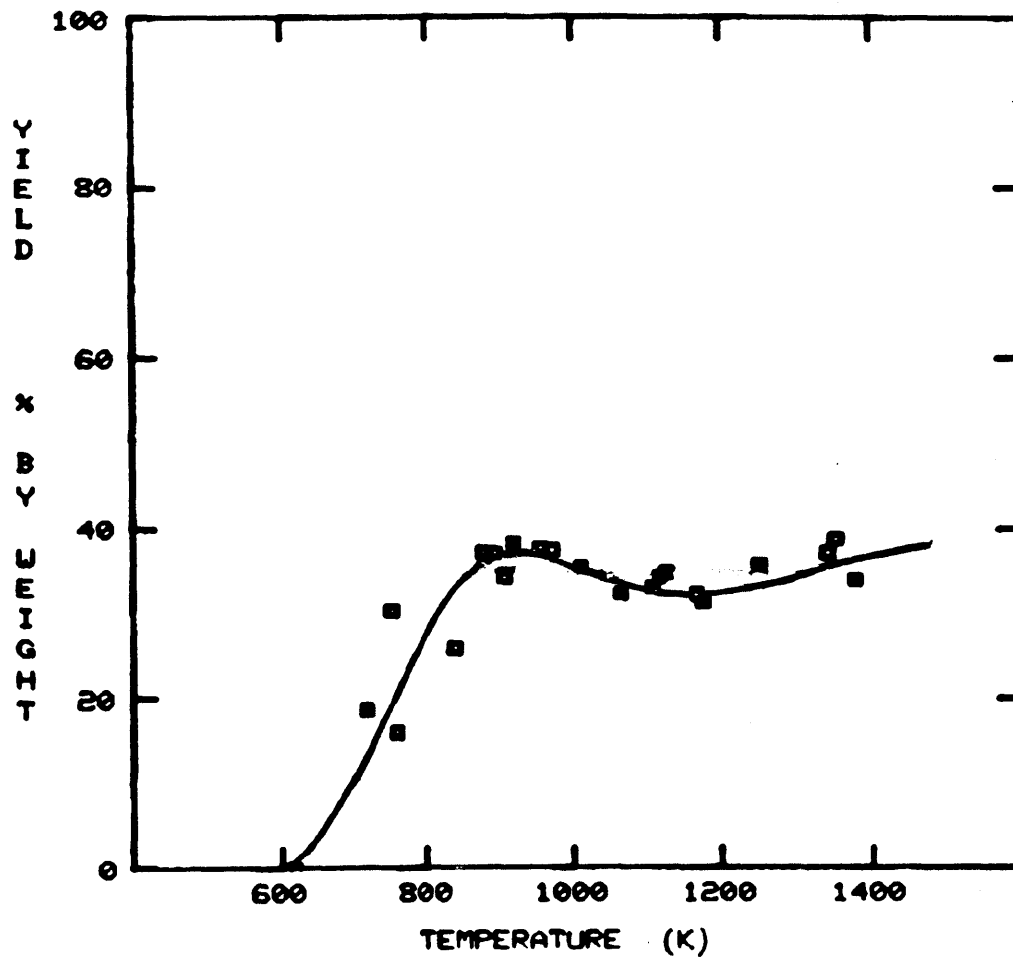
Fig. 4.1-2   Total gas yield from pyrolysis
of sweet gum xylan.
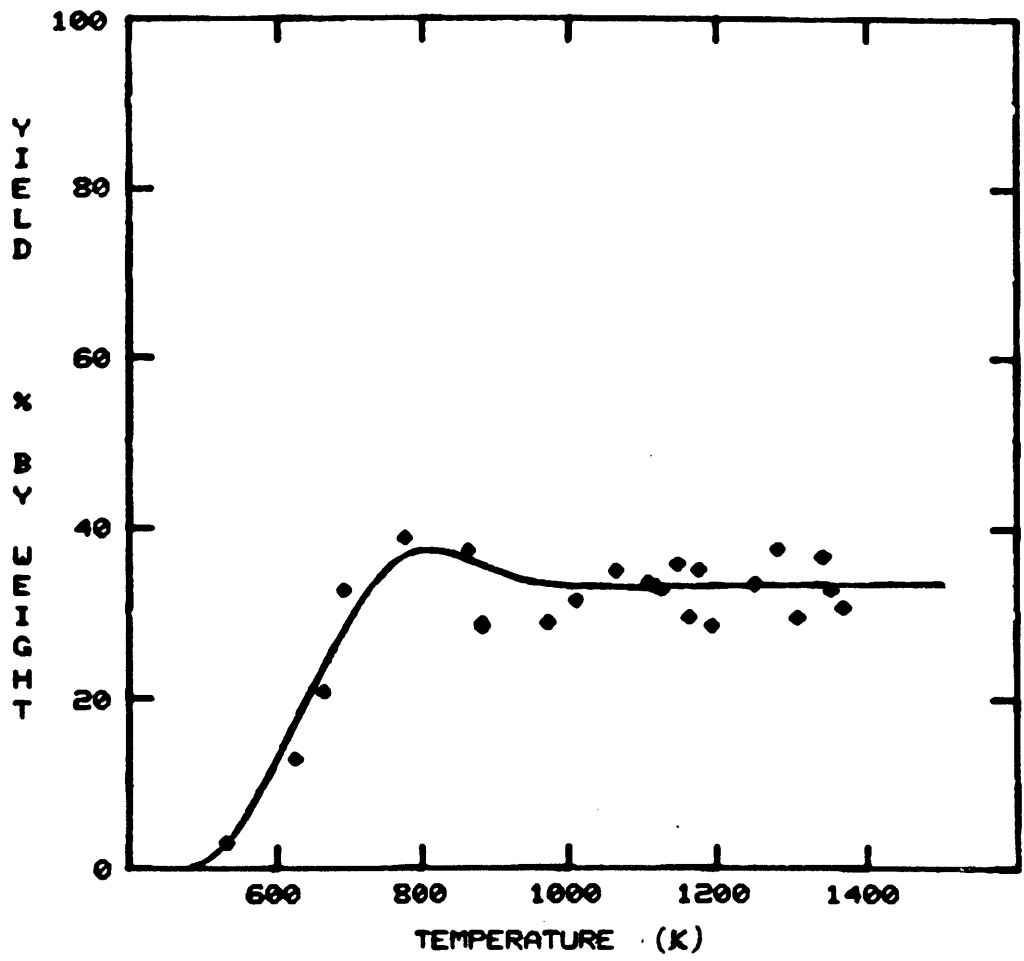
Fig. 4.1-3   Tar yield from pyrolysis of
sweet gum xylan.

40

4.2 Char Yield

The most striking result from the global pyrolysis data presented is the high ultimate char yield of 25 wt% (of cellulose: 4.2 wt%; lignin: 14 wt%; wood: 7.0 wt%). This finding may be attributed partially to the high ash content (9.0 wt%) of the xylan. In Chapter 2 it was pointed out that woods have ash contents around 0.5 wt%. If the xylan in wood contained 9.0 wt% ash, the wood would contain 2.7 wt% ash if the cellulose and lignin are assumed to be ash free.

To correct the global and individual gas yields from xylan pyrolysis for the high ash content, which is due to the xylan isolation procedure (see Fig. 2.1-1), the scheme outlined in Fig. 4.2-1 was implemented. The material balances for each experimental point are preserved in this numerical procedure; Figs. 4.2-2 through 4.2-4 show the corrected char, total gas and tar yield from xylan. The major effect of the correction is in increasing the ultimate yield of total gas and tar by about 10% of their previous values to 38 wt% and 35 wt%, while correspondingly decreasing the char yield by roughly 8 wt% to an ultimate value of 17 wt%.

Appendix D contains the experimental data for the production of individual product gases from xylan pyrolysis. The remainder of the data presented in this chapter have been corrected and are thus on an ash-free basis. Any noteworthy differences which have arisen in the interpretation of the data due to the corrective scheme, have been saved for discussion in Section 4.4.

Fig. 4.2-1 Corrective calculations for char, tar and gas yields

(a) ORIGINAL XYLAN SAMPLE :
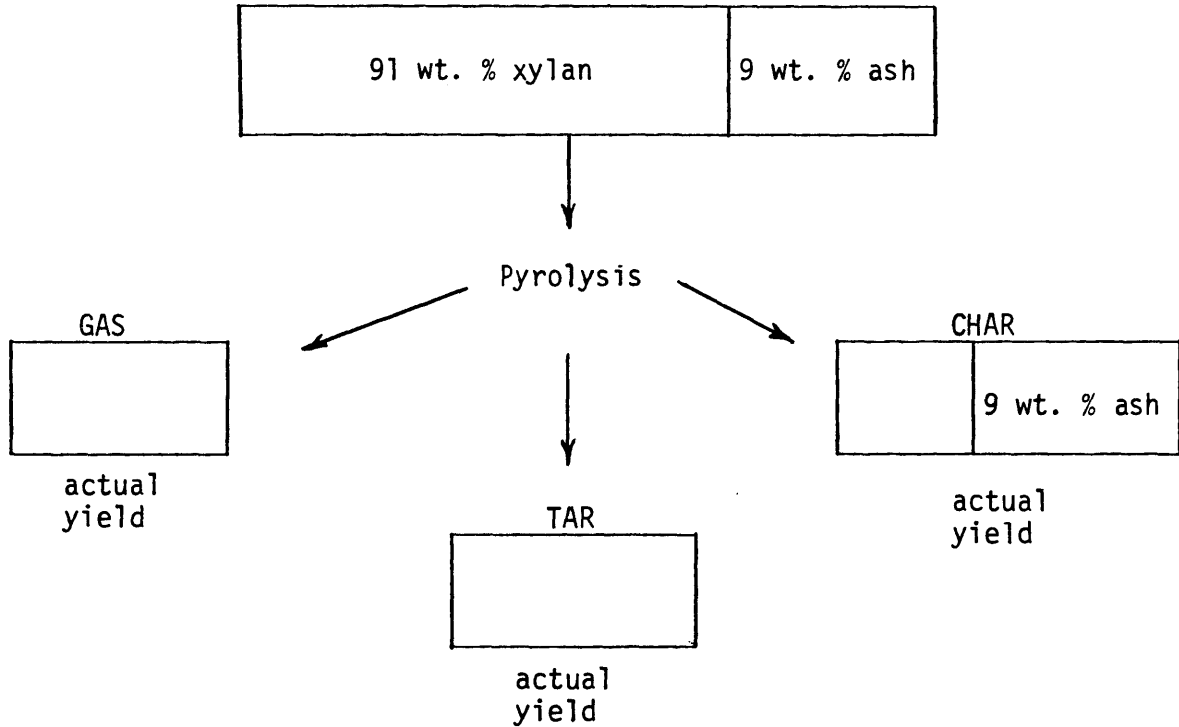
$$\sum \text{ actual yields} = 100 \text{ wt. } \%$$

(b) CORRECTED YIELDS BASED ON 91 WT. % XYLAN :

$$\text{Corrected gas yield} = \frac{\text{Actual Gas Yield}}{0.91}$$

$$\text{Corrected tar yield} = \frac{\text{Actual Tar Yield}}{0.91}$$

$$\text{Corrected char yield} = \frac{\text{Actual Char Yield} - 0.09}{0.91}$$

(+)

$$\text{Total yield} = 100 \text{ wt. } \%$$
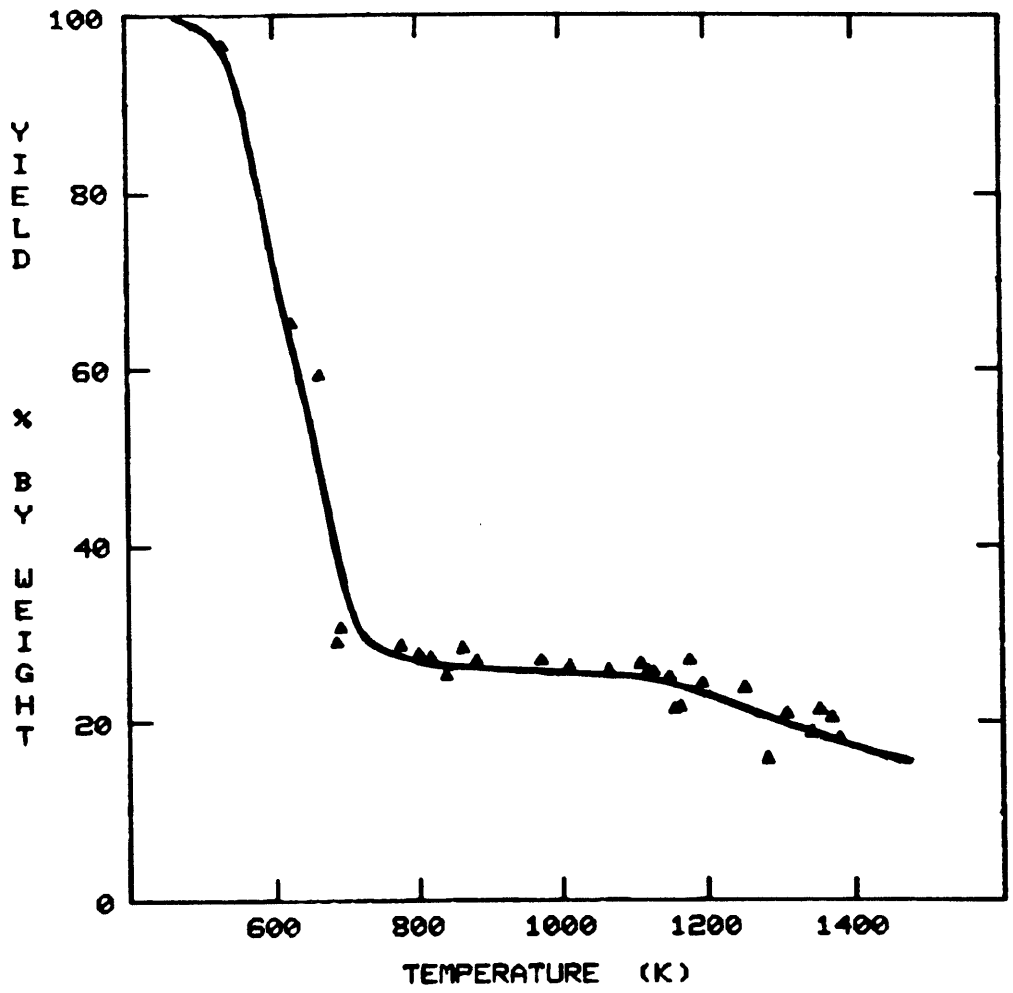
Fig. 4.2-2   Char yield from xylan pyrolysis,
            corrected for ash content.

43
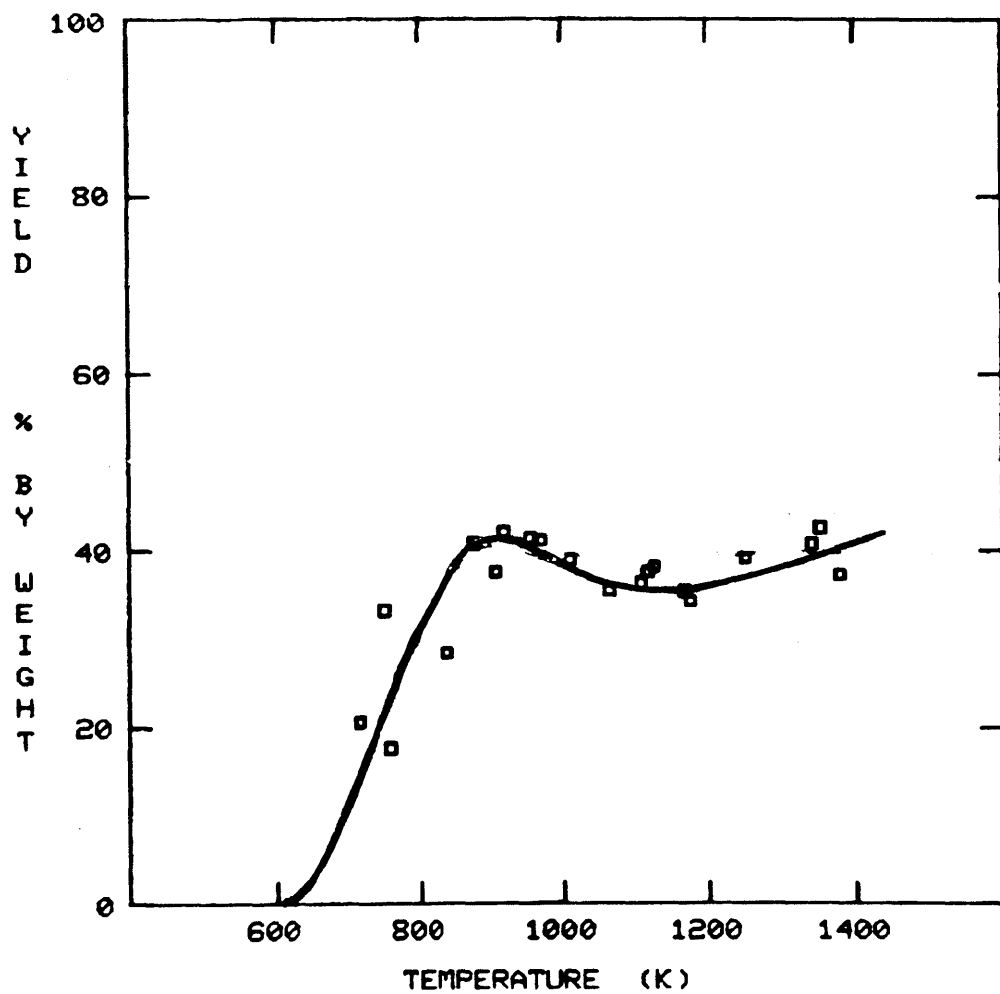
Fig. 4.2-3 Total gas yield from xylan
pyrolysis, corrected for ash
content.
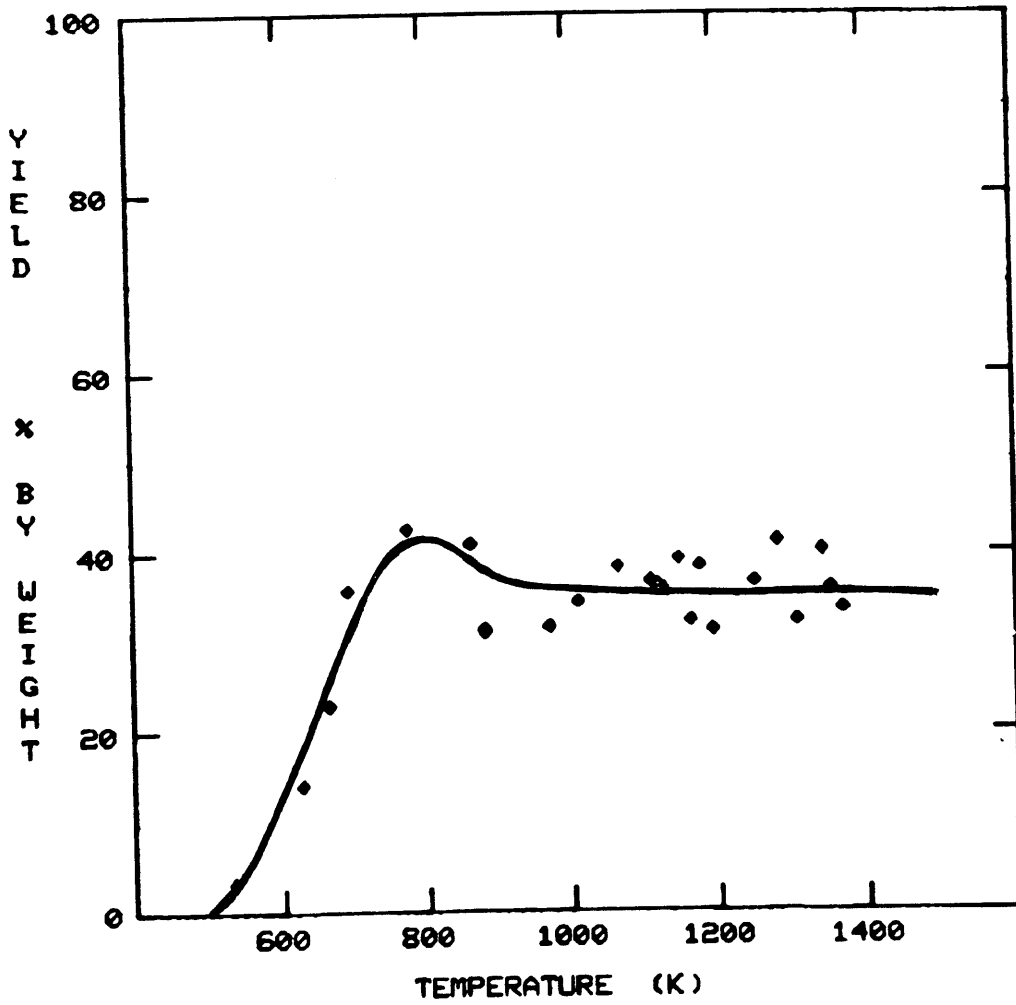
Fig. 4.2-4   Tar yield from xylan pyrolysis,
             corrected for ash content.

4.3 Kinetic Modelling of Pyrolysis Products

The second section of the results focuses on individual gaseous species evolved. The data for each gas were first curve-fitted by eye to reveal the ostensible trend (indicated by the dashed line), and later were fit by a nonlinear least squares regression routine named POWELL (see Appendix C), according to the single reaction first order model used by Franklin (1980), Hajaligol (1980) and Nunn (1981). The curve fit generated by a program named CLFITI (Franklin, 1980) using POWELL's best fit parameters is shown on the same figures as the smooth continuous curve, but plots yield as a function of "idealized temperature" (see Appendix B). When only the latter curve appears on a plot, the model is said to exactly follow the ostensible trend.

Figure 4.3-1 illustrates the production of methane from xylan. The amount of methane generated at temperatures below 800K is less than 0.05 wt%. In the range 800-1300K the increase is virtually linear, and only gives a slight sign of tapering away at the highest temperatures.

The yields of ethylene and ethane shown in Fig. 4.3-2 and 4.3-3 respectively are closely modelled by first order kinetics. The production of each is discernible at about the same peak temperature (700K). Ethane production is complete by 1100K while ethylene evolution continues to about 1150K. Ethylene has an ultimate yield of 0.42 wt%; that of ethane is 0.12 wt%.

It is difficult to find the ostensible trend in the water data due to the scatter. Nevertheless, the first order model gives a

46

Fig. 4.3-1   Methane yield from sweet gum
xylan pyrolysis.
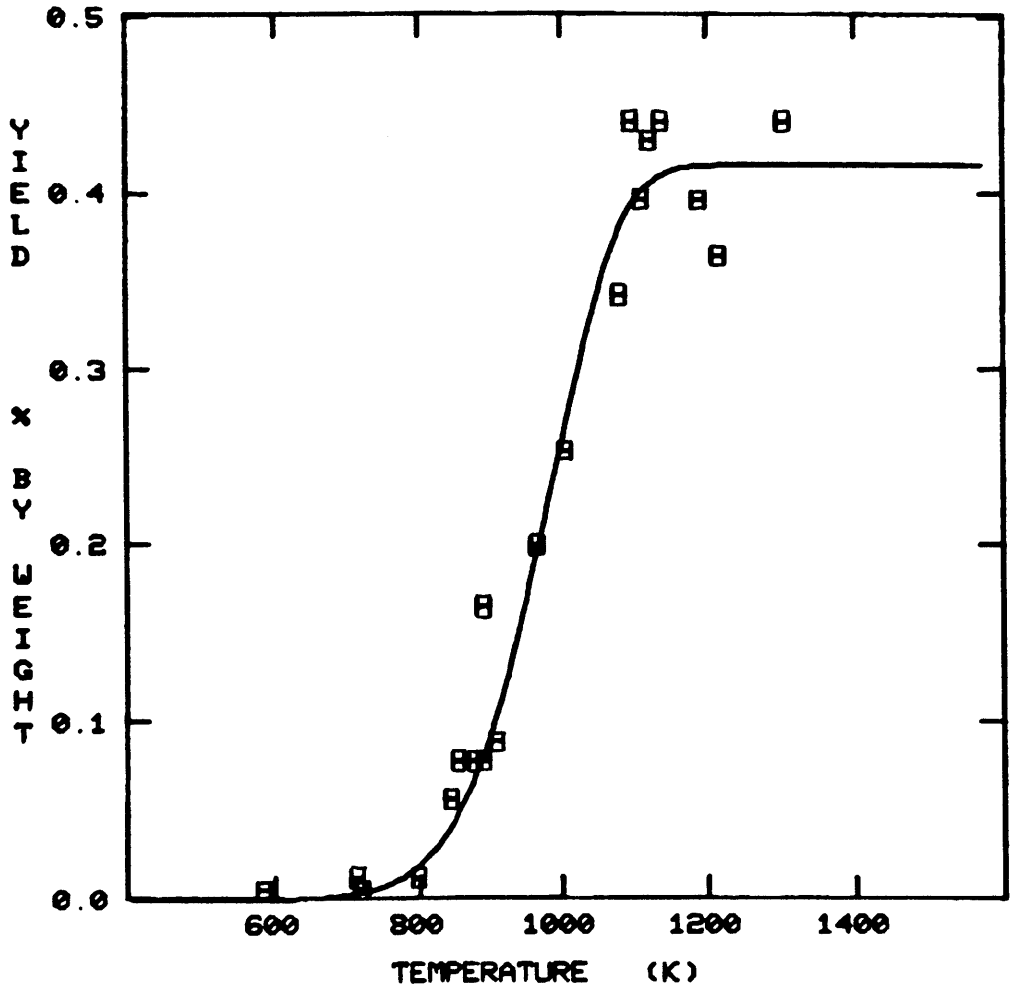
Fig. 4.3-2   Ethylene yield from sweet gum
              xylan pyrolysis.

48
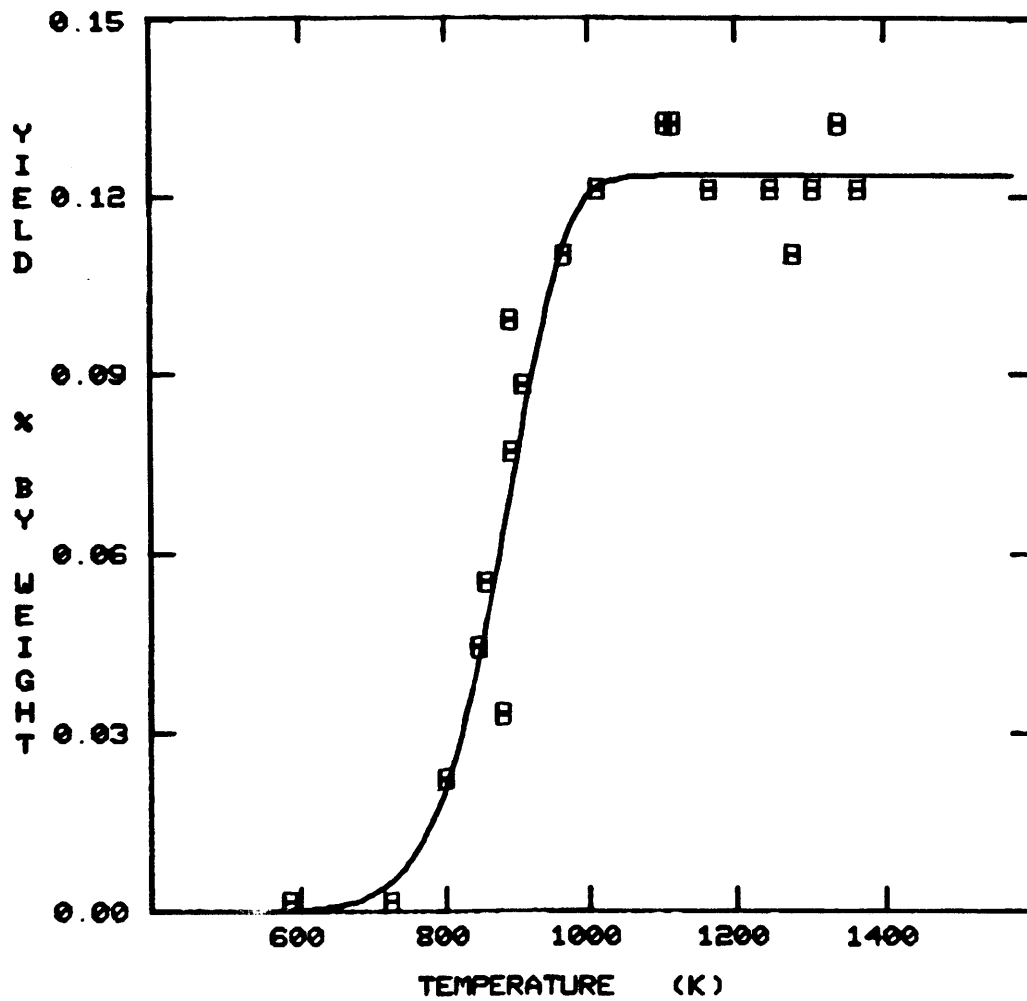
Fig. 4.3-3 Ethane yield from sweet gum
xylan pyrolysis.

reasonable approximation to the data as shown in Fig. 4.3-4. The ultimate calculated yield is 5.2 wt%, but the true value could range from 4.5-6.5 wt%.

As with water, there is much scatter in the formaldehyde data (Fig. 4.3-5). The yield increases linearly with temperature with a break in the slope at 1050K. However, the kinetic model gives a plausible S-shaped curve fit with an ultimate yield of 0.12 wt%. (See Table 4.2-1 for the standard error of estimate.)

Figs. 4.3-6 through 4.3-9 show the yields for propylene, methanol, acetaldehyde and ethanol respectively. The methanol and acetaldehyde yields seem to peak between 900-950K. Other than that, these four products can generally be considered to satisfactorily follow the kinetic model.

On a weight basis carbon dioxide and carbon monoxide account for most of the gases produced. Fig. 4.3-10 shows that carbon dioxide's yield follows the kinetic model well, but only until 1200K. Between 1200-1400K, however, the yield drops 2 wt% (absolute) to 14 wt% total. The same is not true of carbon monoxide. The overall curve for carbon monoxide (Fig. 4.2-11) is consistent with a series of steps at 800K, 1000K and 1150K respectively. However, the curve fitted by the model also approximates the data relatively well, but overspecifies the ultimate yield as an exaggerated 27 wt%. Therefore, for greater accuracy, each hypothetical step was separately fit by its own single reaction first order model. The results for steps 1 and (2+3) combined (800K and 1000K) are depicted in Figs. 4.3-12 and

Fig. 4.3-4 Water yield from sweet gum
xylan pyrolysis.
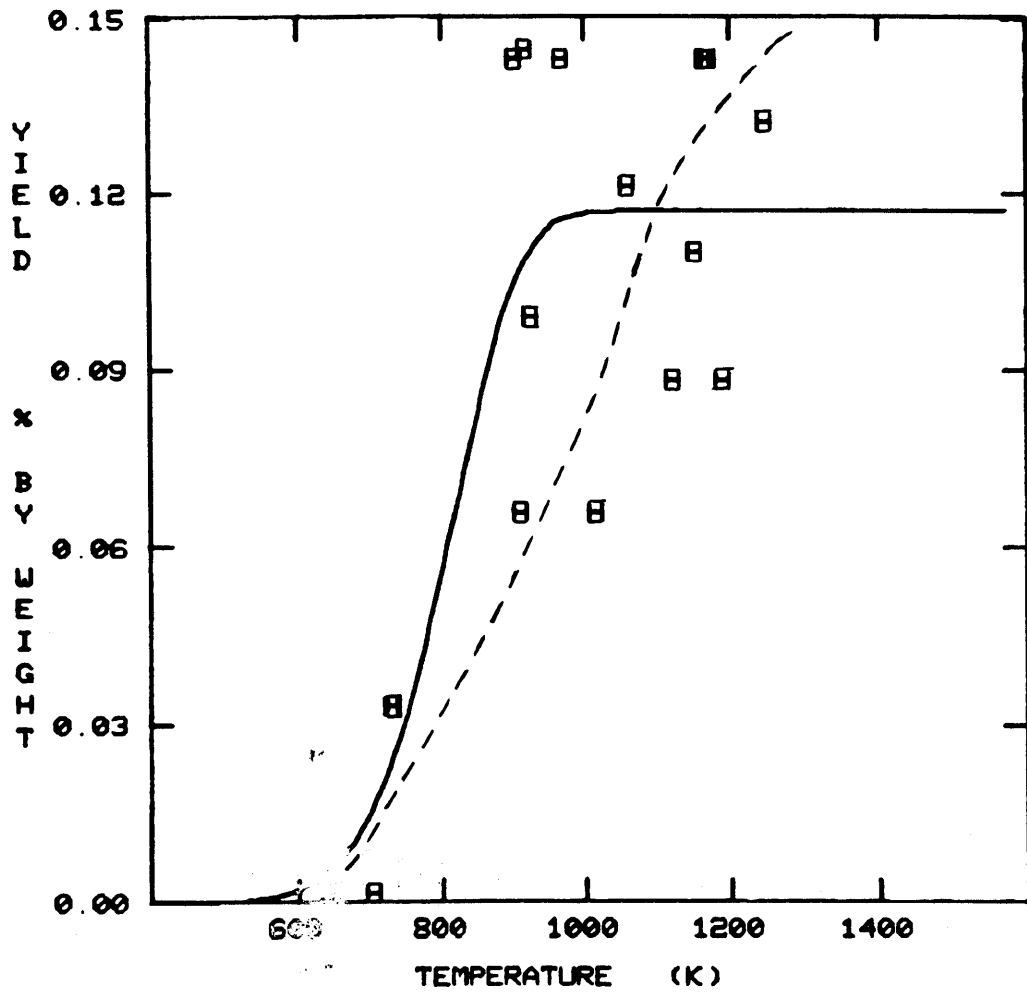
Fig. 4.3-5 Formaldehyde yield from sweet
gum xylan pyrolysis.
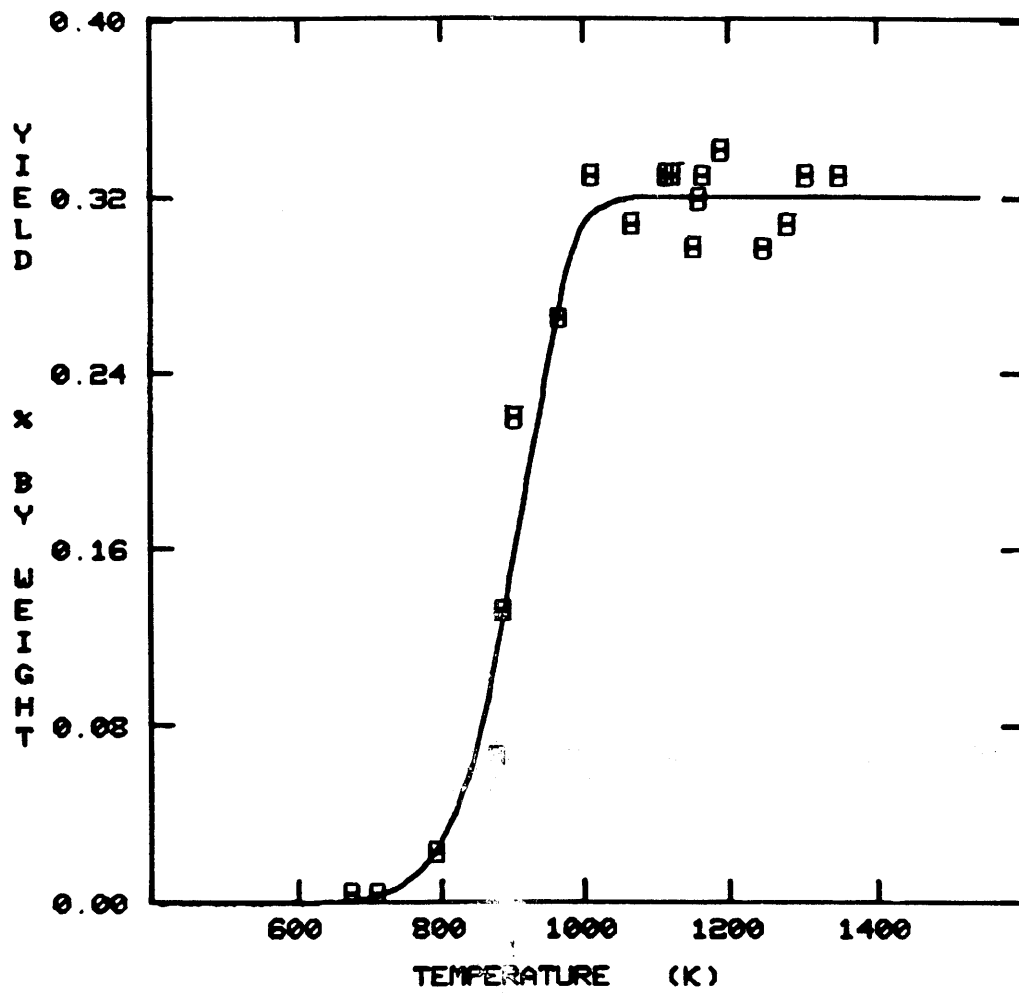
Fig. 4.3-6   Propylene yield from sweet
             gum xylan pyrolysis.
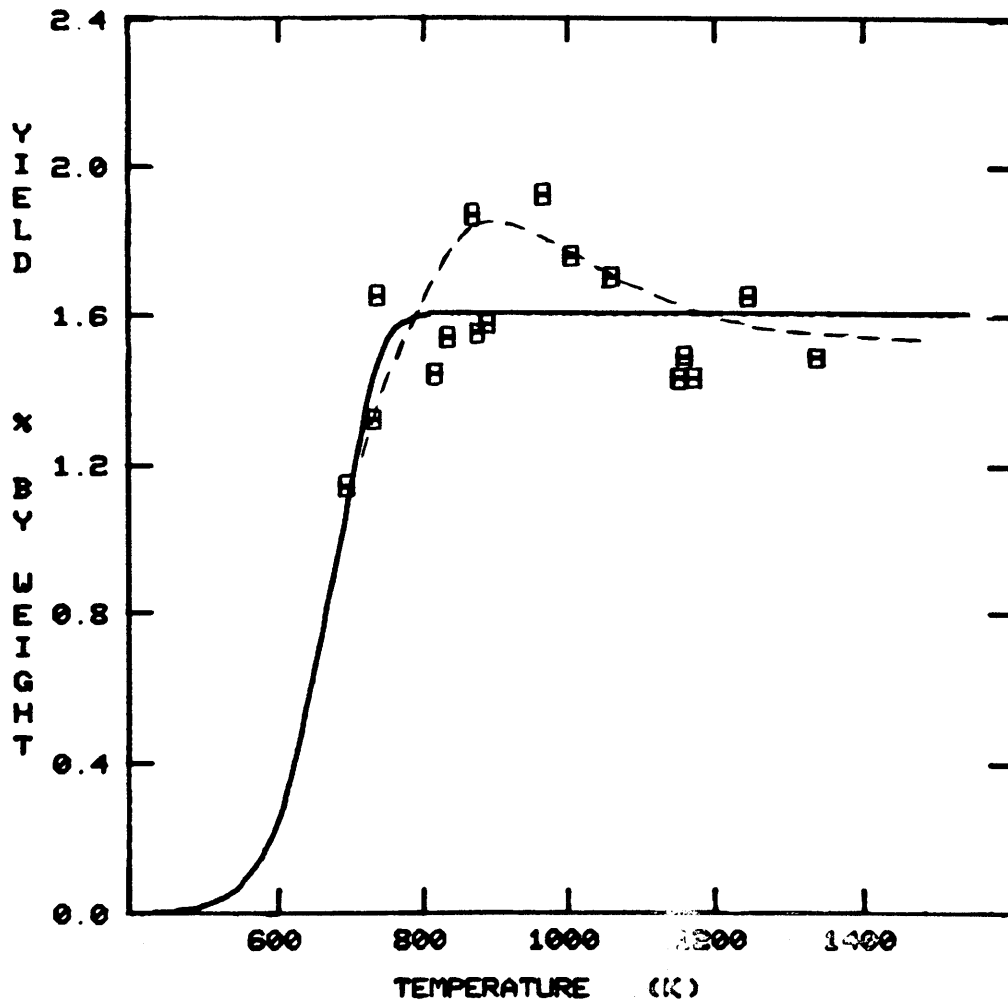
Fig. 4.3-7   Methanol yield from sweet
gum xylan pyrolysis.
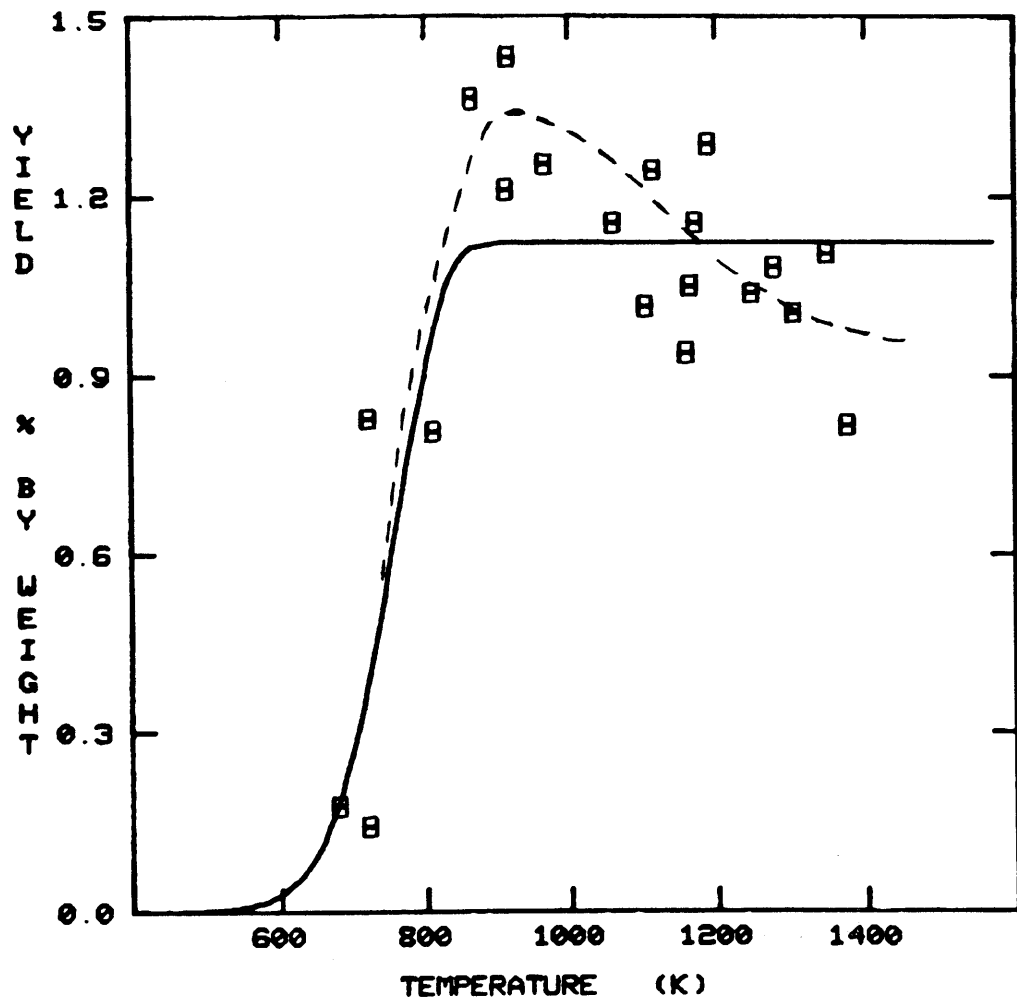
Fig. 4.3-8   Acetaldehyde yield from sweet
gum xylan pyrolysis.
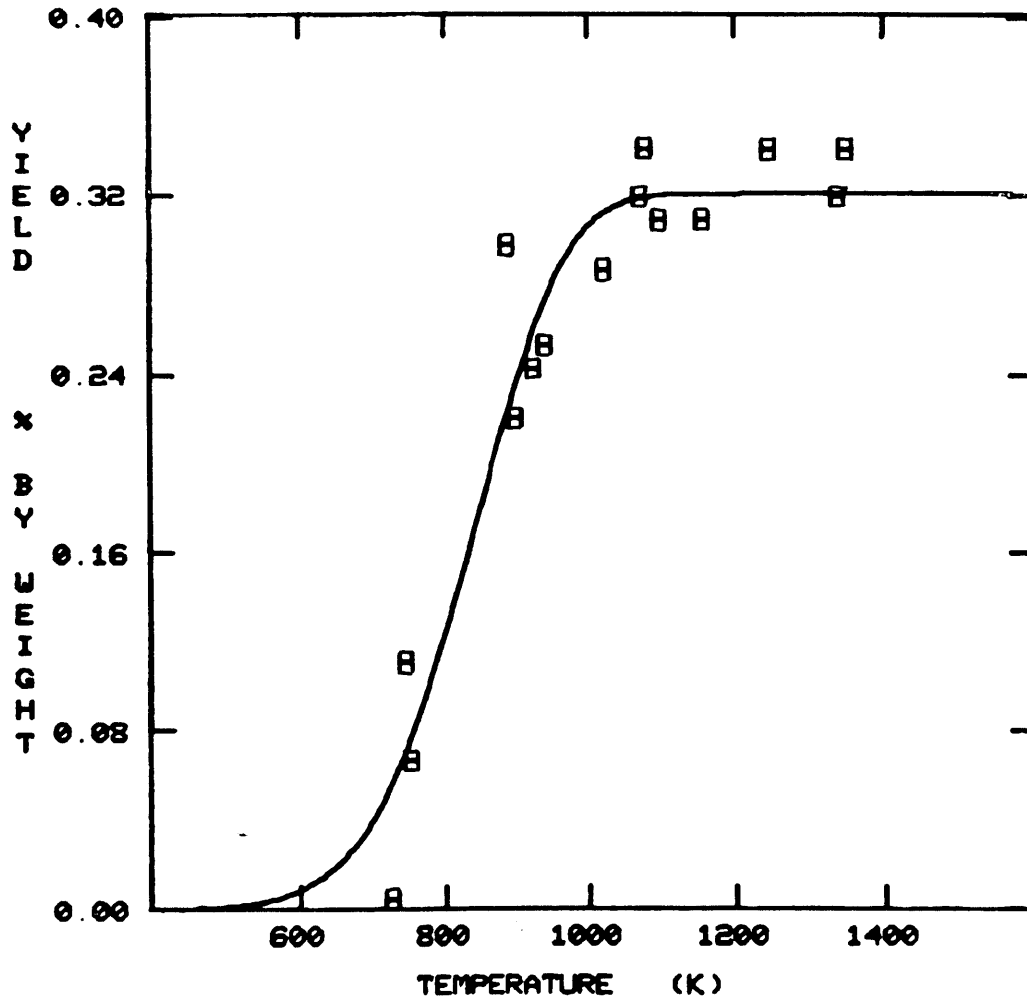
Fig. 4.3-9 Ethanol yield from sweet gum
xylan pyrolysis.
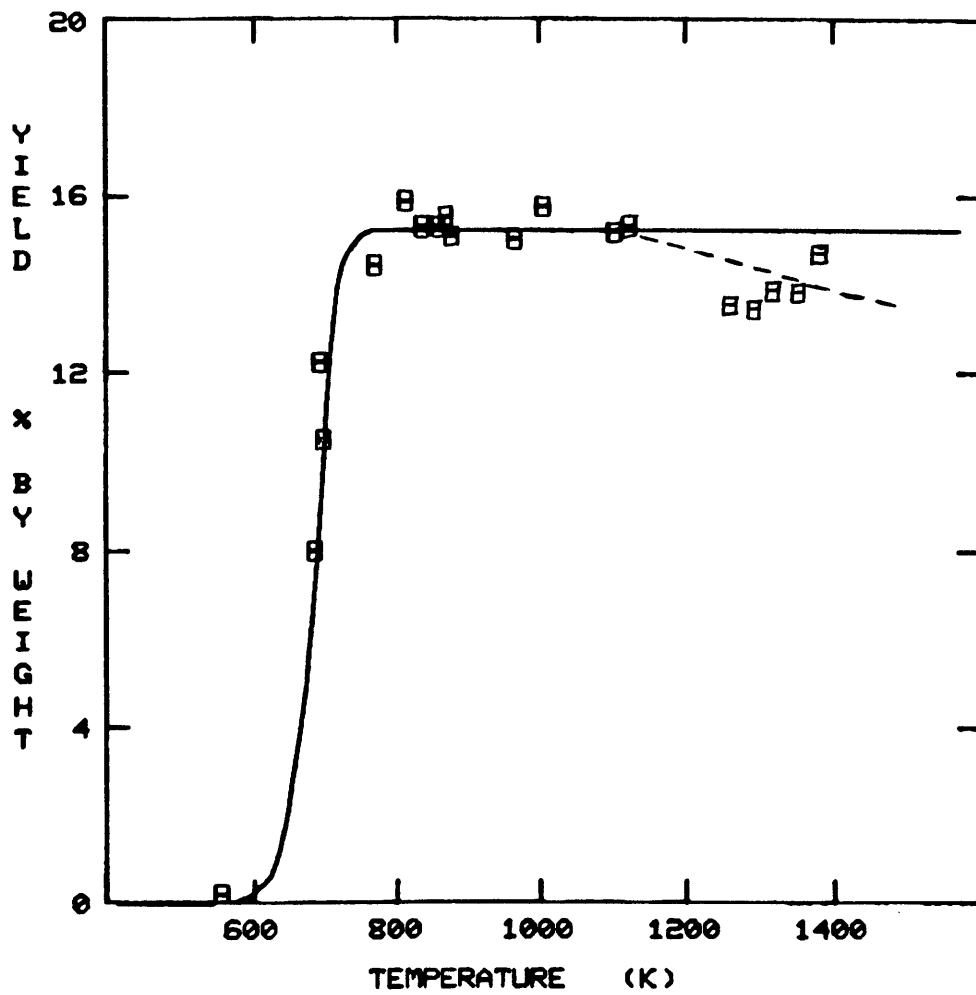
Fig. 4.3-10   Carbon dioxide yield from
                sweet gum xylan pyrolysis.
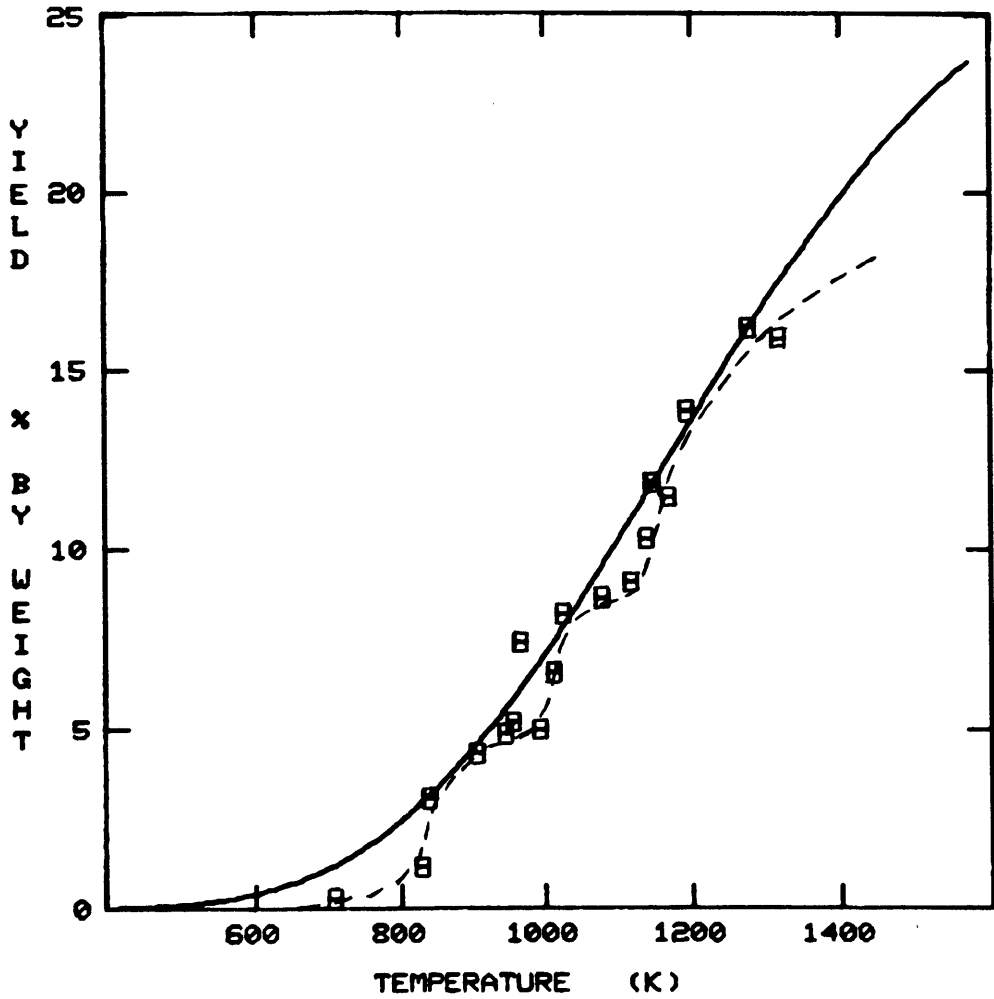
Fig. 4.3-11 Carbon monoxide yield from
sweet gum xylan pyrolysis.

4.3-13. Step 3 could not be independently fitted due to the paucity

of high temperature data. The sum of the ultimate yields for carbon

monoxide's three steps is 17.3 wt% which is in much closer agreement

with experiment.

Table 4.3-1 lists the activation energies (E^*), Arrhenius

preexponential factors $(\log_{10} k)$, ultimate yields (V^*) and the

standard errors of estimate from POWELL's regressions for all

gaseous compounds from sweet gum xylan pyrolysis.

In addition to modelling yields of individual gases, the global

weight loss, total gas yield and tar yields were also separately

fitted for best values of E^*, $\log_{10} k$ and V^*. Figs. 4.3-14 through

4.3-16 respectively show the modelled curves for these three "products".

Though the single reaction first order decomposition model cannot

predict a peak in a product's yield, methanol, acetaldehyde, water

and tar yields, which all show a peak, were fitted by the model

strictly for comparison with Hajaligol's (1980) and Nunn's (1981)

data.

4.4 Comparison of Cellulose with Hemicellulose

Before proceeding with a discussion of the simulation of wood

(section 4.5), it is instructive to compare the pyrolysis behavior of

the two largest wood constituents: cellulose and hemicellulose. When

this simulation was first attempted by Nunn (1981), it was postulated,

in the absence of data for the pyrolysis of hemicellulose, that
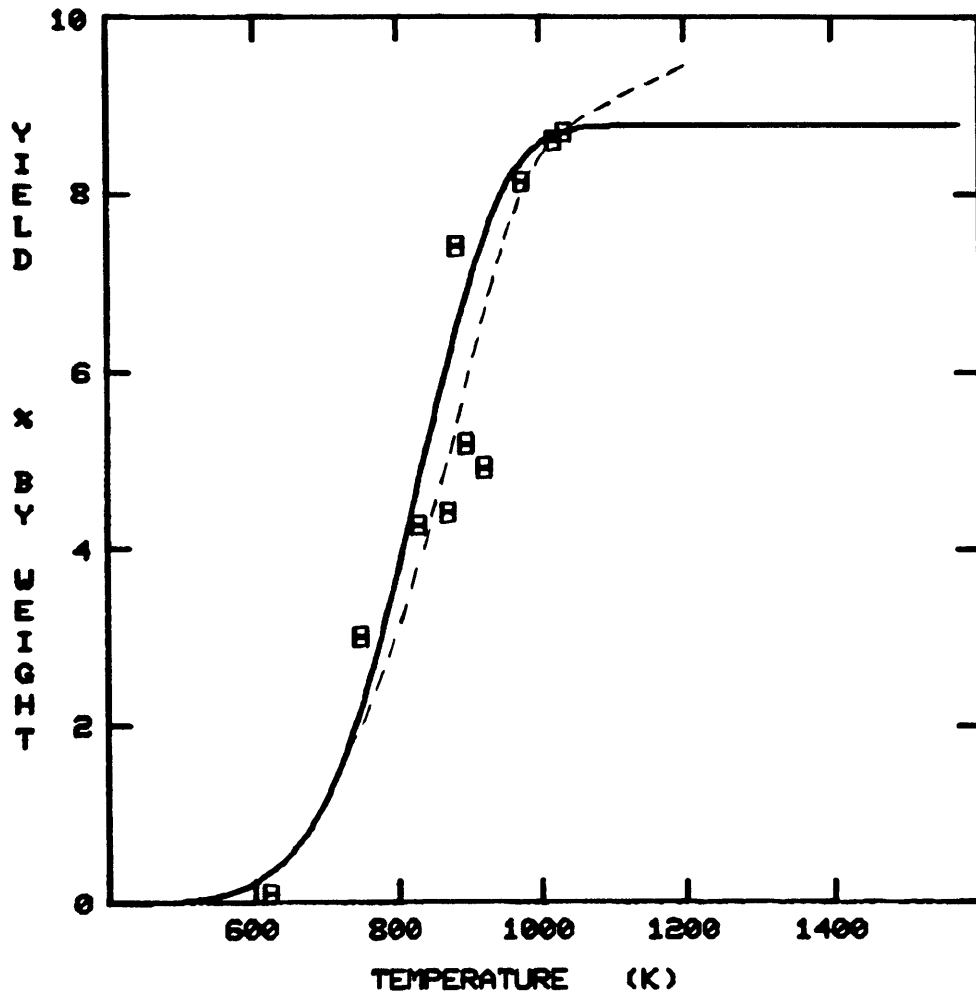
Fig. 4.3-12 Carbon monoxide yield (Step 1).
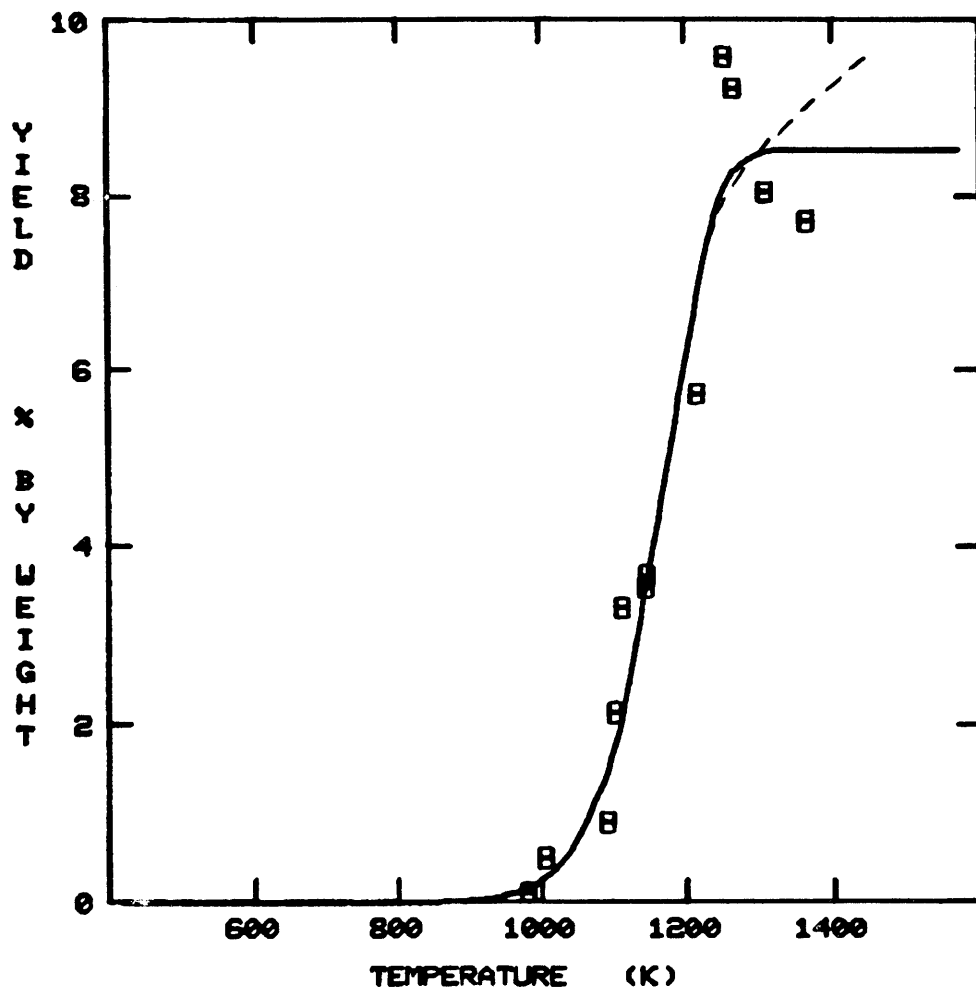
Fig. 4.3-13 Carbon monoxide yield (Step 2).

Table 4.3-1   Kinetic parameters for pyrolysis of sweet gum xylan [a]

Product	E (kcal/g-mol)	$\log_{10}k$ ($k = sec^{-1}$)	V* (wt. %)	Standard error of estimate (wt. %) [d]
Weight loss	12.8 ± 1.0	4.1 ± 0.4	83.6 ± 0.5	2.1
Tar	29.0 ± 8.0	10. ± 3.0	35.8 ± 0.8	3.9
Gas	11.7 ± 3.5	3.7 ± 1.0	38.0 ± 1.0	4.1
CH_4	12.0 ± 2.0	2.3 ± 0.5	1.1 ± 0.1	0.009
CO_2	36.0 ± 4.0	12. ± 1.0	15.2 ± 0.2	0.66
CO [b]	6.0 ± 2.0	0.8 ± 1.0	27.0 ± 21.	2.0
H_2O	29.0 ± 19.	9.0 ± 6.0	5.2 ± 0.2	0.67
HCHO	14.0 ± 6.0	4.0 ± 2.0	0.12 ± 0.01	0.027
C_3H_6	25.0 ± 4.0	6.0 ± 1.0	0.32 ± 0.006	0.002
CH_3OH	14.0 ± 8.0	5.0 ± 3.0	1.62 ± 0.04	0.16
CH_3CHO	17.0 ± 7.0	5.0 ± 2.0	1.12 ± 0.05	0.18
CH_3CH_2OH	12.0 ± 2.0	3.1 ± 0.6	0.32 ± 0.01	0.003
C_2H_4	21.0 ± 3.0	4.8 ± 0.7	0.42 ± 0.02	0.003
C_2H_6	21.0 ± 4.0	5.0 ± 1.0	0.12 ± 0.004	0.001
CO (step 1) [c]	12.0 ± 8.0	3.0 ± 3.0	8.81 ± 0.02	0.23
CO (steps 2 + 3) [c]	41.0 ± 8.0	8.0 ± 2.0	8.5 ± 0.5	0.53

[a] Data presented as : "best fit value ± one standard deviation of fit value"

[b] Single reaction model

[c] Step-wise model involving 3 independent reactions

[d] Defined as :

$$\sqrt{\sum_{j=1}^{n} (V_{j,model} - V_{j,exp.})^2 / (n-3)} \quad ; n \quad \text{data points.}$$
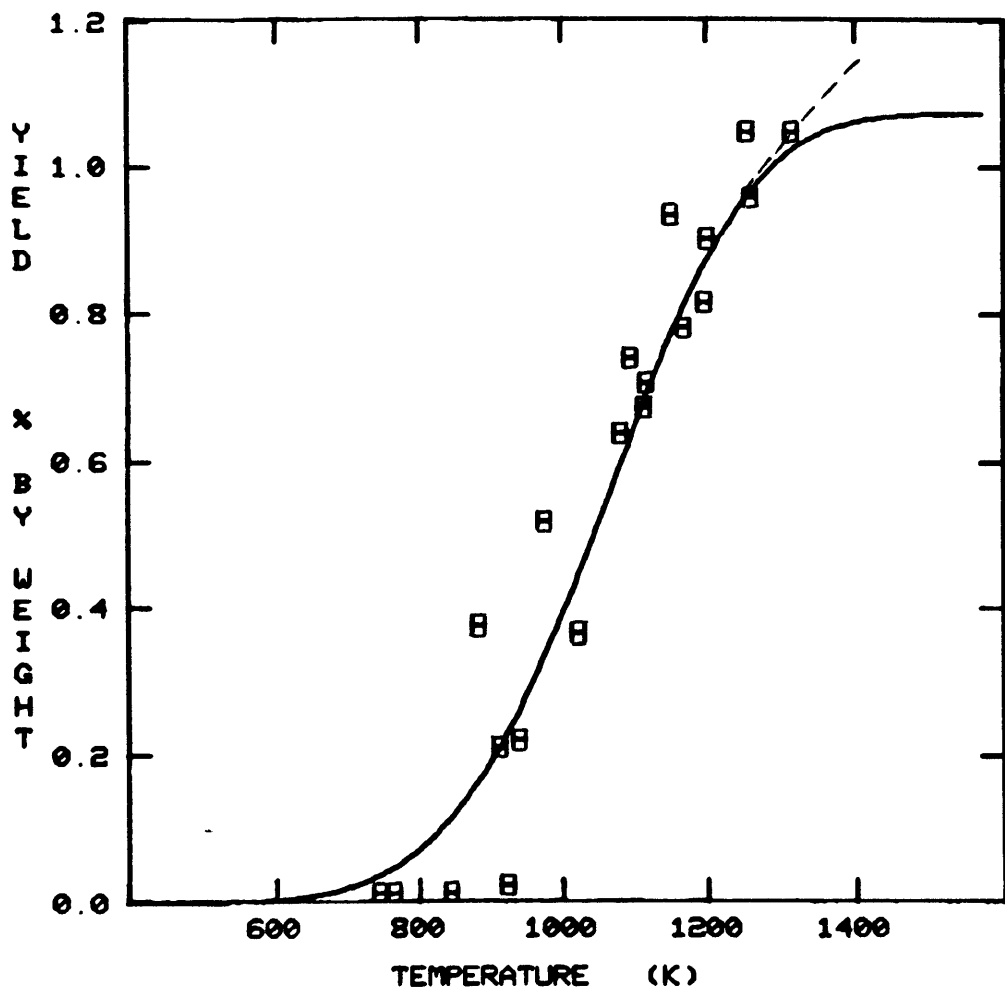
62
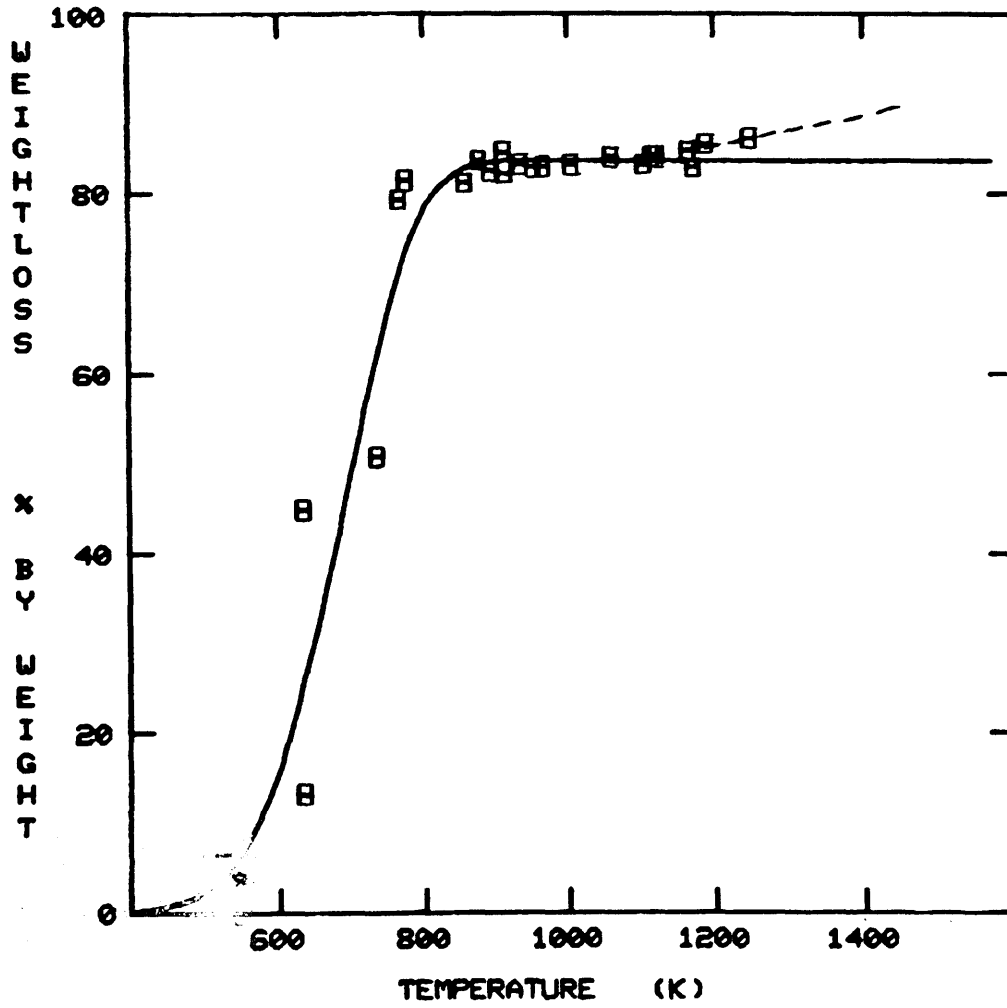
Fig. 4.3-14   Weight loss from sweet gum
xylan pyrolysis.
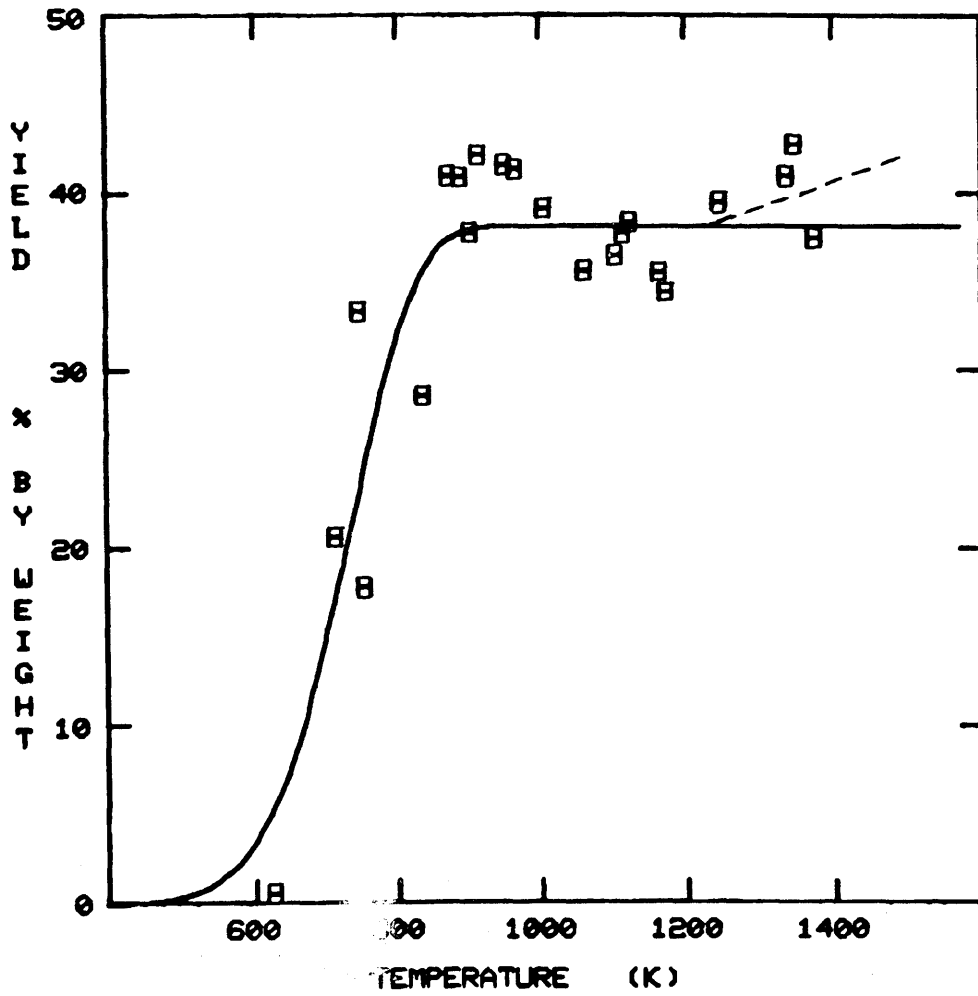
Fig. 4.3-15   Total gas yield from sweet
gum xylan pyrolysis.
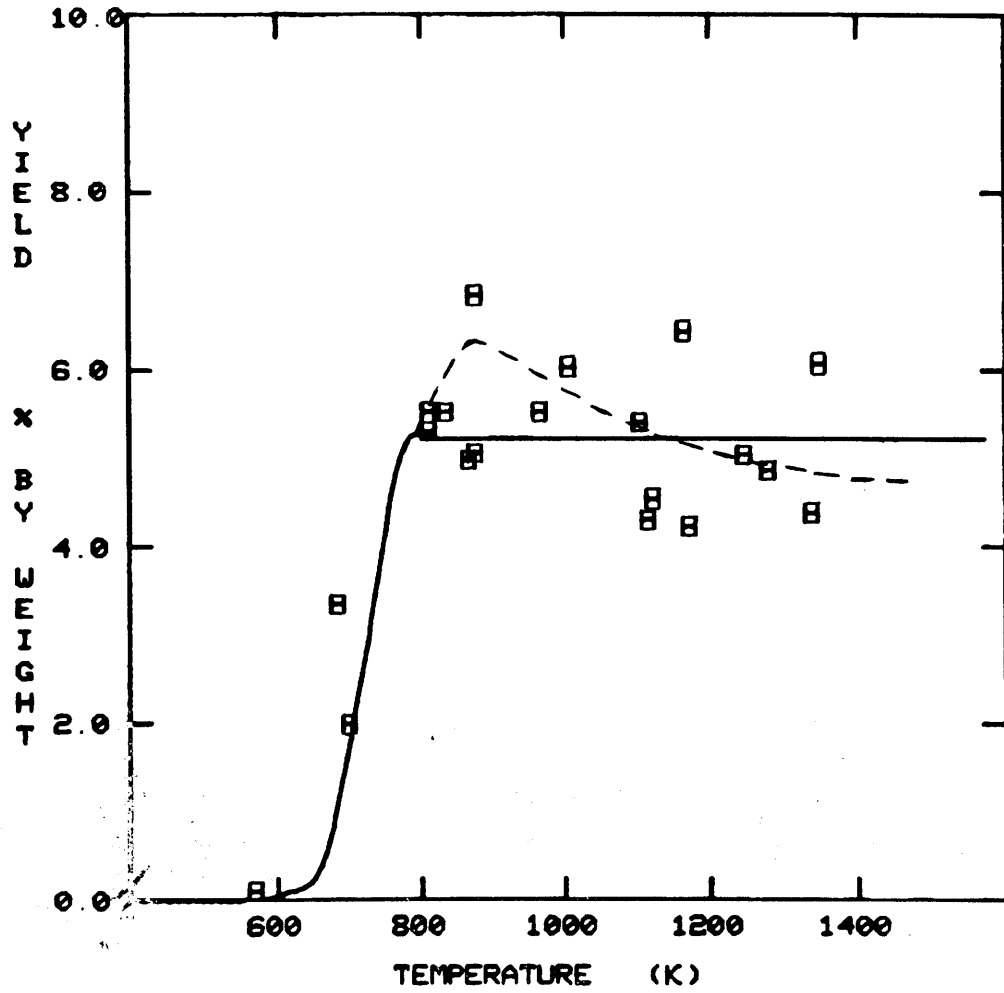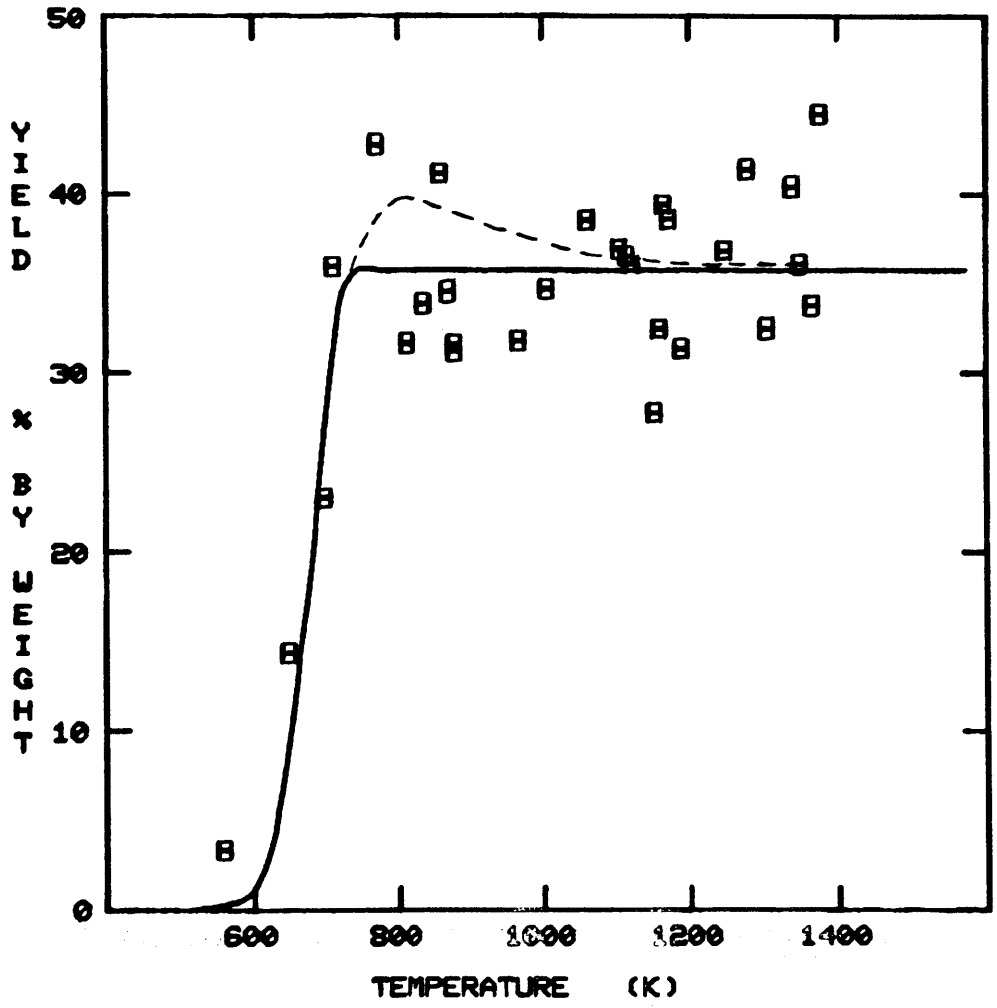
Fig. 4.3-16 Tar yield from sweet gum
xylan pyrolysis.

cellulose and hemicellulose behaved similarly. The following is meant to provide a picture of the accuracies and inaccuracies of that hypothesis.

Fig. 4.4-1 indicates that the initial rate of methane production is greater for sweet gum xylan than for filter paper cellulose at least for temperatures between 700K and 950K. However, the increase in methane production thereafter is 2.5 times greater for cellulose. Both compounds reach their ultimate yields: 2.6 wt% for cellulose, 1.1 wt% for xylan by 1300K.

While it is not clear whether ethylene formation from xylan occurs at a lower temperature than the same from cellulose (see Figs. 4.4-2 and 4.4-3), ethane is produced from xylan at a noticeably lower temperature. The ultimate yield of ethylene is achieved for both species around 1150K (2.1 wt% for cellulose versus only 0.44 wt% for xylan). However, ethane production is initially more rapid for xylan: 0.12 wt% by 1000K; the yield from cellulose reaches 0.25 wt% at a significantly higher temperature of 1150K.

At temperatures below 800K, xylan evolves chemical water more readily than cellulose as shown in Fig. 4.4-4. In fact, water production from xylan ceases before 30% of the ultimate water yield from cellulose is attained. In order to compare xylan data with comparable cellulose data, the yields of water and formaldehyde had to be combined because individual water and formaldehyde data are not available for cellulose. However, the yield of formaldehyde is so small for both species (c.f. 0.11 wt% from xylan) that the curves can be considered to
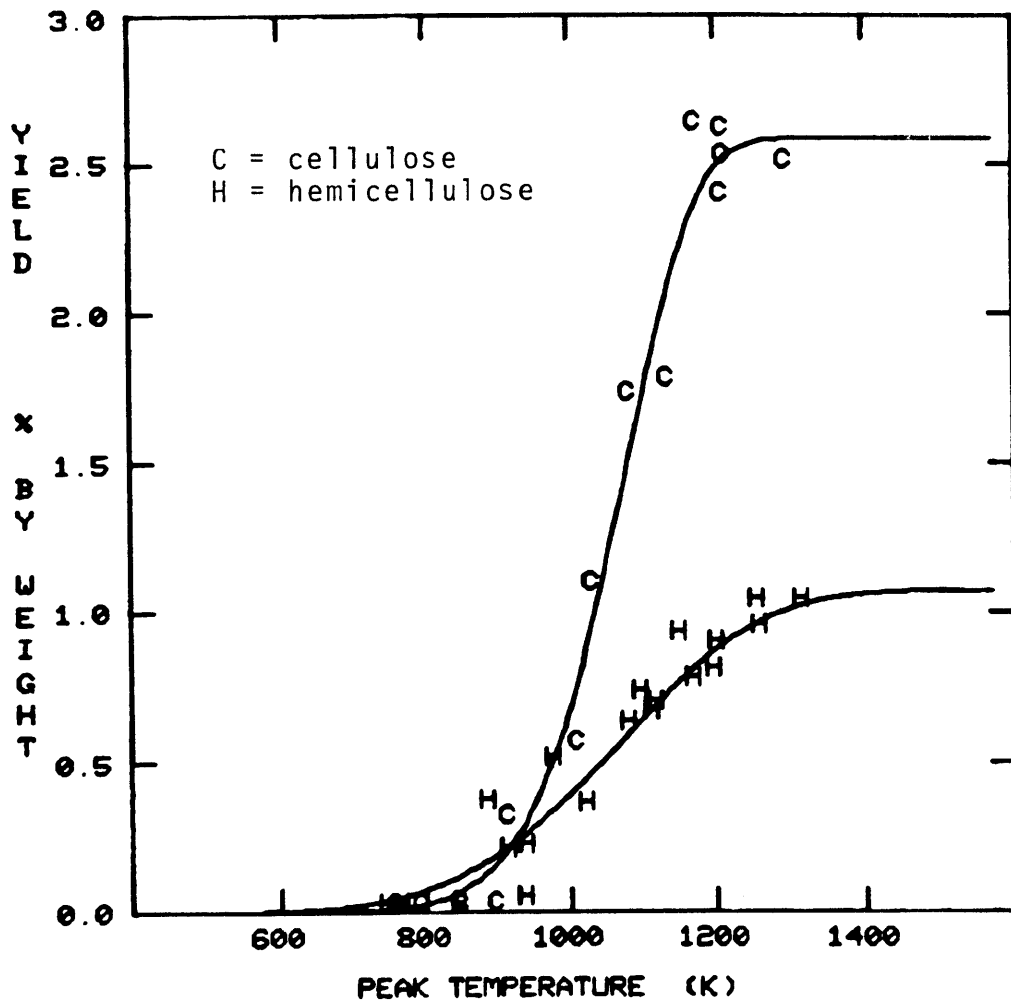
Fig. 4.4-1 Comparison of methane yields
from filter paper cellulose
and xylan.
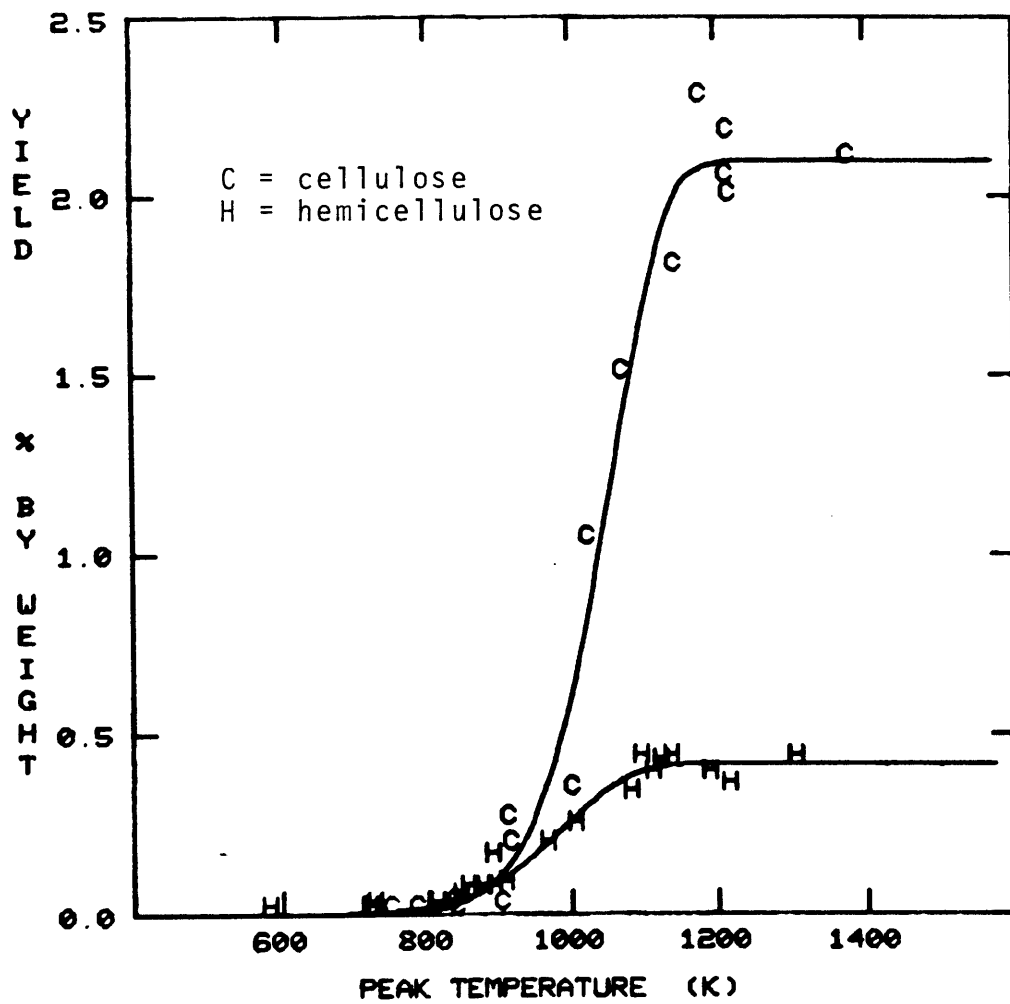
Fig. 4.4-2   Comparison of ethylene yields
from filter paper cellulose
and xylan.

68
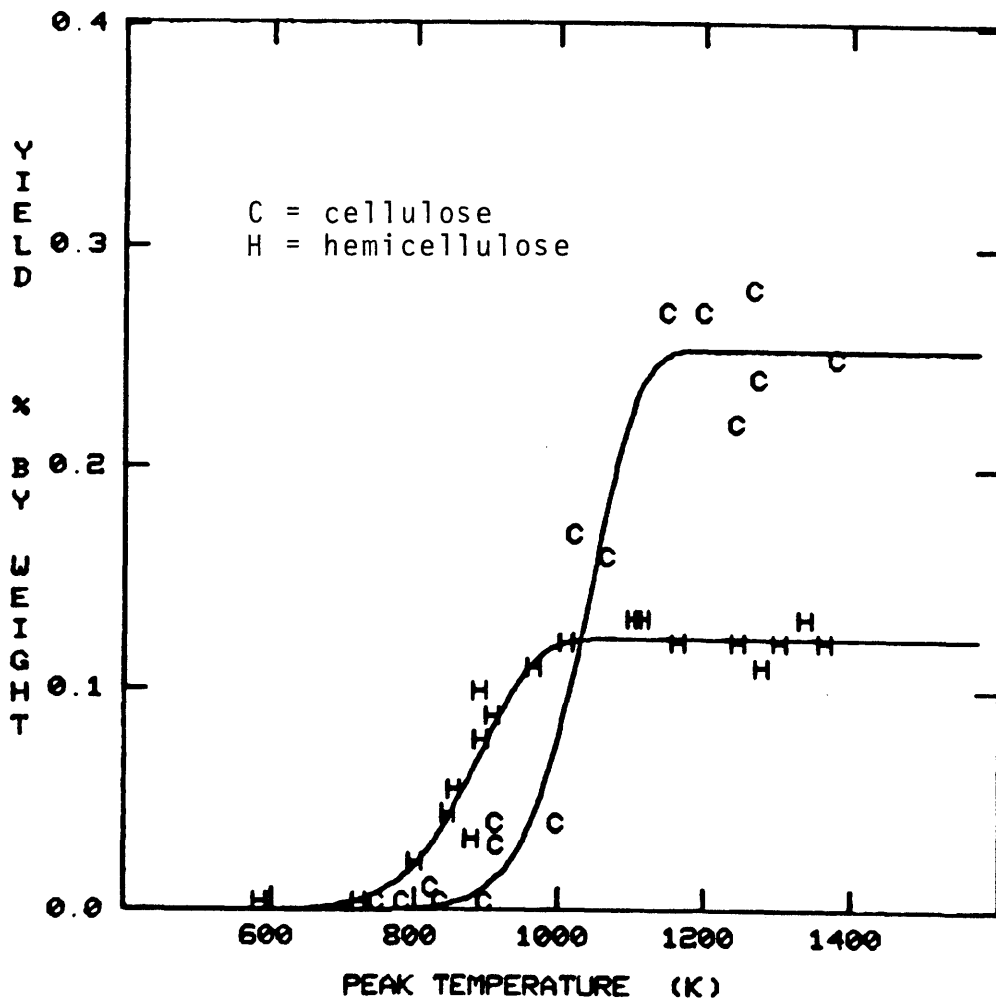
Fig. 4.4-3   Comparison of ethane yields
from filter paper cellulose
and xylan.
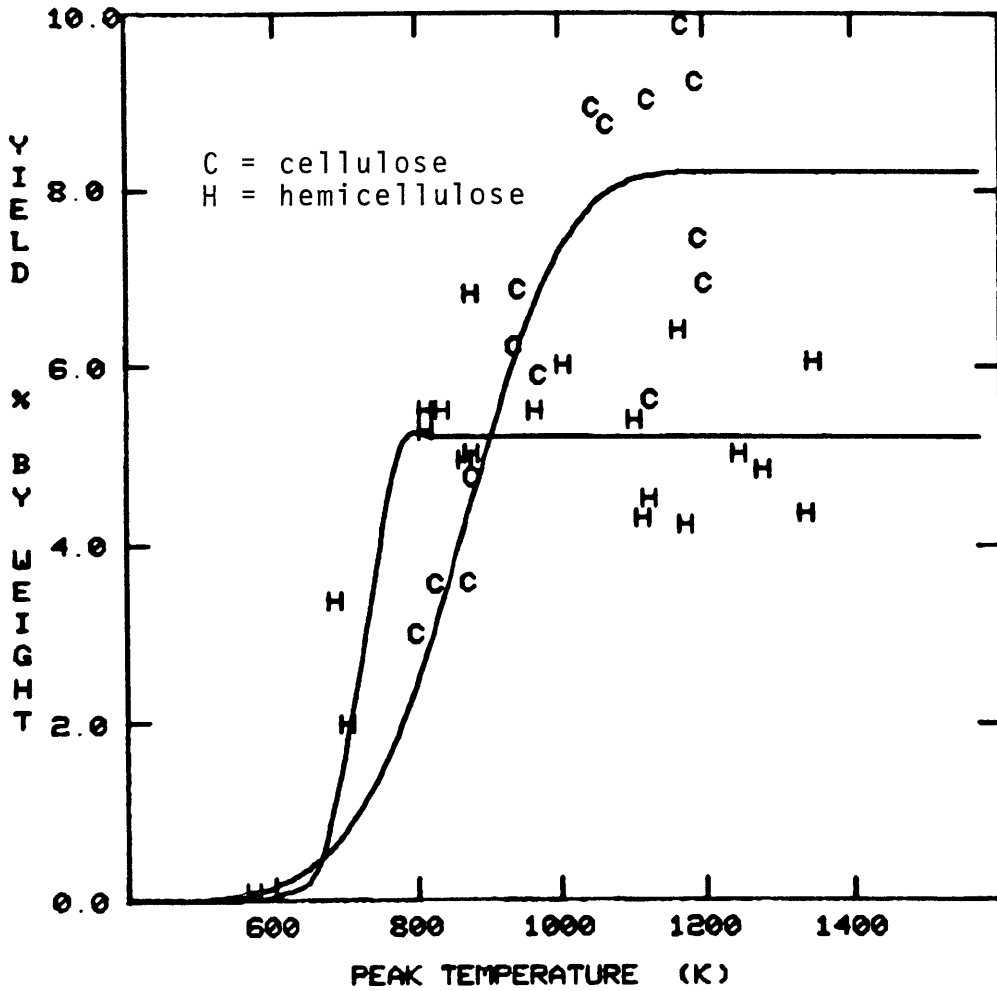
Fig. 4.4-4   Comparison of water + formaldehyde
             yields from filter paper cellulose
             and xylan.

represent only the water yields without significant loss in accuracy.

As for the light hydrocarbon gases discussed previously, propylene is generated starting at a lower temperature for xylan than for cellulose. Yet, both reach their ultimate yields by 1000K. The ultimate yield from cellulose is twice that from xylan. Fig. 4.4-5 presents these results.

The general trend found for light hydrocarbons, i.e. their evolution at lower temperatures from xylan than from cellulose is also true of carbon monoxide, although its rate of production from xylan is not quite so fast as it is from cellulose. This is shown in Fig. 4.4-6. Carbon dioxide yield on the other hand (Fig. 4.4-7) is more closely like that of water because its production from xylan is complete before any is evolved from cellulose. Carbon dioxide and water are the only compounds which are produced in significant quantities both at a lower temperature and a faster rate from xylan than cellulose.

In conclusion, as might be expected from the differing structural conformations for celluloses and hemicelluloses, their pyrolytic behavior is dissimilar. Even with regard to weight loss and total gas production, shown in Figs. 4.4-8 and 4.4-9 respectively, filter paper cellulose and sweet gum xylan behave differently. Thus, the wood simulation model used by Nunn (1981) must be revised in the light of these new findings, and especially the fact that xylan is much more reactive than is cellulose.
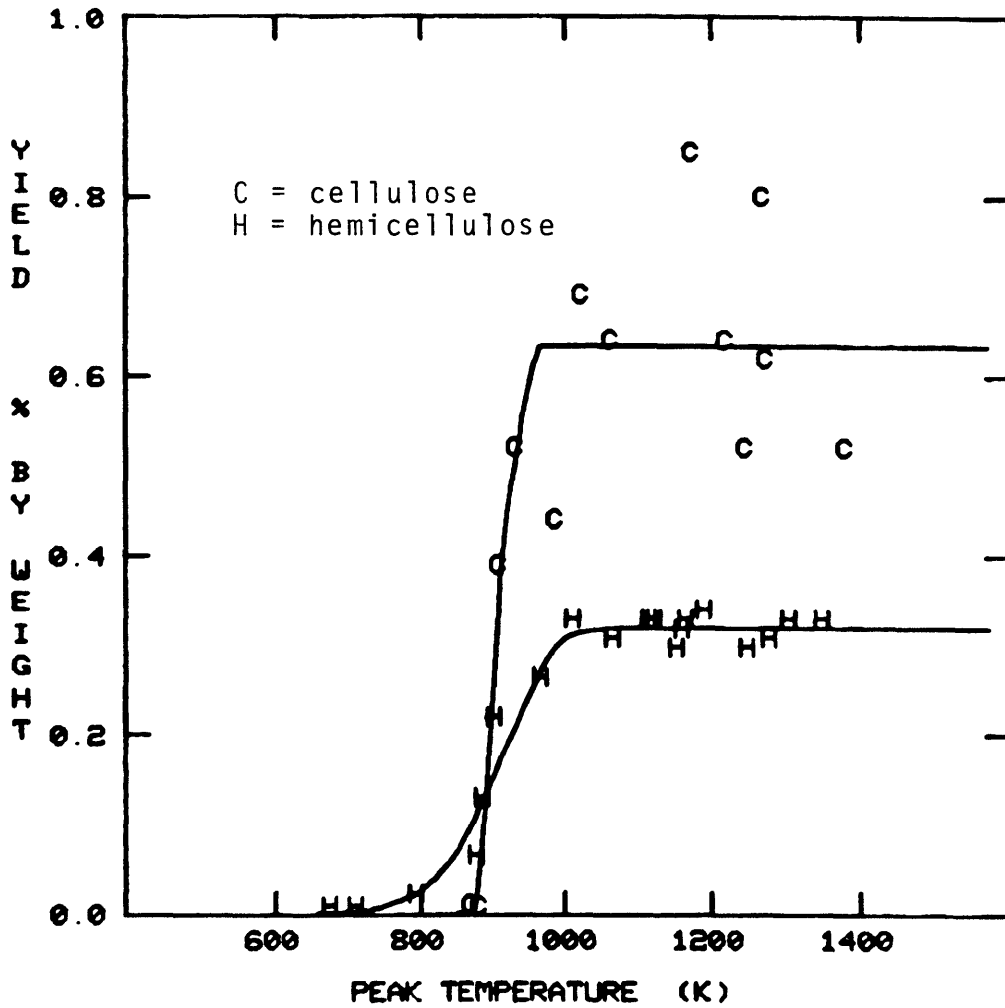
Fig. 4.4-5   Comparison of propylene yields
             from filter paper cellulose
             and xylan.

72
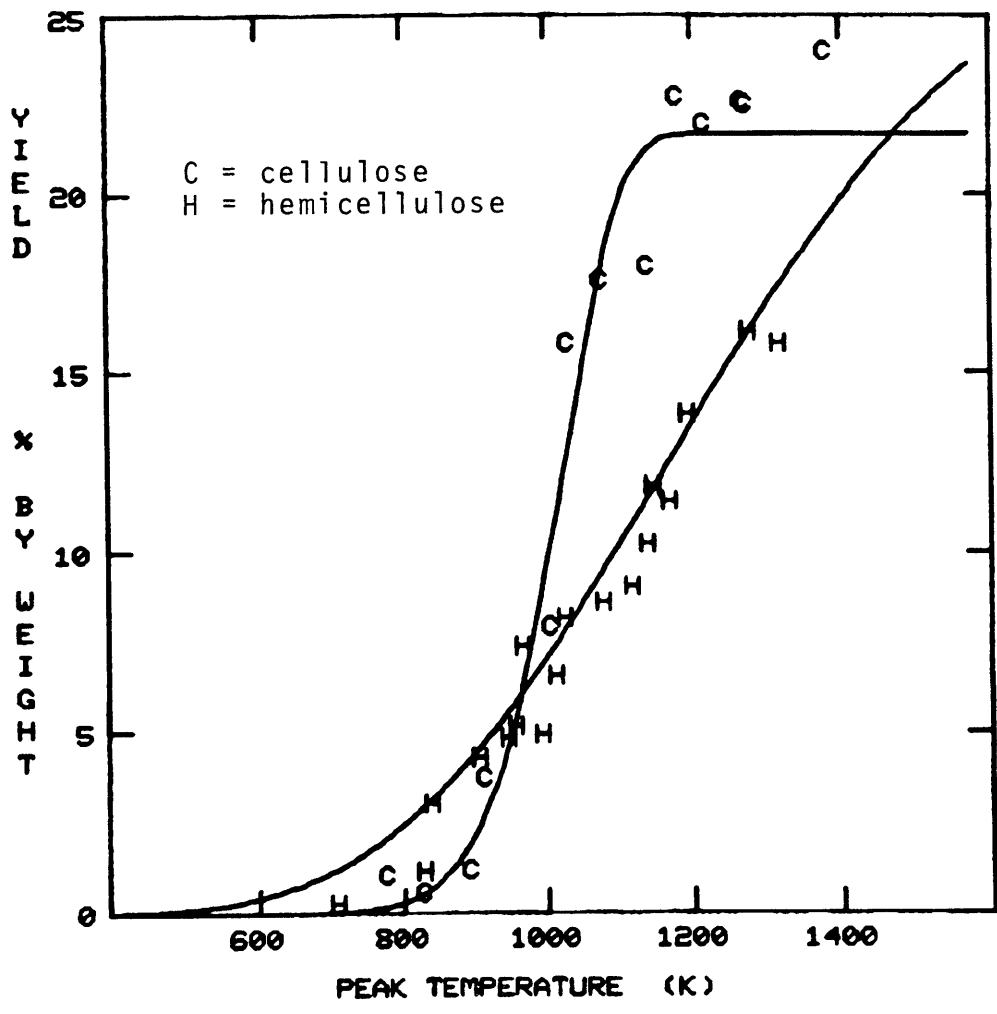
Fig. 4.4-6   Comparison of carbon monoxide
             yields from filter paper
             cellulose and xylan.
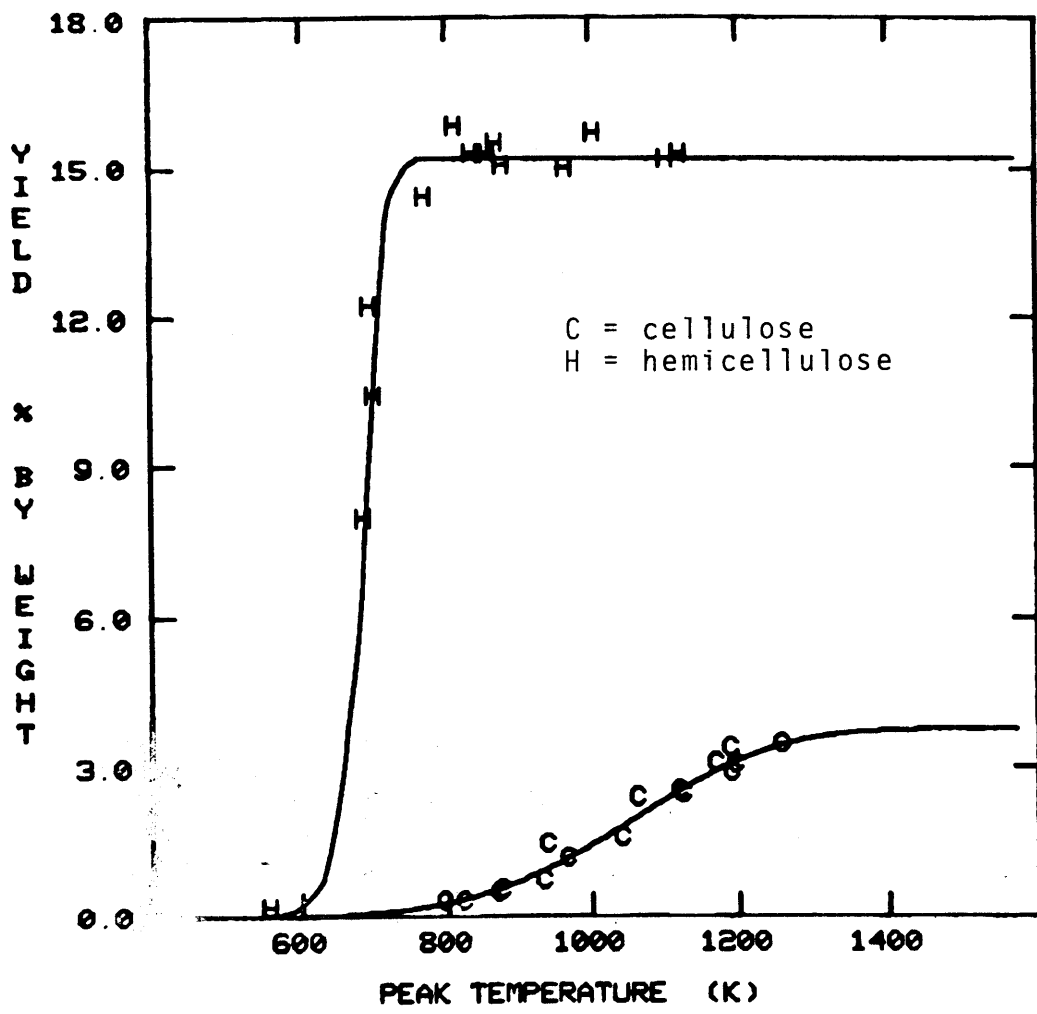
Fig. 4.4-7   Comparison of carbon dioxide
            yields from filter paper
            cellulose and xylan.
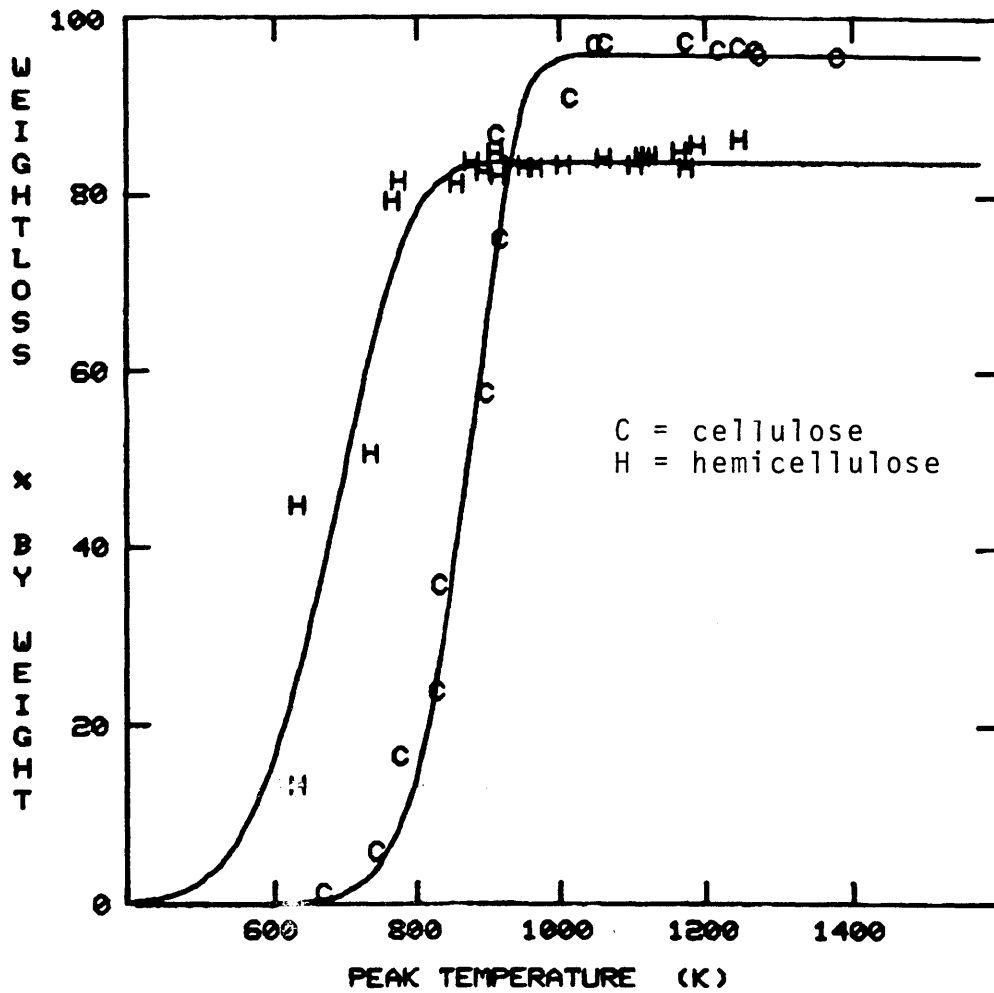
Fig. 4.4-8   Comparison of weight loss from
              filter paper cellulose and
              xylan.
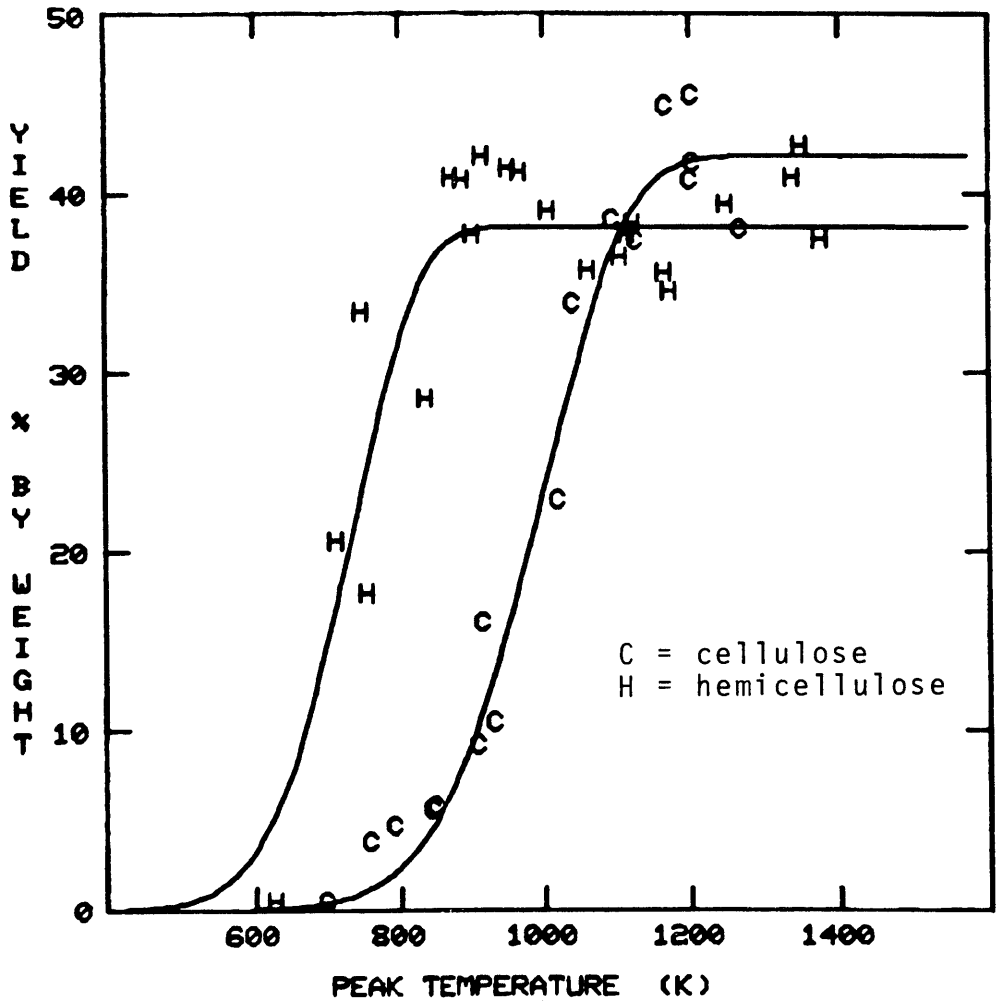
Fig. 4.4-9   Comparison of total gas yields
from filter paper cellulose
and xylan.

4.5 Simulation of Wood

An assessment of the extent to which the rapid pyrolysis of wood can be simulated from comparable information on its constituents is one of the primary objectives of this research. The simulation algorithm to be tested assumes that the yield of each pyrolysis product from wood is given by the sum of the yield of this product from each of its three major constituents (cellulose, hemicellulose and lignin) each weighted by the weight fraction of that constituent in the parent wood. For sweet gum hardwood, the fractional composition was taken to be 42.5 wt% cellulose, 30.6 wt% hemicellulose and 26.9 wt% lignin based on information from Andrews (1980).

The equations describing the simulation follow. The simulated integral yield of product i

$$Y_i(g(t)) = \sum_{j=1}^{3} W_j Y_{i,j}(g(t))$$

where

W_j = weight fraction of constituent j in wood

$Y_{i,j}$ = integral yield of product i from pyrolysis of constituent j in wood

$g(t)$ = the temperature-time history of the pyrolysis sample

As mentioned, the values for W_j were obtained from Andrews (1980). The values of $Y(g(t))$ for cellulose were taken from Hajaligol's (1980) study on No. 507 filter paper; the corresponding data for lignin were from Nunn's (1981) work on lignin pyrolysis while the hemicellulose (xylan) $Y(g(t))$ was generated by this research.

77

Figs. 4.5-1(a) through 4.5-7(a) show the experimental data for

individual product gases from sweet gum wood pyrolysis (Nunn, 1981),

and compare the curves fitted to them with the curves obtained from

the simulation (shown by the dotted lines). Side by side, Figs.

4.5-1(b) through 4.5-7(b) present the identical data which Nunn (1981)

obtained along with his simulation for wood which assumed wood was

73.1 wt% cellulose and 26.9 wt% lignin. In the absence of data on

hemicellulose, Nunn had assumed cellulose and hemicellulose behaved

identically.

The individual product gases whose yields are better simulated

by the current work than by Nunn's simulation include methane,

ethylene, ethane and propylene (Figs. 4.5-1 through 4.5-4). The

most noticeable improvement arises due to the closer fit provided

in the plateau or ultimate yield region at high peak temperatures.

Although the present simulation overpredicts the ultimate yields

for these four specific compounds, the simulated curves remain within

the scatter of experimental data from wood pyrolysis, and are superior

to Nunn's simulation which overshot the data by a substantially

greater amount.

The corresponding pair of simulations shown in Fig. 4.5-5(a)

and (b) for carbon monoxide show no great differences between each

other. Nunn's simulation and the simulation from this study do an

almost identical job, but do not accurately model wood's behavior for

carbon monoxide evolution. The same is not true for water and

formaldehyde production; while both simulation curves (Figs. 4.5-6(a,b))
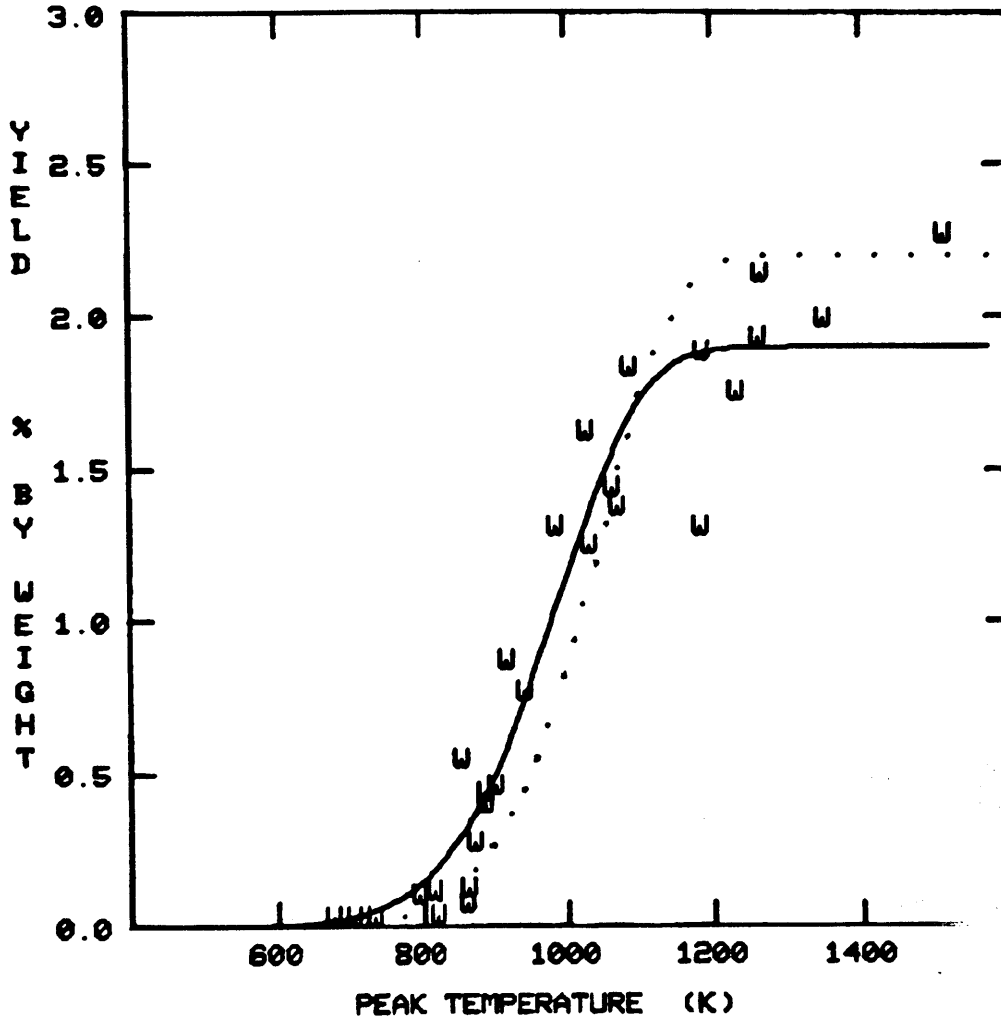
Fig. 4.5-1(a) Modelled fit to data compared
              with simulation (dotted) for
              methane yield from wood pyrolysis.
              (W's are experimental data)
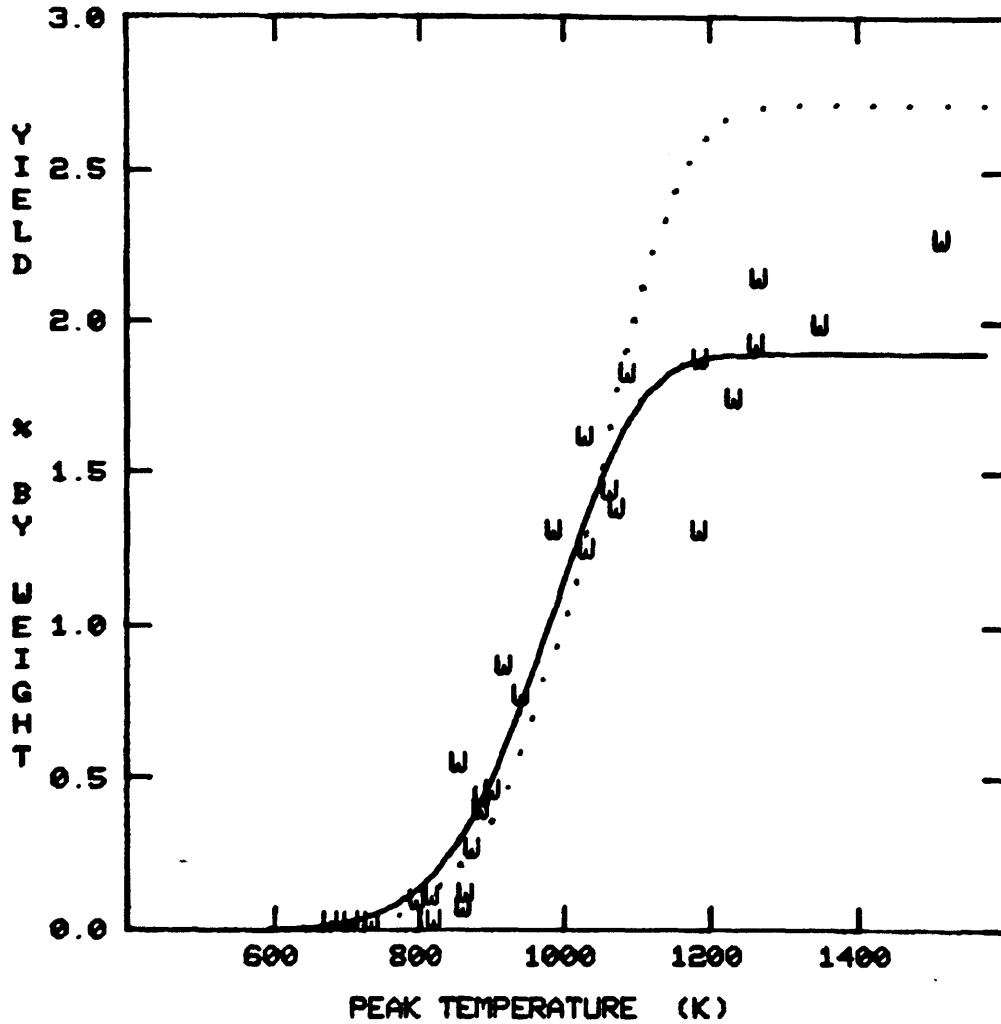
Fig. 4.5-1(b)   Modelled fit to data compared
                with simulation for methane
                yield from wood pyrolysis.
                (Nunn, 1981)
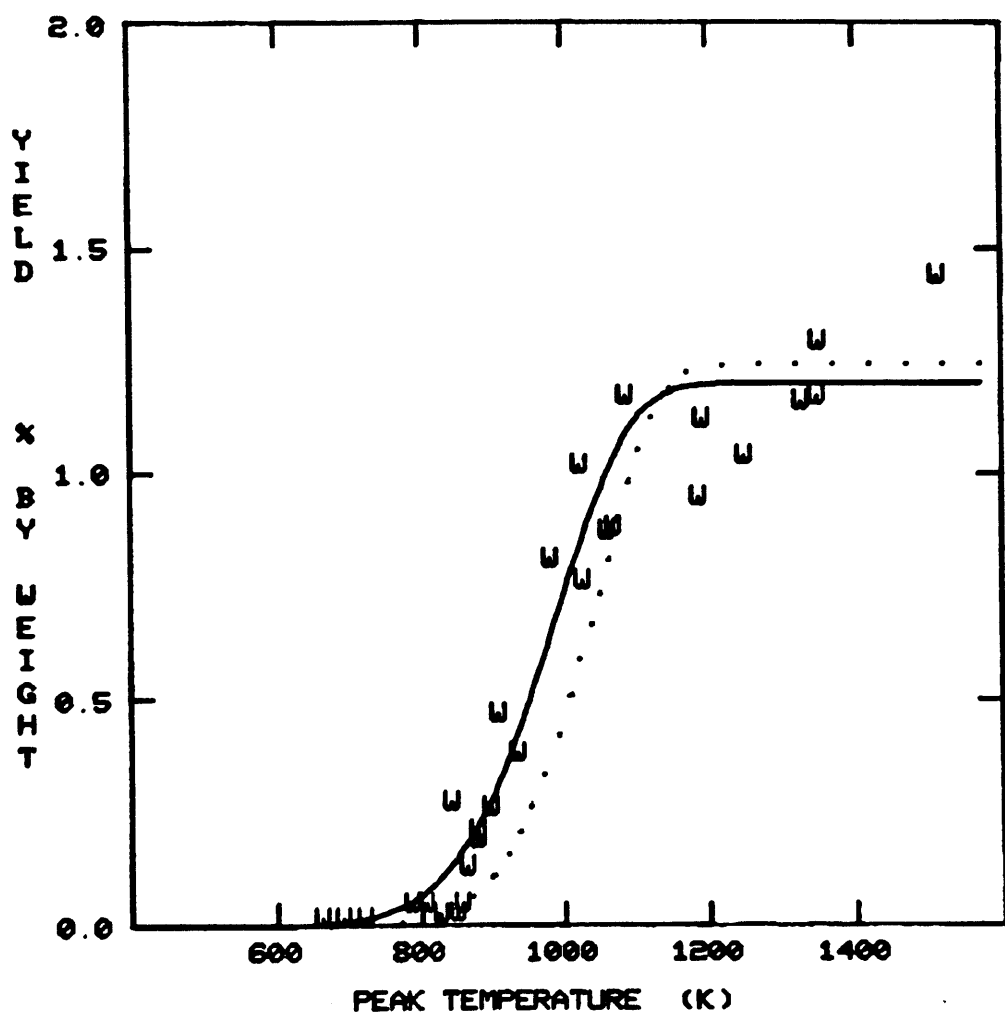
Fig. 4.5-2(a)   Modelled fit to data compared
                with simulation for ethylene
                yield from wood pyrolysis.
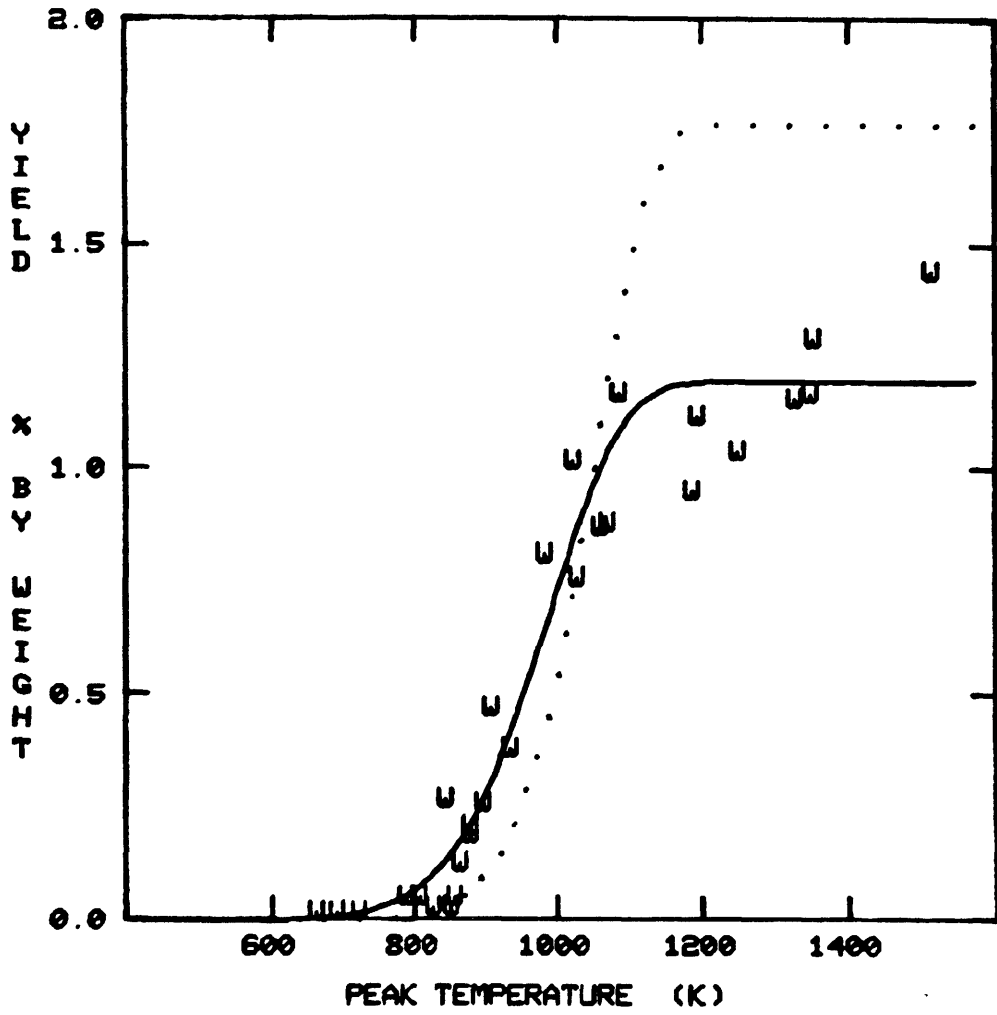
Fig. 4.5-2(b) Modelled fit to data compared
with simulation for ethylene
yield from wood pyrolysis.
(Nunn, 1981)
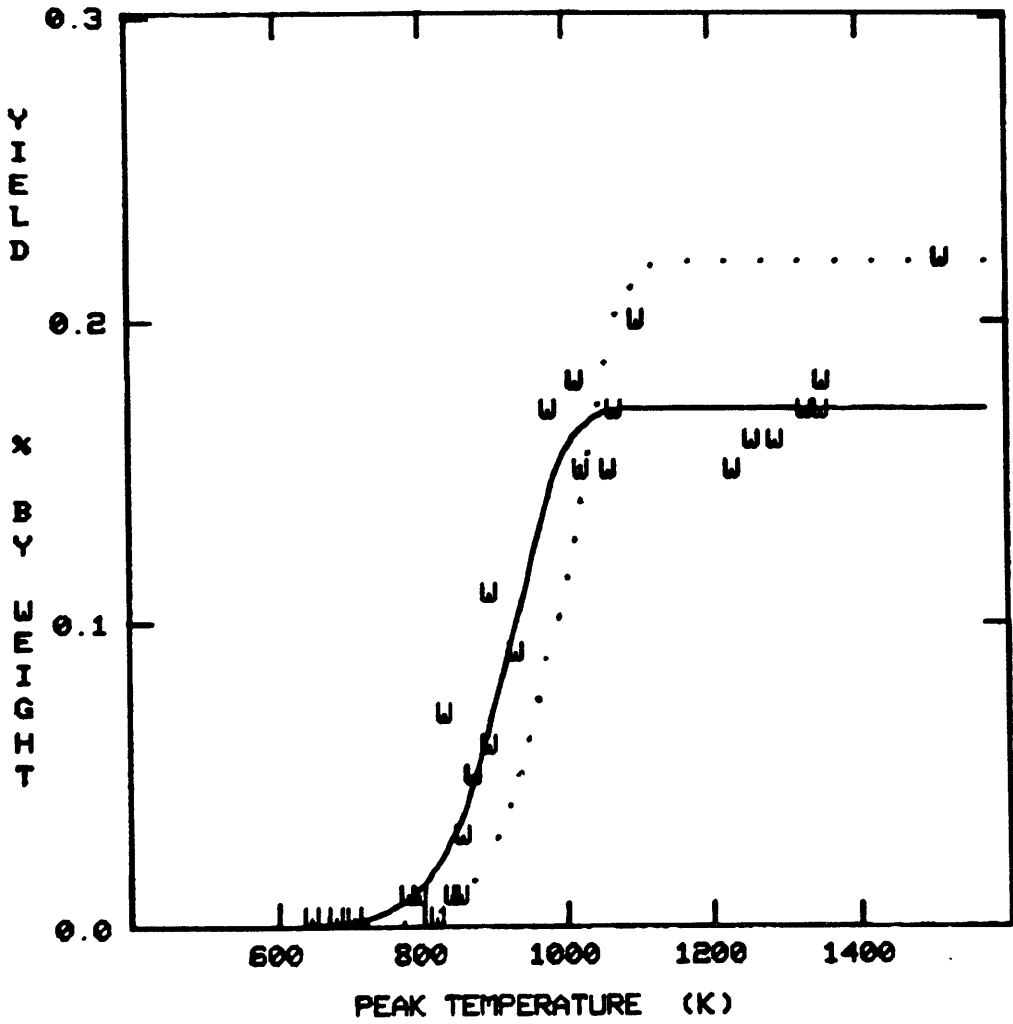
Fig. 4.5-3(a) Modelled fit to data compared
with simulation for ethane
yield from wood pyrolysis.

83
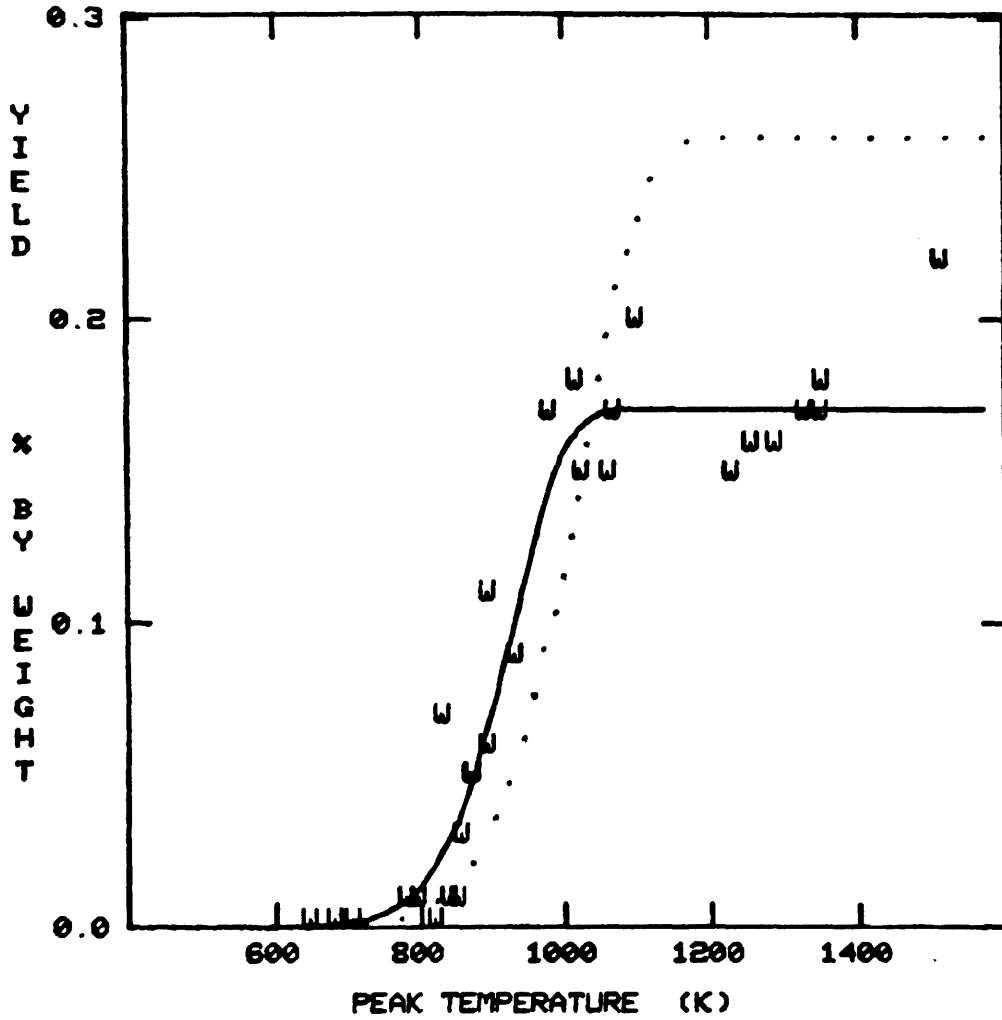
Fig. 4.5-3(b) Modelled fit to data compared
with simulation for ethane
yield from wood pyrolysis.
(Nunn, 1981)

84
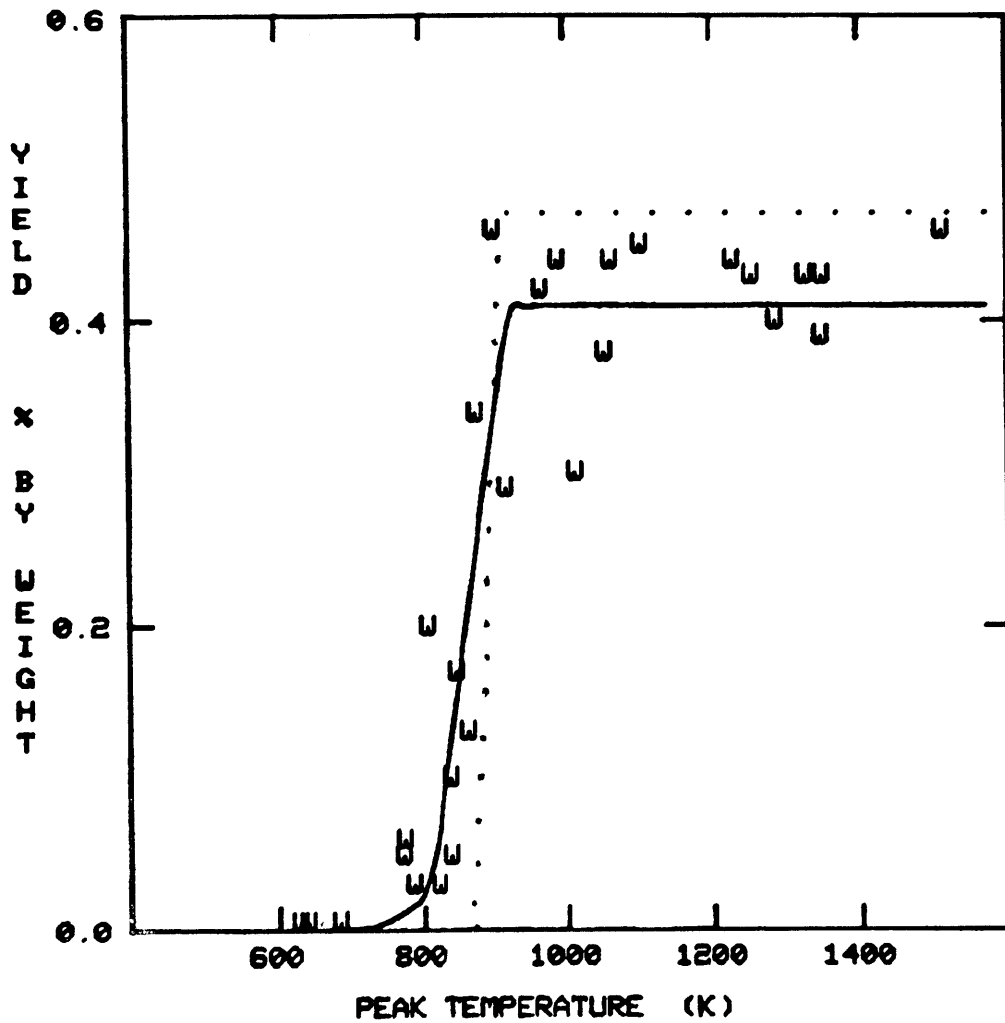
Fig. 4.5-4(a) Modelled fit to data compared
with simulation for propylene
yield from wood pyrolysis.
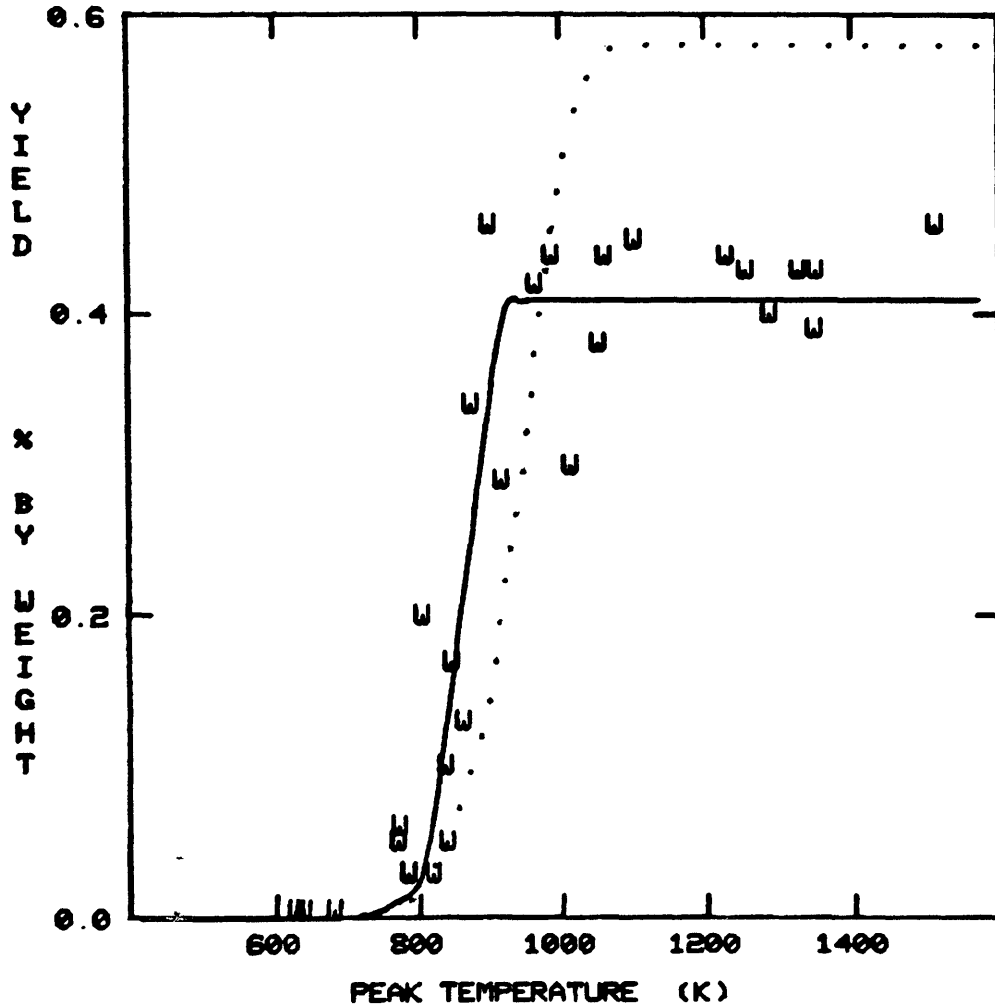
Fig. 4.5-4(b)   Modelled fit to data compared
                with simulation for propylene
                yield from wood pyrolysis.
                (Nunn, 1981)
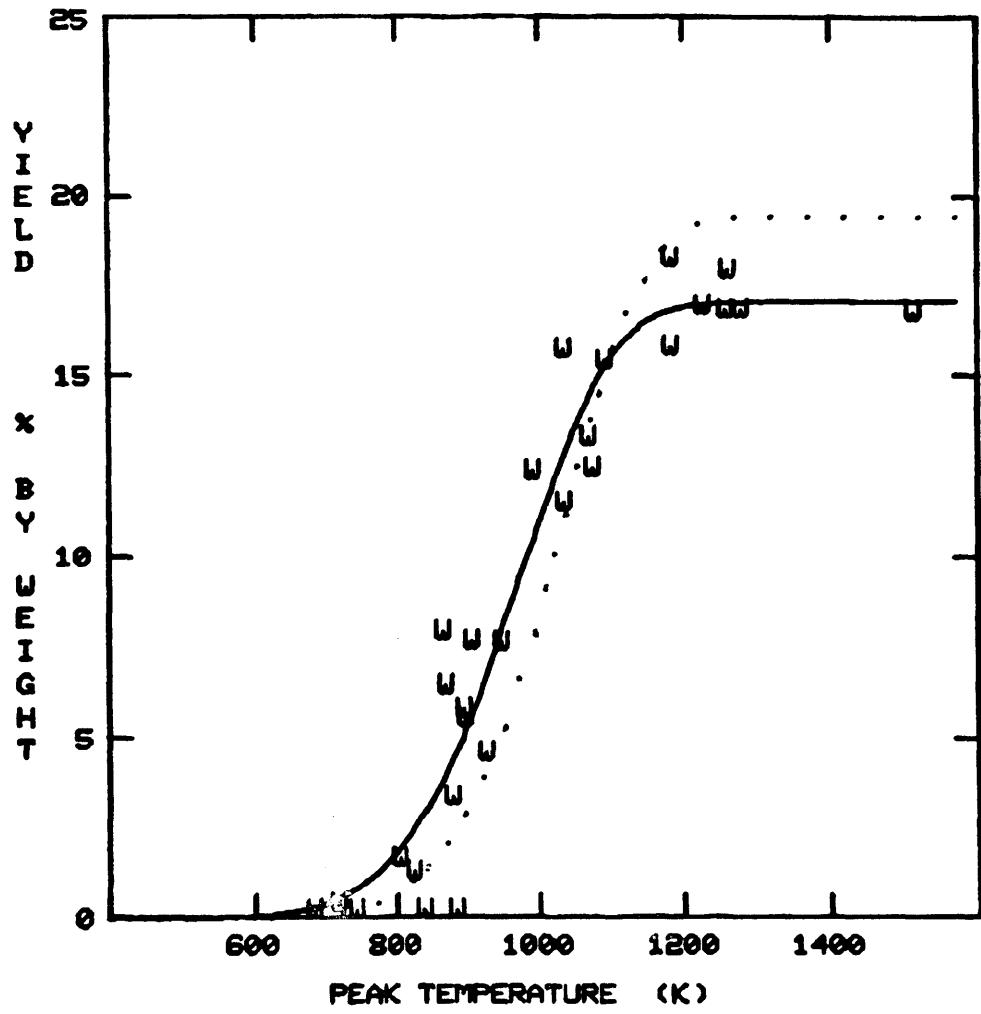
Fig. 4.5-5(a) Modelled fit to data compared
with simulation for carbon
monoxide yield from wood pyrolysis.
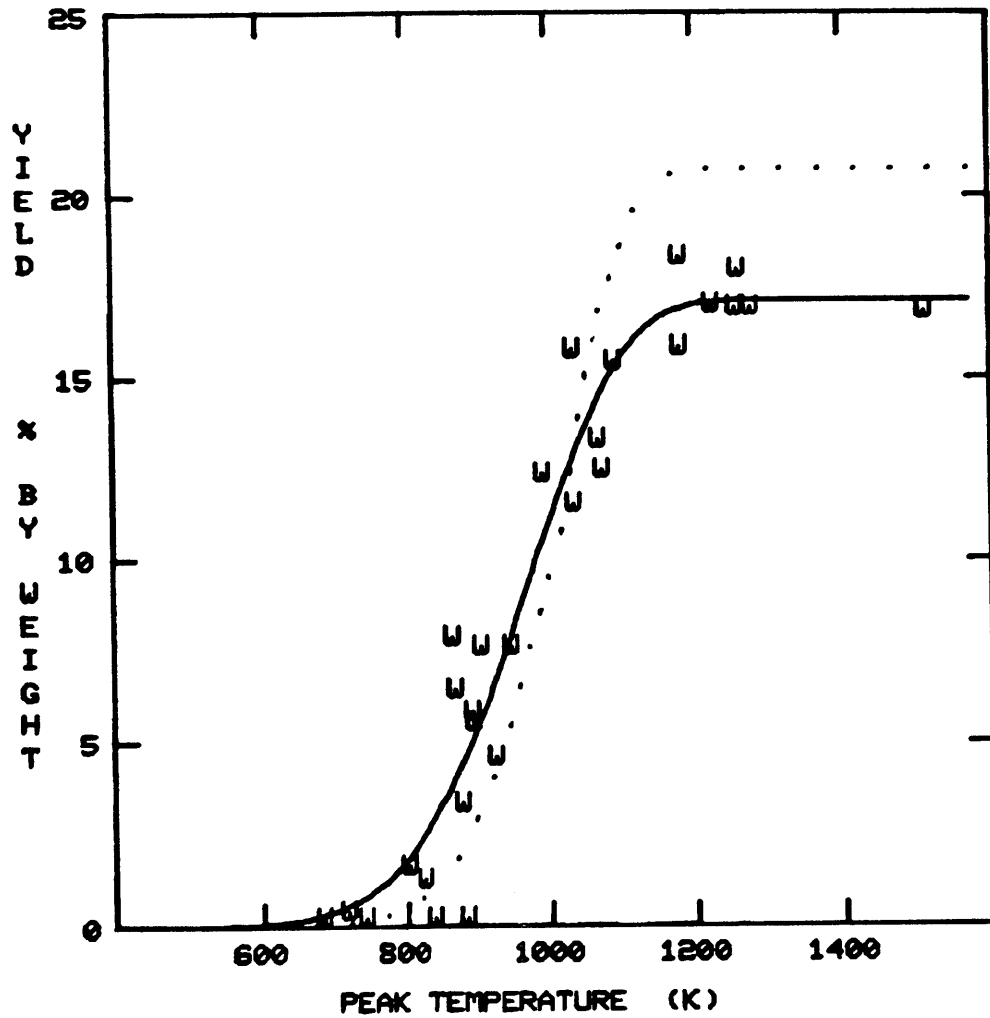
Fig. 4.5-5(b)   Modelled fit to data compared
                 with simulation for carbon
                 monoxide yield from wood pyrolysis.
                 (Nunn, 1981)
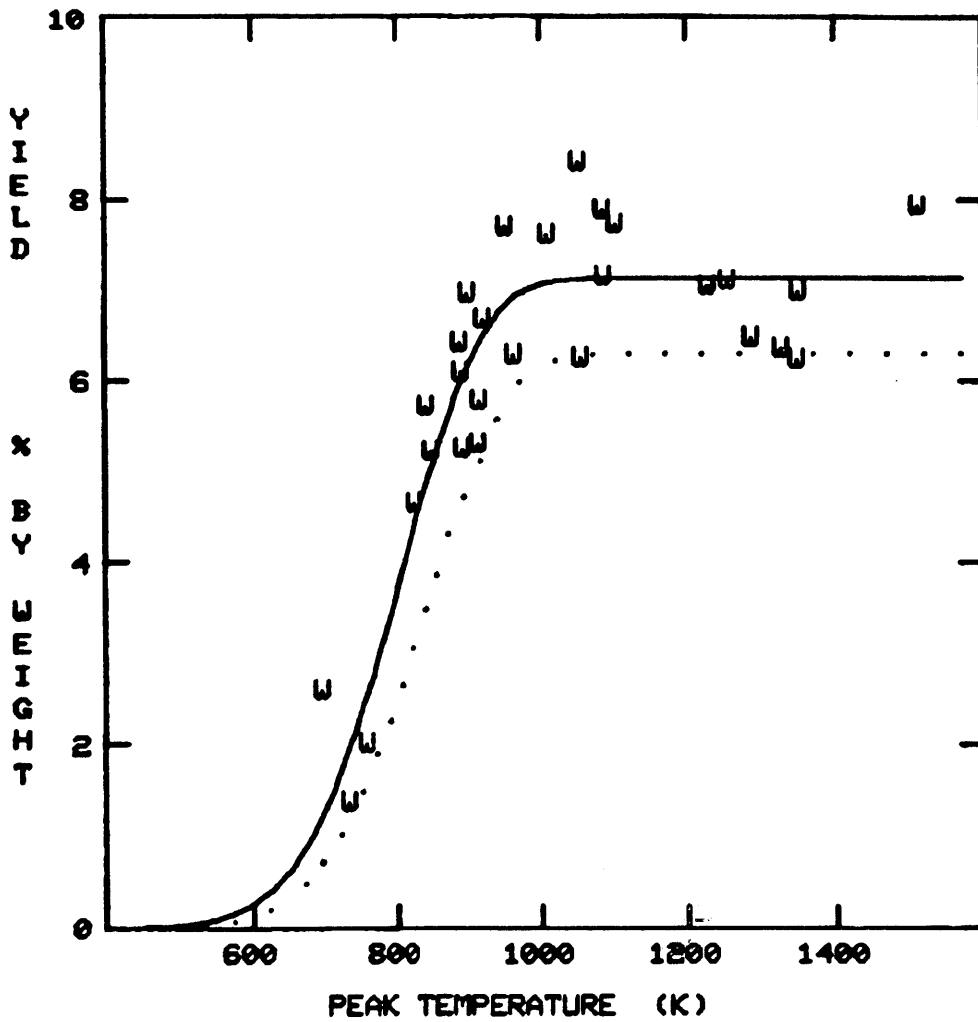
Fig. 4.5-6(a)   Modelled fit to data compared
               with simulation for water +
               formaldehyde yield from wood
               pyrolysis.
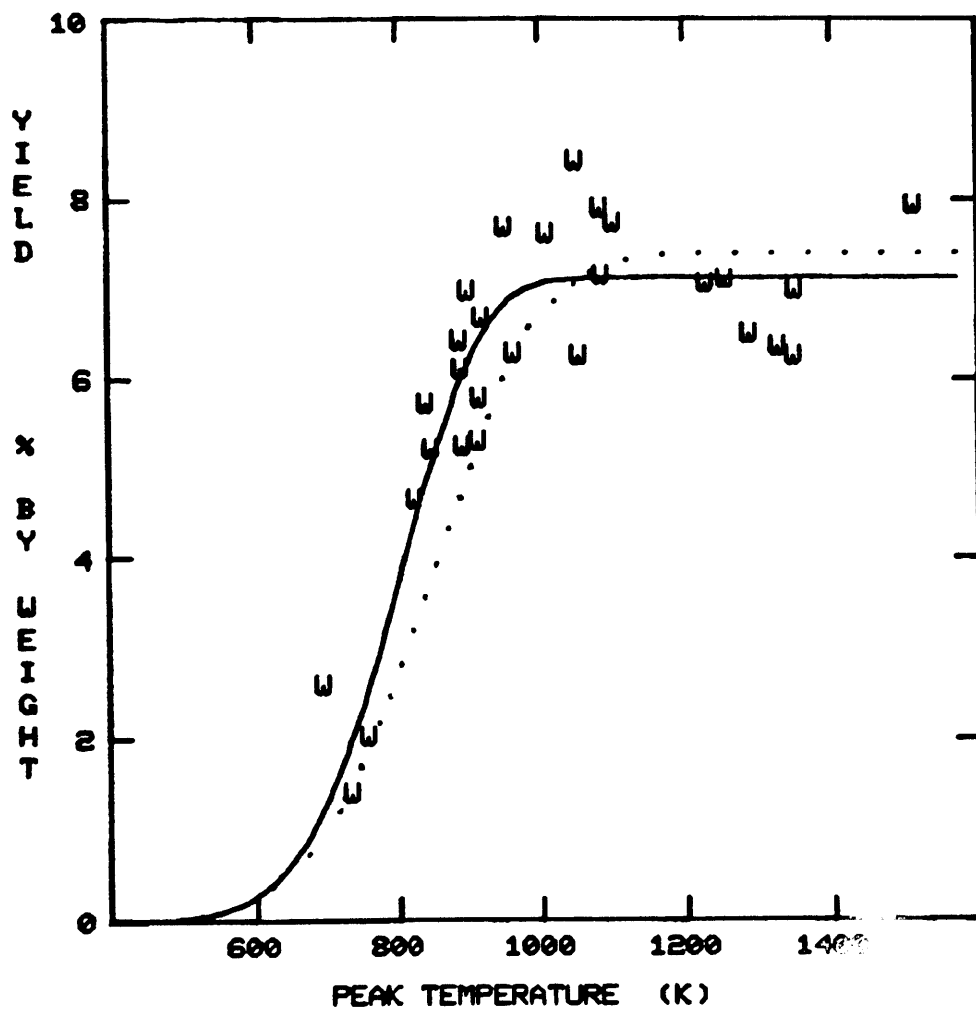
Fig. 4.5-6(b)   Modelled fit to data compared
with simulation for water +
formaldehyde yield from wood
pyrolysis. (Nunn, 1981)

90
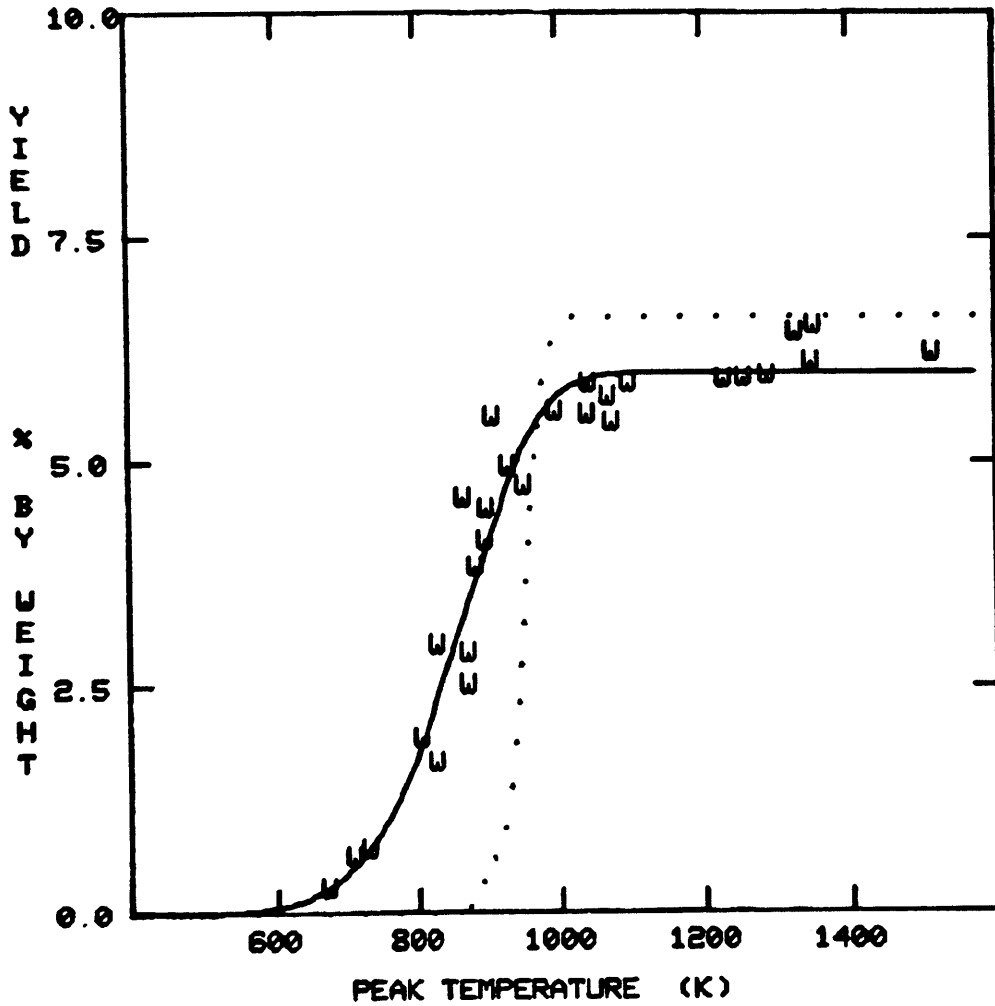
Fig. 4.5-7(a)   Modelled fit to data compared
                with simulation for carbon
                dioxide yield from wood pyrolysis.

91
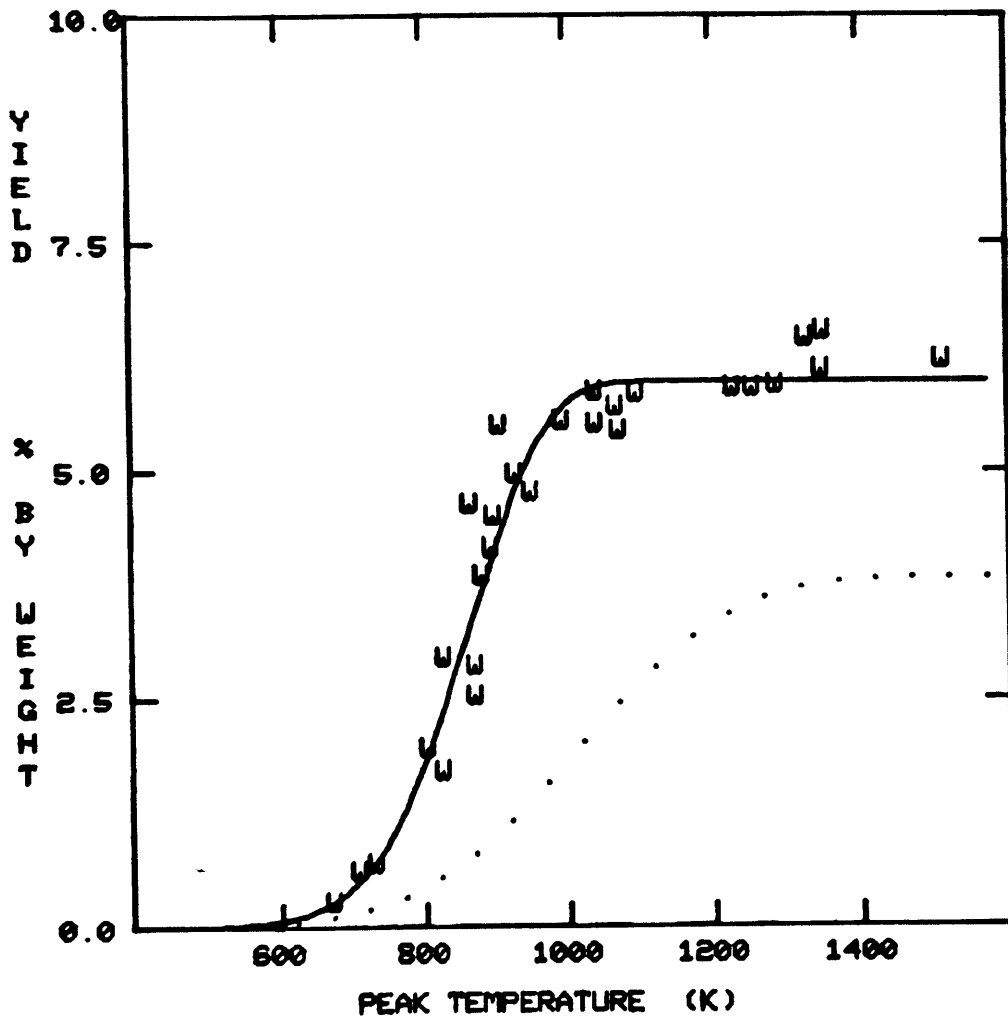
Fig. 4.5-7(b)   Modelled fit to data compared
with simulation for carbon
dioxide yield from wood pyrolysis.
(Nunn, 1981)

are inside the scattered data, each has its strong and weak points. The strong point in Nunn's curve is the closer agreement to data in the high temperature region, while the strong point of the current simulation lies in showing the proper temperature dependence of the yield insofar as predicting the correct temperature at which the ultimate yield of water and formaldehyde is first achieved (1000K).

Carbon dioxide is better modelled by the simulation from this study than by Nunn's model. While both simulations are far from ideal, the major redeeming qualities of the present simulation are its rather accurate prediction of the temperature (1000K) at which carbon dioxide achieves its ultimate yield and its closer reduction of the absolute value of that yield.

Figs. 4.5-8 and 4.5-9 show the simulations for total weight loss and gas production. The current work consistently underestimates the data for wood for both cases over the entire temperature range. Nunn's simulation also underestimates the wood data in the steeply rising section of both plots, but is remarkably accurate in matching the ultimate yields. In general, Nunn's simulation for weight loss more closely matches the data from the pyrolysis of wood than any other simulation matches the rest of the data for wood.

Table 4.5-1 lists the best fit kinetic parameters for the pyrolysis of sweet gum wood and compares them with those derived from the present simulation of wood.
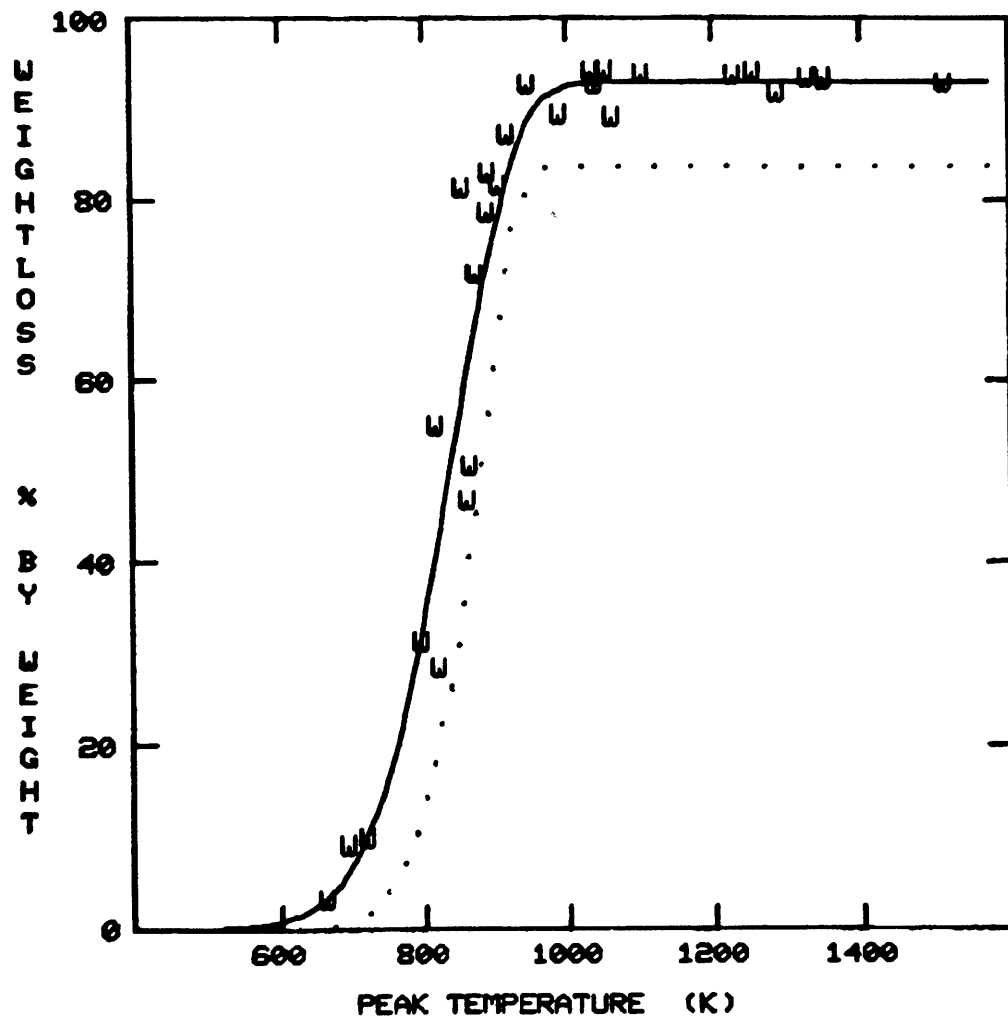
Fig 4.5-8(a)   Modelled fit to data compared
               with simulation for weight loss
               from wood pyrolysis.
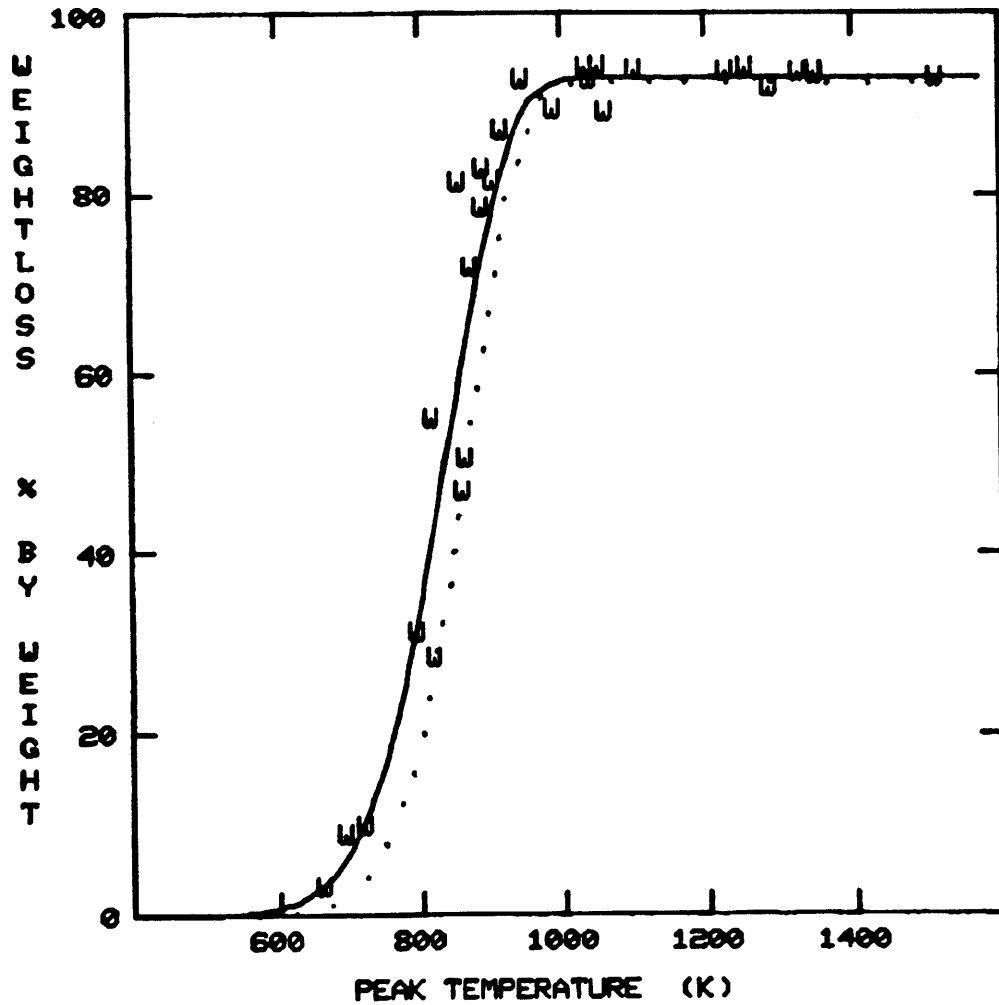
Fig. 4.5-8(b)   Modelled fit to data compared
                with simulation for weight loss
                from wood pyrolysis. (Nunn, 1981)

95
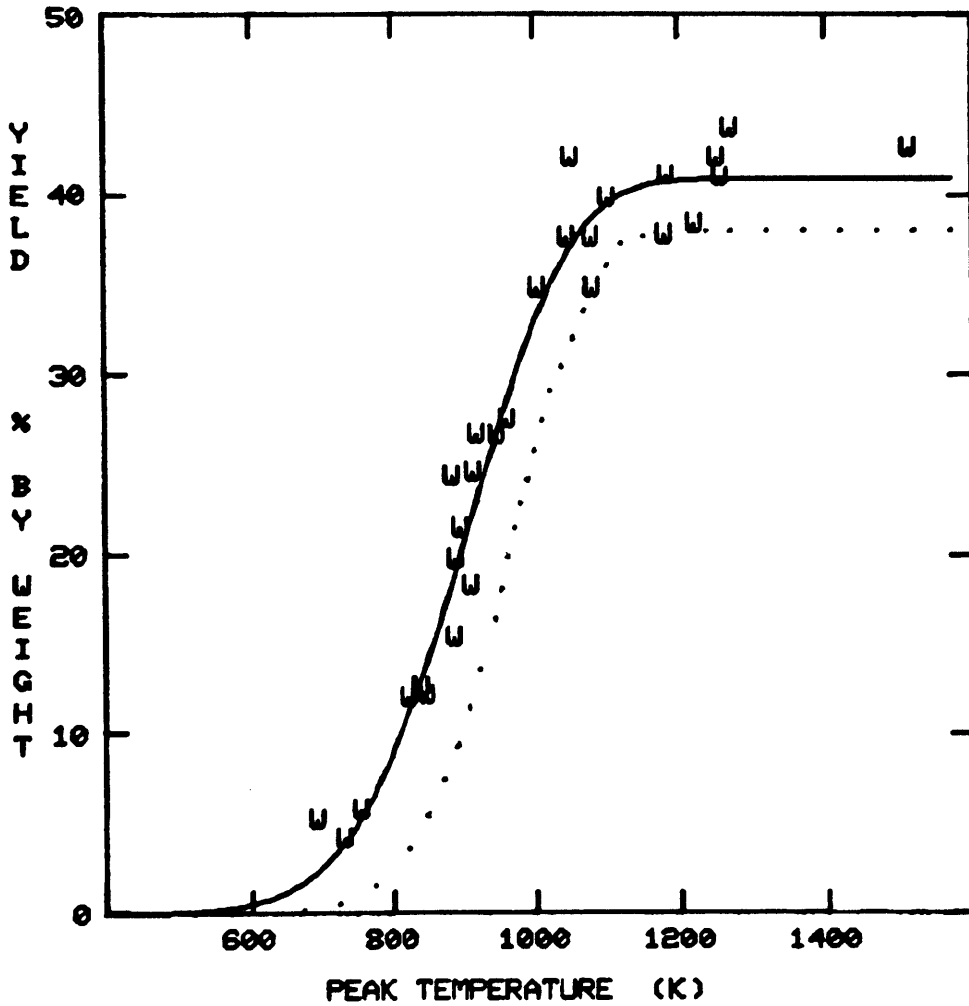
Fig. 4.5-9(a) Modelled fit to data compared
with simulation for total gas
yield from wood pyrolysis.
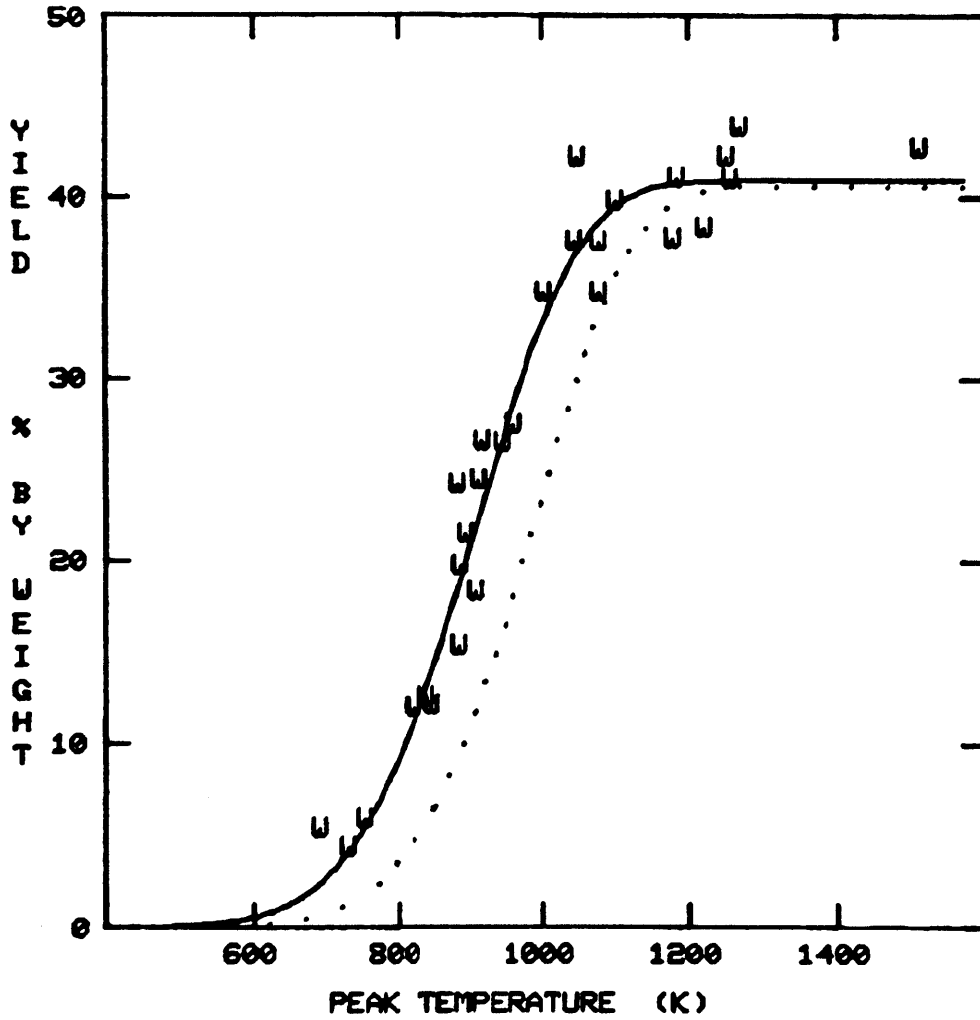
Fig. 4.5-9(b)   Modelled fit to data compared
                with simulation for total gas
                yield from wood pyrolysis.
                (Nunn, 1981)

Table 4.5-1   Comparison of kinetic parameters for sweet gum
hardwood pyrolysis[†] to those predicted from the
wood pyrolysis simulation model.

Component	E (kcal/g-mol)		$\log_{10}k$ $(k = sec^{-1})$		V* (wt. %)		Standard error of estimate (wt. %) [‡]
CH_4	20.7	(16.6)	4.5	(3.8)	2.2	(1.9)	0.05
C_2H_4	26.0	(19.2)	5.7	(4.4)	1.2	(1.2)	0.004
C_2H_6	29.8	(23.7)	6.8	(5.9)	0.22	(0.17)	0.007
H_2O + HCHO	12.7	(11.5)	3.5	(3.3)	6.3	(7.1)	0.10
C_3H_6	245.	(43.8)	59.	(11.)	0.43	(0.41)	0.44
CO_2	82.9	(14.3)	19.	(3.8)	6.6	(5.9)	0.31
CO	18.9	(14.6)	4.1	(3.4)	19.	(17.)	0.63
Weight loss	28.5	(16.5)	7.6	(4.5)	84.	(93.)	0.62
Gas	19.0	(11.8)	4.5	(2.9)	38.	(41.)	0.91

[†] Values in parenthesis are data from Nunn (1981)

[‡] See Table 4.3-1.

4.6 Char Gasification

There are several factors which may eventually be found to
explain why the ultimate yields for individual gases obtained from
simulation are greater than the same from wood. One of the postulated
factors is secondary reactions of volatiles with char at temperatures
above 1150K. This phenomenon would result in gaseous yields sub-
stantially higher than the ultimate yields for gases generated by
primary reactions (mainly those at temperatures less than 1150K).

Though the reactor provides a large escape and quench volume
for volatiles evolving from the neighborhood of the sample screen,
visual inspection of their recirculation patterns in the reactor
(as revealed by the movement of tar fog during and after each run)
shows that for peak temperature runs higher than 1200K, some of the
evolved primary gases re-contact the heater screen before it reaches
the peak temperature.

The role of such effects in carbon monoxide and carbon dioxide
generation was emphasized since, combined, these two products comprise
about 60 wt% of all volatiles. In addition, the overshoot for V^*
in the simulation for these gases were 3.0 wt% and 3.8 wt%
respectively which is a large fraction of the total gas yield of 40 wt%.
There is one new feature found in the data for carbon dioxide production
from xylan which cannot be explained by the secondary cracking of tar
postulated above. Beyond 1200K, carbon dioxide production decreases
by 2 wt% instead of increasing beyond its plateau at 15.2 wt%. Thus,

still another hypothesis which considered a char gasification reaction was formulated. The char gasification reaction is:

$$C_{char} + CO_2 \rightleftharpoons 2CO$$
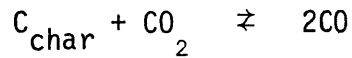
Experiments described below have proven the existence of this reaction for xylan pyrolysis.

Dershowitz (1979) examined the analogous process in a pulverized Montana coal char. Based on intrinsic kinetics, he showed that the equilibrium in the reaction

$$C_{char} + CO_2 \rightleftharpoons 2CO$$
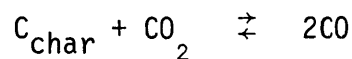
lies to the right ($\log_{10} K_p \sim 1.7$) at 1200K. At higher temperatures, the production of CO is even more greatly favored.

Tables E.1, E.2 (Appendix E) and 4.6-1 list the experiments performed, and give the data relevant to proving the occurrence of the gasification reaction. The objective of these specially designed experiments was to separate the contributions to the observed xylan pyrolysis behavior of (a) primary thermal decomposition of the xylan and (b) secondary gasification of the pyrolysis-derived char. Therefore, the apparent generation of carbon monoxide in three steps was thoroughly reexamined and evaluated in light of the hypothesized occurrence of char gasification. The ultimate char yields from these experiments, when compared with those for the regular peak temperature pyrolysis runs, gave a strong indication of whether or not char gasification was occurring.

The first two experiments (H-38 and H-39) performed were "holding time" experiments designed to show the qualitative nature of secondary reactions. In both runs, the char yield was lower than that expected for a standard "peak temperature" run at 1023K which is 32.5 wt%. Although carbon dioxide reached its ultimate yield by 1023K, the experiments both indicated a small increase in carbon dioxide yield due to the added chance for reaction during the 19 seconds of "holding time". The carbon monoxide yields also increased substantially. It is not clear from these experiments whether the greater yields of both gas species stems from further primary pyrolysis or from secondary reactions; it is most likely from a combination of the two.

The next pair of experiments, summarized in Table E.2, were directly concerned with peak temperature runs, and had the objective of approximately determining the temperature above which secondary reactions become important. A preliminary study of the carbon monoxide "three step" yield pattern suggested that this temperature might be either 1073K or 1193K, corresponding to the base of the second and third steps respectively (cf. Fig. 4.3-11). In each experiment, the char yield was expected to equal that corresponding to the second, higher peak temperature run (1373K). Indeed, the char yields matched according to prediction (cf. Fig. 4.2-2), confirming that any secondary reactions which may have occurred also occur during standard pyrolysis runs. Furthermore, experiment H-40 seems to confirm that while carbon dioxide production is essentially

nil past 1073K, carbon monoxide is still being produced by what evidently are primary reactions. (No other gaseous component exists in sufficient quantity to be able to generate such large amounts of carbon monoxide from secondary reactions.) That we are seeing only primary reactions is also evidenced by the discrepancy in carbon dioxide and carbon monoxide yields from their expected values at a peak temperature run at 1373K. This difference, thus, must be shown to be the result of secondary reactions.

In experiment H-41, the evacuation of all gases from the reactor after the first peak temperature run, followed by the injection of 4 cc-atm of carbon dioxide before the second run to 1373K, was designed to force secondary reactions between gas and char. The final yields of carbon dioxide and carbon monoxide qualitatively prove the existence of the char gasification reaction. However, the net gas yields indicate that only one-half of the total carbon monoxide produced in the second run can be attributed to originate from carbon dioxide. The remainder then must have come from primary reactions in the char.

Experiment H-42, outlined in Table 4.6-1(a), finally integrated all observations into a consistent picture of the nature of char gasification for xylan. Upon quantifying the gases evolved by each successive peak temperature run, it was firmly established that carbon dioxide reaches its ultimate yield of 15.5 wt% gradually by 1373K. At temperatures even as low as 1023K, the carbon dioxide yield is within 7% of its ultimate value. Similarly, it is known that

102

Table 4.6-1(a)   Experiment H-42 confirming the three step
                  yield curve for carbon monoxide , and the
                  char gasification reaction

Temperature - time history
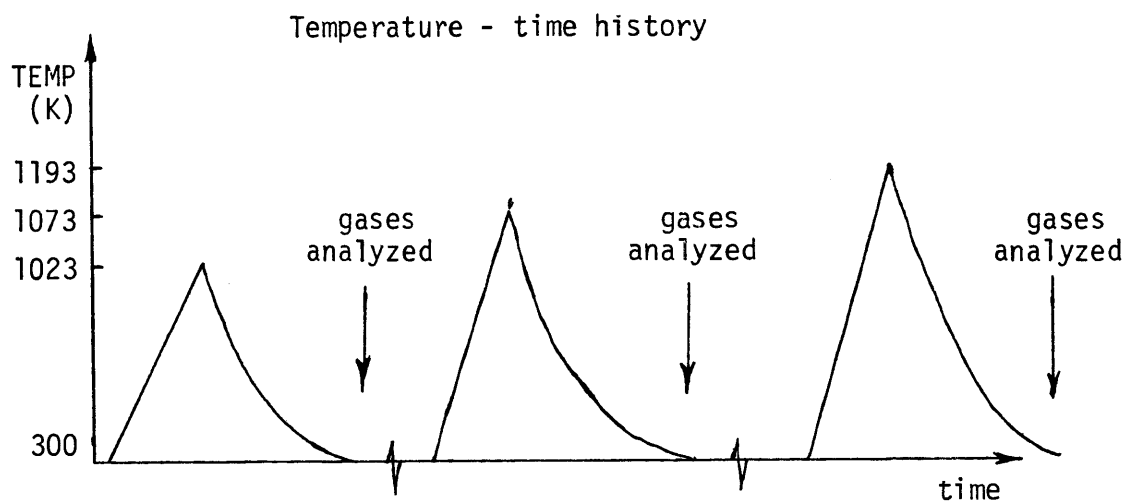
STEP 1: Peak temperature run to 1023 K
STEP 2: Peak temperature run to 1073 K
STEP 3: Peak temperature run to 1193 K

INDIVIDUAL YIELDS:

	CO_2	CO
Step 1 (1023K)	14.4 wt. %	8.9 wt. %
Step 2 (1073K)	0.76	2.75
Step 3 (1193K)	0.22	1.9

CUMULATIVE YIELDS:

	CO_2		CO	
Step 1 (1023K)	14.4 wt. %	(15.0)*	8.9 wt. %	(8.5)*
Step 2 (1073K)	15.2	(14.8)	11.7	(12.)
Step 3 (1193K)	15.5	(13.6)	13.5	(17.)

---

* Values in parentheses indicate expected yields

103

Table 4.6-1(b)   Calculations proving validity of stoichiometry
                  in char gasification reaction for xylan char.
                  (Data from Table 4.6-1(a))

Difference in CO_2 yield attribuable to char gasification:

$$15.5 - 13.6 \text{ wt. } \% = 1.9 \text{ wt. } \% \text{ at } 1200K.$$

Difference in CO yield attribuable to char gasification :

$$17.0 - 13.5 \text{ wt. } \% = 3.5 \text{ wt. } \% \text{ at } 1200K.$$

Postulated reaction: $CO_2 + C$ (char) $\longrightarrow$ 2CO
Molecular weights   44   12   2(28)

Basis = 50 mg xylan sample.

1.9 wt. % CO_2 = 2.16 X 10^{-5} g-mol CO_2
3.5 wt. % CO = 6.25 X 10^{-5} g-mol CO
Expected CO   = 2 (2.16 X 10^{-5} g-mol) = 4.3 X 10^{-5} g-mol CO.

Difference (6.25 - 4.3) X 10^{-5} g-mol = 1.9 X 10^{-5} g-mol (0.8 wt. %)
            due to continued primary reaction formation of CO.

the evolution of carbon monoxide by primary reactions does exhibit

a three-step behavior: the first plateau at 8.4 wt% is reached by

923K; the second shorter plateau at 11.6 wt% is achieved by 1150K.

The third plateau, the existence of which may be deduced from the

available data, though it lies at the high temperature periphery

of our data, is at about 13.7 wt% of carbon monoxide and is attained

by perhaps 1250K. The most important element in the interpretation

of H-41 which allows us to justify this third plateau for carbon

monoxide at 13.7 wt% is that calculations show (see Table 4.6-1(b))

that the deviations from 15.5 wt% carbon dioxide and from 13.7 wt%

carbon monoxide can be attributed to a stoichiometric char gasification

reaction (i.e., $CO_2 + C \rightarrow 2CO$).

4.7 Step Behavior of Carbon Monoxide

Suuberg (1977) in an extensive study of the devolatilization

behavior of a Montana Lignite and a Pittsburgh Seam Bituminous coal

observed step behavior for several gas species' yields. The reaction

conditions for the rapid pyrolysis behavior were varied over a wide

range of heating rates and pressures. Despite this variation in

conditions, a three step behavior for the production of carbon

monoxide from the coals is proposed as is done here for the pyrolysis

of xylan.

The supporting evidence is strong for the coals, and is justified

based on the assumption that carbon monoxide production proceeds via

different mechanisms depending on the peak temperature of the pyrolysis. The complex petrographic structure of coal provides enough justification for this hypothesis and did not force Suuberg to constrain the suggested applicability of this mechanism to carbon monoxide evolution alone; methane, ethylene and carbon dioxide, for example, also exhibit two step yield behavior.

A similar argument may be proposed for xylan but only for carbon monoxide. Looking at xylan's structure illustrated in Fig. 2.1-3(a), we find that carbon monoxide may be generated from the carboxylic glucoronic acid group, from the H_3CO- side group, from the C-O-C chain which links adjacent pentose sugar units together, and lastly from the oxygen-carbon group in the ring structure itself. Based on relative bond strengths (Benson, 1976) it is reasonable to postulate that the first step in carbon monoxide production (see Fig. 4.3-11) between 550 and 1050K is due to the rupture of the H_3CO- side groups on the pentose ring in the 4-ortho position of the xylan backbone. The second step (1050 to 1200K) is probably the result of the cleavage of one carbon-oxygen bond between the five carbon sugars, while the high temperature plateau (1200 to 1400K) would be from carbon monoxide formation from carbon and oxygen atoms within a 6-membered ring. Fig. 4.7-1 points out the specific groups mentioned. A final comment is needed to emphasize that the glucoronic acid group is most likely the precursor to carbon dioxide production and normally will not yield the monoxide.

1. Most likely
   position

3. Third possible
   position

2. Second most likely
   position
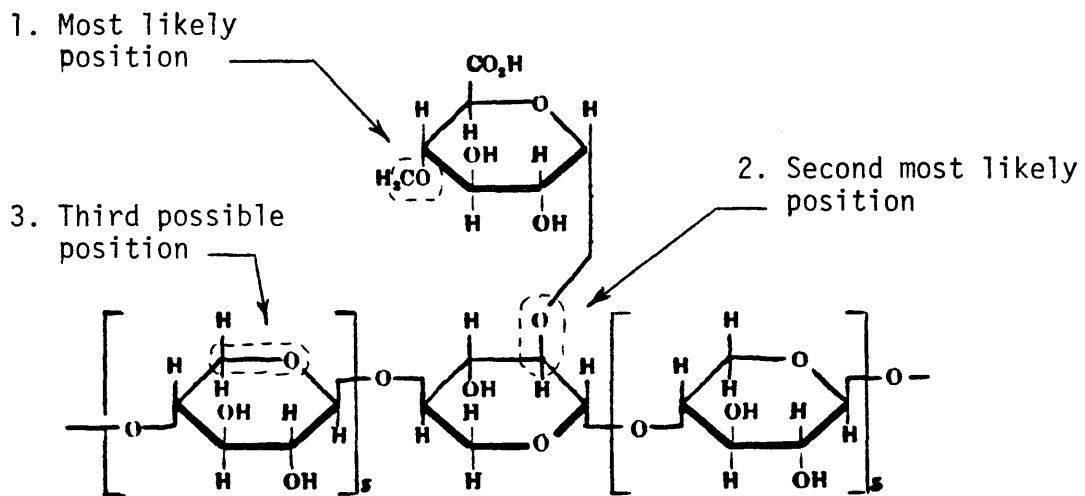
Fig. 4.7-1 Three possible locations in xylan's
            structure which might yield carbon
            monoxide upon pyrolysis.

4.8 Effects of Potassium in Xylan Pyrolysis

Mineral additives such as NaOH, H_3PO_4, $ZnCl_2$ and $(NH_4)_2HPO_4$ have

been added to xylan (Shafizadeh, 1972; 1976) and to holocellulose

(Fang and McGinnis, 1976). The differences resulting therefrom were

tabulated next to those of their "neat" pyrolyses. It is found that

char yields increase substantially, tar yields decrease substantially

while the yields of light hydrocarbons vary -- some, such as furan,

ethanol and water are evolved in larger quantities; others such as

methanol and carbon dioxide remain essentially constant while acetic

acid, acetaldehyde, and acetone, for instance, decrease in yield

(see Table 2.2-1 and 2.2-2).

A more extensive study performed by Cosway (1981) on the

effects of calcium, sodium and potassium, ion exchanged with carboxylic

hydrogen ions in demineralized subbituminous coal, is more directly

relevant to the present work on xylan. Since Cosway's data were

gathered on an apparatus very similar to the one used here for xylan,

and since the same heating rate (1000 K/s) was used for pyrolysis, the

analogies with and extrapolations from this research are particularly

meaningful. Further, the potassium ions which exist in the xylan

microstructure are replacing the hydrogen ions in glucuronic acid

groups (Chang, 1982(b)), the predominant carboxylic acid group in

xylan.

The main observation made by Cosway concerned the large increase

in char yield due to the metal ions. No mechanism is proposed, but

it is safe to speculate that the reduction in weight loss may be due to catalytic activity of the metal ions, probably in accelerating rates and extents of tar cracking to char and gases. This result can justify a 16 wt% char yield from xylan. The weight loss from coal was reduced from 55% to 38% on a dry mineral matter free (DMMF) basis. Tar yield, too, was found to decrease in the presence of potassium.

As for product gases, Cosway notes that carbon monoxide yield is depressed (from $V^* = 10\%$ DMMF to $V^* = 8\%$ DMMF for potassium substituted coal). Fig. 4.8-1 shows the typical behavior obtained by Cosway for carbon monoxide, methane and other volatiles from sub-bituminous coal pyrolysis. Of the several interesting features in the figure, it is clear that the primary function of the metal ions is not only to lessen the ultimate yield of gas but also to lessen the apparent reactivity of the coal samples. Thus, not only is V^* less than that for demineralized coal, but the curve for gas production is also shifted to the right (i.e., to higher temperatures). The only compound for which this behavior is reversed is carbon dioxide; Fig. 4.8-2 presents Cosway's data for carbon dioxide production.

If we believe the pyrolysis behavior for xylan is affected by the potassium impurity in much the same way as it affects Cosway's coal, then we can give a suitable explanation for the inaccuracies of the simulated curves for wood pyrolysis. All of the simulation curves, be they for weight loss or propylene evolution, have one common feature: all underestimate the analogous behavior of wood during the most rapidly
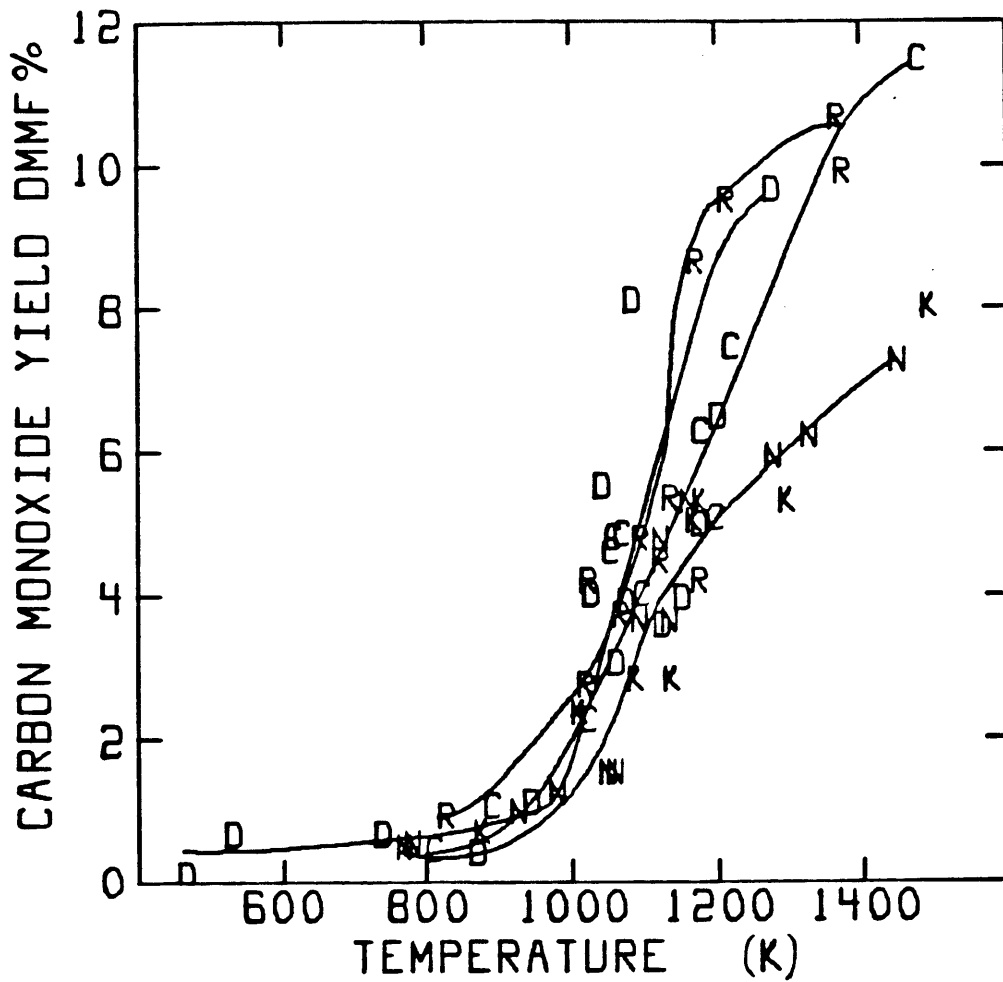
Fig. 4.8-1 Carbon monoxide yield from rapid pyrolysis
of a Montana subbituminous coal; R = raw,
D = demineralized, N = sodium added,
C = calcium added, K = potassium added.
(Cosway, 1981)
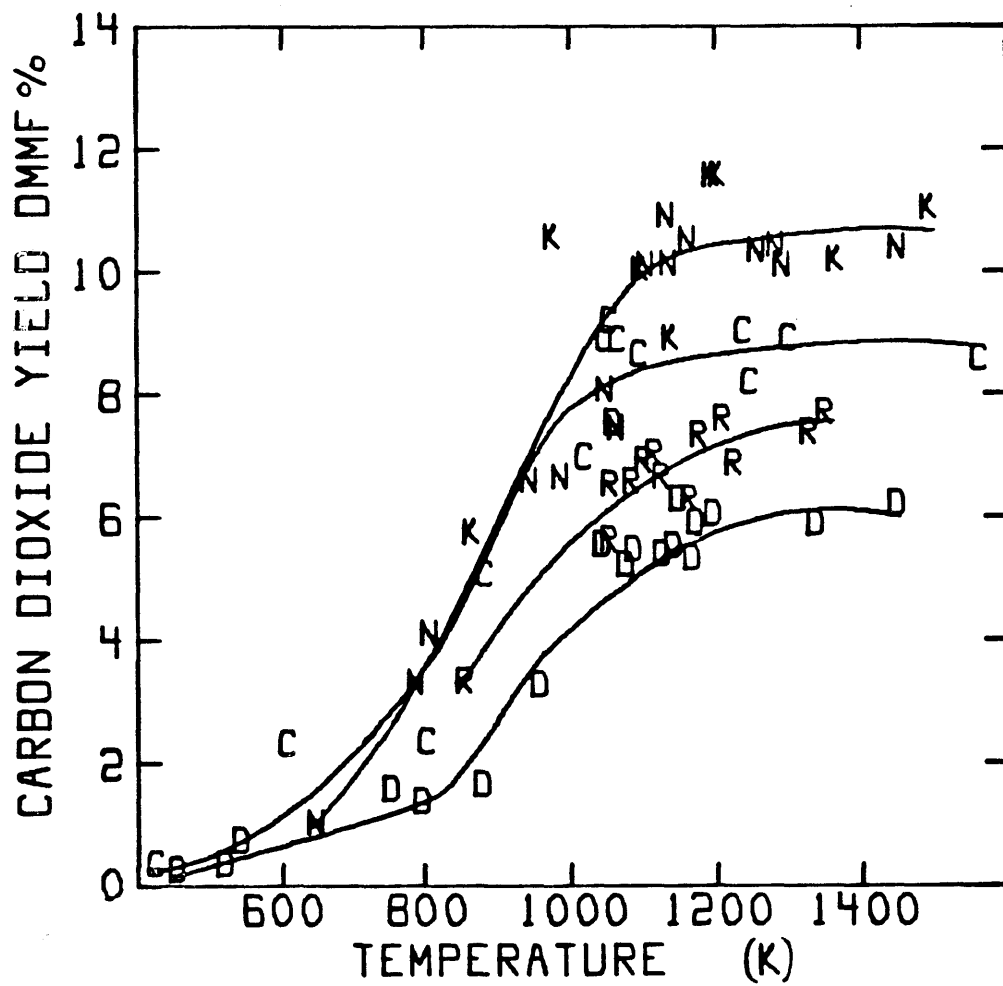
Fig. 4.8-2 Carbon dioxide yield from rapid pyrolysis
of a Montana subbituminous coal; R = raw,
D = demineralized, N = sodium added,
C = calcium added, K = potassium added.
(Cosway, 1981)

rising region of the weight loss or product evolution. It is con-
ceivable that this phenomenon is due to an apparently lowered xylan
reactivity due to potassium's catalytic action. Furthermore, one
may hypothesize that the pyrolysis data from potassium-free xylan
when combined with those of Hajoligol's (1980) cellulose and Nunn's
(1981) lignin, which were both free of potassium, would yield a
simulation curve which would closely match Nunn's wood data.
Nunn's wood had a small potassium content in agreement with the
quantity one might expect to find in woods.

4.9 Experimental Accuracy

The present pyrolysis reactor gives good material balance
closures (between 90 and 100%). The char yield is determined grav-
imetrically and is subject to < 0.1 wt% inaccuracy. The yield of
gases, which are collected in the glass wool and lipophilic traps, is
subject to a somewhat greater inaccuracy because recovery is between
80 and 100%. But the greatest part of the inaccuracy lies in
collecting tars. While tar yield is partially determined gravimetric-
ally from the foil which lines the bottom of the reactor, most of
the tar is recovered on the Kimwipe tissues which are used to wipe
down the reactor's sides and top. About 50% of the tar appears on the
tissues once the solvent is evaporated. Though the control tissue
provides a correction for residual solvent, the solvent sometimes
accounted for 30% of each tissue's accumulated weight.

A final note concerns the yield of heavy oxygenated gases which are eluted after water. Nunn (1981) mentions a possible 30% error in each of those peaks for formaldehyde, methanol, acetaldehyde, ethanol, acetone and furan. Yet it is not of much consequence in the overall material balance of which they represent 1 wt% maximum. More serious is the fact that methanol and acetone, which are in the solvent used to extract tars from the glass wool trap, could never be completely desorbed from the glass wool. As a result, although reasonable qualitative trends may be inferred from the present data on methanol, their quantitative significance is questionable.

5. CONCLUSIONS AND RECOMMENDATIONS

The conclusions to be drawn, given that the experimental apparatus generates consistently reproducible data with material balance closures generally in excess of 90 wt%, are:

(1) The pyrolysis data on sweet gum xylan shows similarities to analogous data obtained from the pyrolysis of filter paper cellulose, milled wood lignin and sweet gum hardwood in terms of (a) the high degree of devolatilization possible, (b) the high tar yield at high temperatures, (c) the light volatile products' distribution, and (d) the good fit of the single step first order reaction model to the data.

(2) The devolatilization behavior of cellulose and hemicellulose are not in as close agreement with each other as expected from their structural similarities, the major differences arising from the greater reactivity of hemicellulose, demonstrated by incipient volatiles evolution at lower temperatures than for cellulose, and the noticeably great differences in ultimate yields for carbon monoxide and carbon dioxide.

(3) The temperature dependence of yields from wood, of all products except char is well simulated by the present model which accounts for the differences in the pyrolysis behavior of cellulose and hemicellulose. This represents a significant improvement over a previous simulation which hypothesized that

these two wood components behaved identically.

(4) The high char yield from xylan is probably due to its high

potassium content, since it is known from other studies on

coal and biomass that inorganic matter catalyzes char formation

in pyrolysis.

(5) The large potassium content of the present xylan may catalyze

the char gasification reaction at temperatures above 1150K

(CO_2 + char $\rightleftarrows$ 2CO). This generates carbon monoxide in greater

quantities than would have been expected from primary pyrolysis

and secondary (tar cracking) reactions.

Additional work must be done in order to discover the reasons for

the differences between simulation and experimental observations for

wood pyrolysis; hence, the recommendations are:

(1) To determine the pyrolysis characteristics of mineral-free

xylan and compare them with filter-paper cellulose pyrolysis

behavior;

(2) To perform a similar study on natural sweet gum cellulose (α-

cellulose) and also compare the results with those of filter

paper cellulose;

(3) To investigate more closely the effects that inorganic minerals

(such as potassium) have on the pyrolytic decomposition reactions

in biomass, especially with regard to catalytic char gasification;

(4) To compare the pyrolysis behavior of wood reconstituted from a

mix of its three major components with that predicted by

simulation; and

115

(5) To study the secondary reactions of tars from wood and its
constituents to establish a more quantitative picture of
their role in global pyrolysis behavior. The possible greater
stability of xylan derived tars indicated in the present
work is of particular interest.

LITERATURE CITED

1.   Andrews, E. K., M.S. Thesis, Dept. of Wood and Paper Science, North Carolina State University, Raleigh, NC (1980).

2.   Benson, S. W., "Thermochemical Kinetics", (2nd ed.), John Wiley and Sons, NY, NY (1976).

3.   Browning, B. L., Methods of Wood Chemistry, Vol. I & II, NY Interscience Publishers (1967).

4.   Caron, R., "Batch Reactor Manual", a report in the Dept. of Chemical Engineering, MIT (1979).

5.   Chang, H.-M., Professor, North Carolina State University, personal communication, July (1982(a)).

6.   Chang, H.-M., Professor, North Carolina State University, personal communication, August (1982(b)).

7.   Cosway, R. G., "Ion Effects in Subbituminous Coal Pyrolysis", S.M. Thesis, MIT, Dept. of Chem. Engineering (1981).

8.   Fang, P., and McGinnis, G. D., "Flash Pyrolysis of Holocellulose from Loblolly Pine Bark", Thermal Uses and Properties of Carbohydrates and Lignins Symposium, Shafizadeh, Sarkanen and Tillman, eds., p. 37 (1976).

9.   Franklin, H. D., "Mineral Matter Effects in Coal Pyrolysis and Hydropyrolysis", Ph.D. Thesis, MIT, Dept. of Chem. Engineering (1980).

10. Hajaligol, M. R., "Rapid Pyrolysis of Cellulose", Ph.D. Thesis, MIT, Dept. of Chem. Engineering (1980).

11. Howard, J. B., "Fundamentals of Coal Pyrolysis and Hydropyrolysis", Ch. 12 of Chemistry of Coal Utilization, Elliott, M. A., ed., John Wiley and Sons Inc., New York (1981).

12. Johnson, R. A., B.S. Thesis, "The Analysis of Gaseous and Light Oil Products from a Two-State Fixed-Bed Coal Pyrolysis Reactor".

13. Joseleau, J. P. and Barnoud, F., "Cell Wall Carbohydrates and Structural Studies of Xylans in Relation to Growth in the Reed Ardendo Donax", Appl. Poly. Symp., 28, 983, John Wiley & Sons Inc., New York (1976).

117

14. Kollmann, F. F. P. and Coté, W. A. Jr., _Principles of Wood Science and Technology_, George Allen and Union Ltd., Heidelberg (1968).

15. Marchessault, R. H. and Liang, C. Y., "The Infrared Spectra of Crystalline Polysaccharides. VIII. Xylans", _J. Polymer Sci._, _59_, 357 (1962).

16. Masen, D. M. and Gandhi, K., "Formulas for Calculating the Heating Value of Coal and Coal Char: Development, Tests and Uses", ACM Fuel Chem. Div. Preprints, _25_(3), Aug. 24-29 (1980).

17. Nunn, T. R., "Rapid Pyrolysis of Sweet Gum Wood and Milled Wood Lignin", M.S. Thesis, MIT, Dept. of Chem. Engineering (1981).

18. Perkin-Elmer Sigma 10B Console Operations Manual, Norwalk, CT (1979).

19. Probstein, R. F., and Hicks, R. E., _Synthetic Fuels_, McGraw Hill Inc., New York (1981).

20. Ruel, K., Joseleau, J. P., Comtat, J. and Barnoud, F., "Ultrastructure Localization of Xylans in the Developing Cell Wall of Graminae Fibers by the Use of an Endoxylanase", _Appl. Poly. Symp._, _28_, 971, John Wiley & Sons Inc., New York (1976).

21. Serio, M. A., Ph.D. Thesis, Dept. of Chem. Engineering, MIT (1983) (to be published).

22. Shafizadeh, F., McGinnis, G. D. and Philbot, C. W., "Thermal Degradation of Xylan and Related Model Compounds", _Carbohyd. Res._, _25_, 23 (1972).

23. Shafizadeh, F. and Chin, P. P. S., "Thermal Deterioration of Wood", in _Wood Technology: Chemical Aspects_, Goldstein, I. S., ed., ACS Symp. Series, _43_(1), 57, Washington DC (1977).

24. Solar Energy Research Institute (SERI), "A Survey of Biomass Gasification", SERI/TR-33-239 (1979).

25. Stamm, A. J., "Thermal Degradation of Wood and Cellulose", _Ind. Eng. Chem._, _48_, 413 (1956).

26. Suuberg, E. M., "Rapid Pyrolysis and Hydropyrolysis of Coal", Sc.D. Thesis, Dept. of Chem. Engineering, MIT (1977).

27. Timell, T. E., "Wood Hemicelluloses", _Adv. Carbohyd. Chem_, _19_, 409 (1965).

118

28. Wenzl, H. F. J., The Chemical Technology of Wood, Academic Press, New York (1970).

29. Yurek, G. J., Professor, MIT Department of Materials Science and Engineering, personal communication (1977).

APPENDIX A - GAS CHROMATOGRAPHY

A.1 Response Factors for Sigma 2B Gas Chromatograph

For each of the identified product gases evolved on pyrolysis, gas samples (for CO, CO_2, CH_4, C_2H_4, C_2H_6 and C_3H_6) of volumes ranging from 0.25 cc to 2.0 cc, and liquid samples (for HCHO, CH_3OH, CH_3CHO, EtOH, acetone and furan) of volumes ranging from 0.25 μl to 2.0 μl were injected into chromatographic columns maintained at 573K. Methane of 99.97% purity (Matheson, ultra-high purity) is used as the standard calibration gas, since it responds to both the thermal conductivity detector (TCD) and flame ionization detector (FID), and thus has a response factor of 1.0.

For gases other than methane, the response factor was calculated from:

$$R_i = \frac{mg_i}{A_i} \frac{A_{CH_4}}{mg_{CH_4}}$$

in which mg_i was regressed versus $A_i/(A_{CH_4}/mg_{CH_4})$ via linear least squares to obtain the response factor (R_i) as the slope of the line. Then, R_i is used in the following formula:

$$mg_i = R_i \frac{0.6544}{A_{CH_4}} A_i$$

where: mg_i = milligrams of component i

R_i = response factor for i

$$mg_{CH_4} = 0.6544 \text{ per cc } (R_{CH_4} = 1.000)$$

$$A_i = \text{TC or FI peak area for } i$$

$$A_{CH_4} = \text{TC or FI peak area for } CH_4$$

Thus, only A_{CH_4} needs to be obtained for a 1cc sample of methane (which contains 0.6544 mg methane) to get all other mg_i.

Table A.1 lists the TC and FI response factors for the gases collected in the glass wool and lipophilic traps.

A.2 Operation of the Sigma 2B Gas Chromatograph

Gas chromatography often involves the separation of a sample on a single column temperature programmed from ambient or sub-ambient initial temperatures to some higher final temperature.

Previous biomass pyrolysis studies in this laboratory utilized a 3.6 m long 0.635 cm ID column packed with Porapak QS (Waters Associates), temperature programmed from 203K to 513K at a constant rate of 16 K/min. In this protocol, the gases emerged from the column in the following order: air, carbon monoxide, methane, carbon dioxide, ethylene, ethane, propylene, water plus formaldehyde, methanol, acetaldehyde, ethanol and heavier oxygenated hydrocarbons.

This method had the drawback of not providing a clear separation between the air and carbon monoxide peaks, nor could it discriminate between water and formaldehyde peaks. To overcome these deficiencies, a new method developed by Serio (1983) proved effective.

Table A.1 Response factors for thermal conductivity (TC) and flame ionization (FI) detectors on the Sigma 2B and Perkin Elmer 3920B gas chromatographs

Component	Sigma 2B TC	Sigma 2B FI	PE 3920B TC
CH_4	1.000	1.000	1.00 [#]
CO_2	1.71 $\pm$ 0.01	*	1.78
CO	1.437 $\pm$ 0.006	*	1.36
C_2H_4	1.37 $\pm$ 0.01	0.791 $\pm$ 0.007	1.26
C_2H_6	0.92 $\pm$ 0.09	0.889 $\pm$ 0.015	1.28
H_2O	1.34 $\pm$ 0.03	*	1.24
$HCHO$	1.34 $\pm$ 0.03	*	1.24
C_3H_6	1.47 $\pm$ 0.02	1.437 $\pm$ 0.006	1.47
CH_3OH	1.466 $\pm$ 0.016	3.5 $\pm$ 0.1	1.34
CH_3CHO	1.68 $\pm$ 0.02	3.01 $\pm$ 0.014	1.34
CH_3CH_2OH	1.63 $\pm$ 0.02	1.93 $\pm$ 0.02	1.55
CH_3COCH_3	1.63 $\pm$ 0.01	1.893 $\pm$ 0.007	1.47
Furan	2.07 $\pm$ 0.03	1.36 $\pm$ 0.05	1.47
CH_3COOH	1.90 $\pm$ 0.014	4.72 $\pm$ 0.04	1.91

* No FI response

[#] Old response factors used CO_2 as the standard gas

The novel technique uses a 0.92 m long x 0.635 cm ID column packed with 80/90 mesh 5A molecular sieve in series with the 3.6m long Porapak QS column described above. It is possible, via a switching mechanism at the gas inlet port to these columns (see Figure A.2) to reverse the in-series positioning of the two columns. From Fig. A.2 we see that valve position A corresponds to having the molecular sieve column (#2) first, followed by the Porapak column (#1), with no communication between the sample and the columns. Valve position B allows the gases to enter the Porapak column first and then the molecular sieve column. In this position the carrier gas sweeps through the sample loop before entering the columns. Thus, the valve must initially be at position B to allow the gases to enter the column system. This position also results in the entire sample being deposited first on the Porapak column. This is necessary since certain components, e.g., CO_2, H_2O, are nearly irreversibly adsorbed on the molecular sieve column.

Two distinct temperature programs were used with the new method, one for the glass wool trap and the other for the lipophilic trap. This is necessary due to the differences in product gas distribution in each trap. Nonetheless the main features of the gas analysis are the same for both traps, and their description follows.

Initially, the valve is in position B and all the gases are swept into the Porapak column at ambient temperature. The valve stays in that position until air and then methane exit the molecular

Description of Column and Detector Sequence (Gas Analysis)

Column Sequence Reversal System
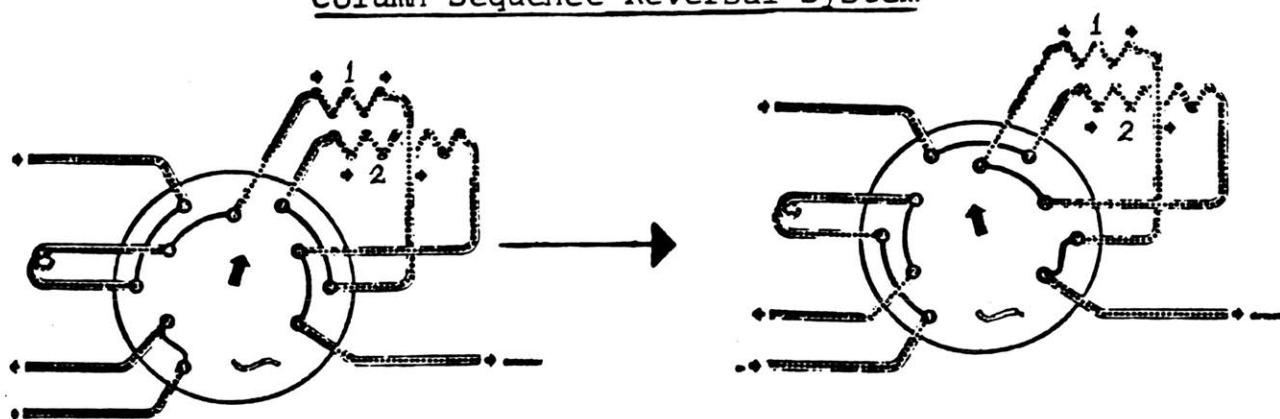
Valve Position B   Valve Position A

Column 2 (Poropak QS)
Column 1 (Molecular Sieve)

Fig. A.2   Columns' configuration in Sigma 2B Gas Chromatograph.
           Switching time = 4.2 minutes for glasswool trap;
           and 7.8 minutes for lipophilic trap. (Johnson, 1982)

sieve column. Due to the retarding effect of the molecular sieve column on carbon monoxide, methane "overtakes" carbon monoxide and is detected first. At this point, the carbon dioxide is nearly at the connection between the two columns. The valve is switched to position A so that the carbon dioxide comes out of the Porapak column to go straight into the detectors, not to the molecular sieve column, and hence is detected right after methane. All the carbon monoxide which was on the molecular sieve column when the valve is switched from position B to A then retraces its path back to the Porapak column, passes through it a second time, and exits to the detectors with ethylene and ethane.

The net result is a clean separation not only between air and carbon monoxide, but also between carbon monoxide and carbon dioxide, which are major gaseous products of xylan pyrolysis. In addition, the versatility of the temperature programming in the Sigma 2B allows two different ramp rates during a single analysis, while the integrator offers "skim" correction for peaks which "tail" enhancing the sensitivity and accuracy of the quantitative gaseous determinations. The skim correction allows a more accurate determination of peak areas for gases found in minute quantities. These peaks are frequently superimposed on larger peaks, the latter of which tail due to the particular gas' adsorption/desorption characteristics on the Porapak column (see Fig. A.3).
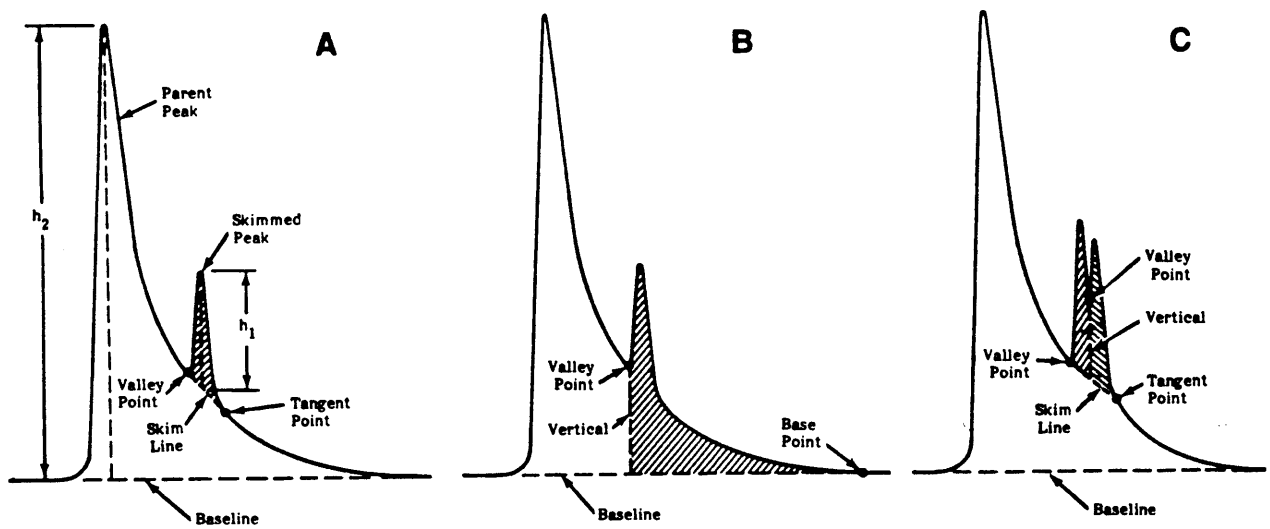
Fig A-3   *Areas of Unresolved Peaks Obtained with Peak Skimming*
(A and C) and without Peak Skimming (B). C is a Special
Case in Which Two Unresolved Peaks Are Skimmed from
the Trailing Edge of a Large Peak and Separated by
a Vertical to the Skim Line.
(From Perkin-Elmer Sigma 10B Console Operations Manual, 1979)

APPENDIX B - MATHEMATICAL ANALYSIS OF DATA

Howard (1981) describes different mathematical models which have proven effective in quantitatively defining the high temperature pyrolytic behavior of coals and biomass materials. These models range in sophistication from simple single step first order expressions to more complicated multiple reaction models which have a distribution of activation energies for each product species. In order to ensure consistency with previous biomass pyrolysis modelling at MIT (Hajaligol, 1980; Nunn, 1981) and to facilitate comparison between sets of best fit parameters for various wood components, a single reaction first order decomposition model was used to fit the data in this work.

In this model the rate of formation of species i with a yield of V_i (wt%) at time t is given by:

$$\frac{dV_i}{dt} = k_i \, (V_i^* - V_i) \tag{1}$$

where V_i^* = ultimate value of V_i (i.e., for long times and high temperatures)

k_i = Arrhenius rate constant for species i

The model dictates a rate of formation for product species i as being proportional to the departure of V_i from V_i^*. The Arrhenius factor has the usual dependence on temperature:

$$k_i = k_i^o \exp(-E_i/RT) \hspace{4cm} (2)$$

where k_i^o = preexponential factor

E_i = Activation energy for species i

R   = universal gas constant

T   = temperature

A nonlinear fitting routine (POWELL, see Appendix C) which minimizes the sum of squared errors between calculated and experimental yields is used to compute values for V_i^*, E_i and $\log_{10} k_i^o$. To do the regressions, POWELL calls a subroutine "FUN" which is the function (or model) to which the data are being fitted. POWELL is supplied with initial guesses for V_i^*, E_i and $\log_{10} k_i^o$ as well as time-temperature histories for each experimental run. FUN contains the integrated form of Eq. (1):

$$\ln \frac{V_i^* - V_i(T')}{V_i^*} = - \int_0^{t'} k_i^o \exp(-E_i/RT(t)) \, dt$$

Thus, POWELL calls FUN for each yield data point to compute the yield $V_i(T')$ from the experimental time-temperature history (yield at time t' for a run to a peak temperature T'), compares the answer with the experimentally obtained value for $V_i(T')$, and adjusts V_i^*, E_i and $\log_{10} k$ to minimize the square of their difference. Fifteen data points with their corresponding time-temperature histories are supplied per run, with time intervals of 0.3-0.9s between data points. These data include the initial rapid heat-up (3 points: 1s duration)

followed by 8.9s of cool-down after the peak temperature is reached (12 points).

Once acceptable best fit parameters are obtained from POWELL, they are used as input data to a curve fitting program: CLFITI (Franklin, 1980). An interpolated yield versus temperature curve is generated, starting at 373K totalling 25 data points at 50K intervals, using idealized time-temperature histories. These ideal time-temperature histories are calculated based on a constant heating rate of 1000 K/s to the peak temperature, followed by an exponentially decaying cooling with an initial cooling rate of 200 K/s. CLFITI also computes the idealized peak temperature to which the sample would have had to be pyrolyzed in order to achieve the measured experimental yield. This temperature is then used with ideal time-temperature histories to calculate the ideal yield from subroutine FUN, and is also the temperature used in plots of yield versus "peak temperature".

APPENDIX C

(Powell)

```
C                          M       IS THE NUMBER OF DATA POINTS
C                          N       IS THE NUMBER OF UNKNOWNS
C                          F       IS A VECTOR OF LENGTH N CONTAINING THE RESIDUALS
C                          X       IS THE VECTOR OF UNKNOWNS
C                          E       ABSOLUTE ACCURACY LIMIT VECTOR OF LENGTH N ON THE
C                  CHANGE IN VALUES OF THE UNKNOWNS BETWEEN ITERATIONS
C                  ESCALE  PARAMETER LIMITING THE STEP SIZE; NORMALLY X(I) WILL NOT BE
C                          CHANGED BY MORE THAN ESCALE*E(I) IN A SINGLE STEP
C                          (SUGGESTED VALUE = 1000.)
C                  IPRINT  PRINTING INDEX
C                  MAXFUN  MAXIMUM LIMIT ON NUMBER OF FUNCTION EVALUATIONS
C                          W       STORAGE VECTOR
C
        COMPILER DOUBLE PRECISION
        PARAMETER NN=10            ;NUMBER OF PARAMETERS
        PARAMETER MM=100           ;NUMBER OF DATA POINTS
        PARAMETER ND=10            ;MAX. # DATA ITEMS/POINT
        DIMENSION E(NN), F(MM),X(NN)
        COMMON W(1330),NDATAS,DATAS(ND,MM)
        CALL FOPEN(1,'@DATA')
        NI=1
        NO=10
        READ(NI)N,M,MAXFUN,IPRINT
        FORMAT(8I10)
        READ(NI)ESCALE
        FORMAT(8E10.4)
        DO 100 I=1,N
100     READ(NI)X(I),E(I)
        WRITE(NO,3)
3       FORMAT(///,10X,27HPOWELL REGRESSION ALGORITHM )
C
        CALL SSQMIN(M,N,F,X,E,ESCALE,IPRINT,MAXFUN,FF,NI,NO)
C
        WRITE(NO,4)FF
4       FORMAT(/,2X,'THE SUM OF THE SQUARES OF RESIDUALS = ',1E16.8)
        WRITE(NO,5)
5       FORMAT(/,2X,'FINAL PARAMETER VALUES:',/)
        WRITE(NO,6)(J,X(J),J=1,N)
6       FORMAT(4(3(' Param. ',I2,':',G16.8),/))
        READ(1,END=1)I   ;IF READ SUCCESSFUL, SUPRESS CALL TO ANOVA
        CALL FPLOT(M,F,N,X)      ;MAKE EPLOT PLOT FILES
        IF (I.NE.0) GOTO 1   ;SUPRESS CALL TO ANOVA ONLY IF DATA IS = 0
        WRITE(NO,1002)
1002    FORMAT(/,' Call to ANOVA suppressed by '0' in last line of data file')
        GOTO 7
1       CONTINUE
        TYPE ' '
        WRITE(NO,1000)
1000    FORMAT(' Calling ANOVA.. ',Z)
        CALL ANOVA(N,X,M,F,FF,.0005,10)
7       CONTINUE
X       DO 10 I=1,M
X10             TYPE 'I,F(I)=',I,F(I)
        END
```

```
        COMPILER DOUBLE PRECISION
        SUBROUTINE SSQMI(M,N,F,X,E,ESCALE,IPRINT,MAXFUN,FF,NI,NO)
C
C       THIS SUBROUTINE ACCOMPLISHES THE MINIMIZATION OF
C           CHI-SQUARE VIA THE ALGORITHM DEVELOPED BY
C           FOWELL. THIS PROGRAM IS TAKEN FROM KUESTER AND MIZE,
C           OPTIMIZATION TECHNIQUES WITH FORTRAN,(MCGRAW HILL,
C           NEW YORK: 1973).
C
        DIMENSION F(M),X(N),E(N)
        COMMON W(1330)
        LOGICAL STOFF,MAXCAL,CONTIN,FIRST
C
X       TYPE 'AT START OF SSQMIN'
        WRITE (NO,12) N,M,MAXFUN,ESCALE
12      FORMAT(/,' Number of parameters = ',I2,4X,'Number of data points = ',
     1   I3,/,' Maximum allowed number of sum-of-squares function evaluations = ',
     1   I5,/,' ESCALE (parameter limiting the step size) = ',G10.4)
        WRITE(NO,13)
13  FORMAT (/,2X,   'Initial guesses:')
        WRITE(NO,31) (I,X(I),I=1,N)
        WRITE(NO,18)
18  FORMAT (/,2X,   'Accuracy of parameters (convergence tolerances):')
        TYPE ' '
        WRITE (NO,23) (I,E(I),I=1,N)
23      FORMAT(4(3(' Param.',I2,':',G16.8),/))
C
C   INITIALIZE
C
        STOFF=.FALSE.
        MAXCAL=.FALSE.
        IPF=IPRINT*(IPRINT-1)
        ITC=0
        IPC=0
        MPLUSN=M+N
        KST=N+MPLUSN
        NPLUS=N+1
        KINV=NPLUS*(MPLUSN+1)
        KSTORE=KINV-MPLUSN-1
        NN=N+N
        K=NN
C
C   INITIAL FUNCTION EVALUATION
C
        CALL CALFUN(M,N,F,X)
X         TYPE 'JUST AFTER CALLING CALFUN IN SSQMIN'
X         TYPE 'X=',X(1),X(2),X(3)
X         TYPE 'F',F(1),F(2)
C
        MC=1
        FF=0.0
X         TYPE 'BEFORE FIRST LOOP IN CALFUN'
        DO 1 I=1,M
        K=K+1
        W(K)=F(I)
        FF=FF+F(I)*F(I)
    1 CONTINUE
X         TYPE 'AFTER CALFUN .. FF=',FF
        FOLD=FF
```

```
   100 FIRST=.TRUE.
       K=KST
       I=1
C
C    COMPUTE THE COMPONENTS OF THE GRADIENT IN THE CONJUGATE DIRECTIONS
C
     2 XDUMMY=X(I)
X          TYPE 'AFTER STATEMENT 2, X(1)-',X(1)
       ISMALL=0
       DUMMY=DABS(X(I)*1.D-6)+E(I)
X          TYPE 'BEFORE STATEMENT 5, I,X(I),DUMMY-',I,X(I),DUMMY
     5 X(I)=X(I)+DUMMY
X          TYPE 'X(I)-',X(I)
       CALL CALFUN(M,N,F,X)
       MC=MC+1
       X(I)=XDUMMY
       DO 3 J=1,N
       K=K+1
       W(K)=0.
       W(J)=0.
     3 CONTINUE
       SUM=0.
       KK=NN
       DO 4 J=1,M
       KK=KK+1
C
C    FPLUS-FBEST
C
       F(J)=F(J)-W(KK)
       SUM=SUM+F(J)*F(J)
     4 CONTINUE
       IF (SUM .GT. FF*1.D-12) GO TO 6
C
       WRITE (NO,7) I
     7 FORMAT (5X,3HTHE,I3,'-TH COMPONENT OF THE INITIAL STEP WAS TOO S',
      1'MALL  DOUBLE IT')
       DUMMY=2.0*DUMMY
C
       ISMALL=ISMALL+1
       K=K-N
       IF (ISMALL .LT. 15) GO TO 5
       WRITE(NO,1777)I
  1777    FORMAT(/,' Parameter ',I2,' seems to have no effect on the sum of squares'
      1  ,' of residuals.',/,' Check your FUN subprogram.',
      2  /,' Exiting from SSQMIN at this point.')
       ITC=0
       K=NN
       DO 8 I=1,M
       K=K+1
       F(I)=W(K)
     8 CONTINUE
       GO TO 10
C
C    SUM IS USED TO NORMALIZE G(I,K) AND D(I,J)
C
     6 SUM=1.0/DSQRT(SUM)
       ISMALL=0
       J=K-N+I
C
```

```
:UTIL:LIB:POWELL:SSQMIN

C  W(J) IS D(I,I)   NOTE D(I,J)=0.0 J NOT EQUAL TO I
C
      W(J)=DUMMY*SUM
      DO 9 J=1,M
      K=K+1
C
C  W(K) IS G(I,K) IN THE COORDINATE DIRECTIONS
C
      W(K)=F(J)*SUM
      KK=NN+J
      DO 11 II=1,I
      KK=KK+NPLUSN
C
C  W(II) IS G*GT(I,II)
C
      W(II)=W(II)+W(KK)*W(K)
   11 CONTINUE
    9 CONTINUE
      ILESS=I-1
      IGAMAX=N+I-1
      INCINV=N-ILESS
      INCINF=INCINV+1
      IF (ILESS .GT. 0) GO TO 14
C
C  INVERSE OF G*GT(II,JJ) II,JJ=1,1 BY HOUSEHOLDER METHOD
C      RECALL (I-1)X(I-1) UPPER BLOCK ALREADY DONE
C
      W(KINV)=1.0
      GO TO 15
   14 B=1.
      DO 16 J=NPLUS,IGAMAX
      W(J)=0.
   16 CONTINUE
      KK=KINV
      DO 17 II=1,ILESS
      IIF=II+N
C
C  W(IIF)=W(N+II) IS THE SUM OF G-1(II,J)*G*GT(J,I) J=1,N
C
      W(IIF)=W(IIF)+W(KK)*W(II)
      JL=II+1
      IF (JL .GT. ILESS) GO TO 19
      DO 20 JJ=JL,ILESS
      KK=KK+1
      JJF=JJ+N
      W(IIF)=W(IIF)+W(KK)*W(JJ)
      W(JJF)=W(JJF)+W(KK)*W(II)
   20 CONTINUE
C
C  B IS G*GT(I,I)-SUM OF G*GT(I,II)*G-1(II,JJ)*G*GT(JJ,I)
C       WHICH IS A0
C
   19 B=B-W(II)*W(IIF)
      KK=KK+INCINF
   17 CONTINUE
      B=1./B
      KK=KINV
      DO 21 II=NPLUS,IGAMAX
      BB=-B*W(II)
```

134

```
      DO 22 JJ=II,IGAMAX
C
C   W(KK) IS G-1(II,JJ) WHICH EQUALS A1-1+A1-1*A2*A0-1*A3*A1-1
      W(KK)=W(KK)-BB*W(JJ)
      KK=KK+1
   22 CONTINUE
C   W(KK) IS G-1(I,II) WHICH EQUALS -A0-1*A3 WHICH EQUALS G-1(II,I)
      W(KK)=BB
      KK=KK+INCINV
   21 CONTINUE
C
C   W(KK) IS G-1(I,I) WHICH EQUALS A0-1
C
      W(KK)=B
   15 IF( .NOT. FIRST) GO TO 27
      I=I+1
      IF (I .LE. N) GO TO 2
C
C   0-TH ITERATION INITIALIZATION
C
      FIRST=.FALSE.
      ISAME=0
      FF=0.
      KL=NN
      DO 26 I=1,M
      KL=KL+1
      F(I)=W(KL)
      FF=FF+F(I)*F(I)
   26 CONTINUE
      CONTIN=.TRUE.
   27 IPC=IPC-IPRINT
X        TYPE 'AFTER STATEMENT 27 IN SSQMIN'
      IF (IPC .GE. 0) GO TO 29
C
C   ITERATION PRINTOUT
C
   28 WRITE (NO,30) ITC,KC,FF
   30 FORMAT (/,2X,9HIteration,I3,4X,'Number of sum-of-squares function evaluations
     1'= ',I4,/,2X,'Sum-of-the-squares = ',D16.8,/,2X,'Parameters:')
      WRITE (NO,31) (I,X(I),I=1,N)
   31      FORMAT(/,(3(' Param.',I2,':',G16.8),/))
      WRITE (NO,32)
   32 FORMAT (/,'Residuals (theoretical minus data value) for each data point:')
      WRITE (NO,35) (J,F(J),J=1,M)
   35 FORMAT (/,' ',I3,':',G13.5))
      IPC=IPP
      IF (STOPP) GO TO 33
C
C   CONVERGENCE TESTS
C   1  N+1 VALUES OF F ARE THE SAME
C   2  MAXIMUM OF STEP(I)/E(I) LESS THAN EQUAL TO 1.0 (CONTIN FALSE)
C   3  MAXIMUM OF THE I-TH COMPONENT OF THE ACTUAL STEP TAKEN / E(I)
C        LESS THAN OR EQUAL TO 1.0    CHANGE LESS THAN OR EQUAL TO 1
C
      CHANGE=0.0
   29 IF (CHANGE .NE. 0.0) ISAME = 0
      ISAME=ISAME+1
      IF (ISAME .LE. N) GO TO 291
      IF (IPRINT .LE. 0) GO TO 33
```

```
      WRITE (NO,295)
  295 FORMAT (/,5X,  'N+1 VALUES OF F ARE THE SAME')
      IF (FF .GE. FOLD) GO TO 10
      FOLD=FF
      K=NN
      DO 293 I=1,M
      K=K+1
      W(K)=F(I)
  293 CONTINUE
      GO TO 100
  291 IF (CONTIN) GO TO 34
      IF (CHANGE .GT. 1.0) GO TO 36
   10 IF (IPRINT .LE. 0) GO TO 33
C
C  TERMINAL PRINTOUT
C
      WRITE (NO,38)
   38 FORMAT (/,5X,'SSQMIN FINAL VALUES OF RESIDUALS AND PARAMETERS')
      STOPP=.TRUE.
      GO TO 28
   33 RETURN
C
   36 CONTIN=.TRUE.
C
C  START NEXT ITERATION
C
   34 ITC=ITC+1
X         TYPE 'AFTER STATEMENT 34 IN SSQMIN'
      K=N
      KK=KST
C
C  CALCULATION OF F
C
      DO 39 I=1,N
      K=K+1
      W(K)=0.
      KK=KK+N
      W(1)=0.
      DO 40 J=1,M
      KK=KK+1
C
C  W(I) IS THE SUM OF G(I,K)*F(K) WHICH IS -F(I)
C
      W(1)=W(I)+W(KK)*F(J)
   40 CONTINUE
   39 CONTINUE
      DM=0.
      K=KINV
C
C  CALCULATION OF Q
C
      DO 41 II=1,N
      IIP=II+N
C
C  W(IIP)=W(N+II) IS THE SUM OF G-1(II,J)*(-F(J)) 4=1,N WHICH IS -Q(I)
C
      W(IIP)=W(IIP)+W(K)*W(II)
      JL=II+1
      IF (JL .GT. N) GO TO 43
```

136

```
      DO 44 JJ=JL,N
      JJF=JJ+N
      K=K+1
      W(IIF)=W(IIF)+W(K)*W(JJ)
      W(JJF)=W(JJF)+W(K)*W(II)
   44 CONTINUE
      K=K+1
C
C  MAXIMUM OF F(I)*Q(I)  KL INDEX OF THE DIRECTION OF D(I,J)
C      TO BE REPLACED BY STEP(J)
C
   43 IF (DM .GE.DABS(W(II)*W(IIF))) GO TO 41
      DM=DABS(W(II)*W(IIF))
      KL=II
   41 CONTINUE
      II=N+NPLUSN*KL
      CHANGE=0.
      DO 46 I=1,N
      JL=N+I
      W(I)=0.
      DO 47 J=NPLUS,NN
      JL=JL+NPLUSN
C
C  W(I) IS THE SUM OF (-Q(J)*D(J,I) J-1,N  WHICH IS -STEP(I)
C
      W(I)=W(I)+W(J)*W(JL)
   47 CONTINUE
      II=II+1
C
C  INTERCHANGING KL AND N ROWS OF D(I,J) PUT XBEST IN D(N,J)
C
      W(II)=W(JL)
      W(JL)=X(I)
C
C  CHANGE IS THE MAXIMUM OF ABS(STEP(I)/E(I))
C
      IF (DABS(E(I)*CHANGE) .GT.DABS(W(I))) GO TO 46
      CHANGE=DABS(W(I)/E(I))
   46 CONTINUE
      DO 49 I=1,M
      II=II+1
      JL=JL+1
C
C  INTERCHANGING KL AND N ROWS OF G PUT FBEST IN G(N,K)
C
      W(II)=W(JL)
      W(JL)=F(I)
   49 CONTINUE
      FC=FF
      ACC=0.1/CHANGE
      IT=3
      XC=0.
      XL=0.
      IS=3
      XSTEP=-DMIN1(0.5,ESCALE/CHANGE)
      IF (CHANGE .LE. 1.0) CONTIN=.FALSE.
C
C  LINEAR SEARCH
C
```

```
X       TYPE 'BEFORE CALLING LINMIN'
   51 CALL LINMIN (IT,XC,FC,6,ACC,0.1,XSTEP)
      IF (IT .NE. 1) GO TO 53
      MC=MC+1
      IF (MC .LE. MAXFUN) GO TO 54
      WRITE (NO,56) MAXFUN
   56 FORMAT (5X,I6,  'CALLS TO CALFUN')
      MAXCAL=.TRUE.
      GO TO 53
   54 XL=XC-XL
      DO 57 J=1,N
      X(J)=X(J)+XL*W(J)
   57 CONTINUE
      XL=XC
      CALL CALFU (M,N,F,X)
      FC=0.
      DO 58 J=1,M
      FC=FC+F(J)*F(J)
   58 CONTINUE
      IF (IS .NE. 3) GO TO 59
      K=N
C
C  DETERMINATION OF SECOND BEST POINT
C
      IF (FC-FF) 61,51,62
   61 IS=2
      FMIN=FC
      FSEC=FF
      GO TO 63
   62 IS=1
      FMIN=FF
      FSEC=FC
      GO TO 63
   59 IF (FC .GE. FSEC) GO TO 51
      K=KSTORE
      IF (IS .EQ. 2) GO TO 74
      K=N
   74 IF (FC-FMIN) 65,51,66
   66 FSEC=FC
      GO TO 63
   65 IS=3-IS
      FSEC=FMIN
      FMIN=FC
   63 DO 67 J=1,N
      K=K+1
      W(K)=X(J)
   67 CONTINUE
      DO 68 J=1,M
      K=K+1
      W(K)=F(J)
   68 CONTINUE
      GO TO 51
   53 K=KSTORE
      KK=N
C
C  IF IS=2  XBEST AND FBEST LIE IN W(N+  ) SECOND BEST X AND X LIE IN
C  W(KSTORE+  )=D(N,J)  AND G(N,K)
C  IF IS IS NOT 2 XBEST AND XBEST LIE IN W(KSTORE+  ) AND THE SECOND
C  BEST LIE IN W(N+  )
```

```
C
      IF (IS .NE. 2) GO TO 69
      K=N
      KK=KSTORE
   69 SUM=0.
      DM=0.
      JJ=KSTORE
      DO 71 J=1,N
      K=K+1
      KK=KK+1
      JJ=JJ+1
C
C  XBEST INTO X
C  XBEST-XSECOND INTO D(N,J)
C
      X(J)=W(K)
      W(JJ)=W(K)-W(KK)
   71 CONTINUE
      DO 72 J=1,M
      K=K+1
      KK=KK+1
      JJ=JJ+1
C
C  FBEST INTO F
C  FBEST-FSECOND INTO G(N,K)
C
      F(J)=W(K)
      W(JJ)=W(K)-W(KK)
      SUM=SUM+W(JJ)*W(JJ)
      DM=DM+F(J)*W(JJ)
   72 CONTINUE
      IF (MAXCAL) GO TO 10
      J=KINV
      KK=NPLUS-KL
      DO 76 I=1,KL
      K=J+KL-I
      J=K+KK
C
C  INTERCHANGE KL AND N ROWS OF G-1
C
      W(I)=W(K)
      W(K)=W(J-1)
   76 CONTINUE
      IF (KL .GE. N) GO TO 78
      KL=KL+1
      JJ=K
      DO 79 I=KL,N
      K=K+1
      J=J+NPLUS-I
      W(I)=W(K)
      W(K)=W(J-1)
   79 CONTINUE
      W(JJ)=W(K)
      B=1./W(KL-1)
      W(KL-1)=W(N)
      GO TO 88
   78 B=1./W(N)
   88 K=KINV
C
```

```
C    DETERMINE A1-1 FROM G-1 FOR USE IN CALCULATING NEW G-1
C
      DO 80 I=1,ILESS
      BB=B*W(I)
      DO 81 J=1,ILESS
C
C    W(K) IS G-1(I,J) WHICH IS A1-1=B1-B2*B4-1*B3
C
      W(K)=W(K)-BB*W(J)
      K=K+1
   81 CONTINUE
      K=K+1
   80 CONTINUE
      IF (FMIN .LT. FF) GO TO 82
      CHANGE=0.0
      GO TO 84
   82 FF=FMIN
C
C    CHANGE IS THE MAXIMUM OF THE COMPONENTS OF THE ACTUAL STEP TAKEN
C       DIVIDED BY THE COMPONENTS OF E
C
      CHANGE=DABS(XC)*CHANGE
   84 XL=-DM/FMIN
      SUM=1.0/DSQRT(SUM+DM*XL)
      K=KSTORE
      DO 85 I=1,N
      K=K+1
C
C    W(K) IS D(N,J) THE STEP TAKEN PROPERLY NORMALIZED
C
      W(K)=SUM*W(K)
      W(I)=0.
   85 CONTINUE
      DO 86 I=1,M
      K=K+1
C
C    W(K) IS G(N,K) WHICH IS (FBEST-FSECOND+(SUM OF (FBEST-FSECOND)*FBEST/
C       FMIN)*FBEST)  NORMALIZED
C
      W(K)=SUM*(W(K)+XL*F(I))
      KK=NN+I
      DO 87 J=1,N
      KK=KK+NPLUSN
C
C    W(J) IS THE N-TH ROW OF G*GT
C
      W(J)=W(J)+W(KK)*W(K)
   87 CONTINUE
   86 CONTINUE
      GO TO 14
C
      END
      END$
```

APPENDIX <u>D</u>

(Experimental Data)

Sweet Gum Xylan Pyrolysis Runs at 1000K/s and 3 X 10^5 Pa He

| Run no.	Temp. (K)	Char	Tar	CH_4	CO	CO_2	C_2H_4	C_2H_6	H_2O	HCHO	C_3H_6	CH_3OH	CH_3CHO	Ethanol	Material balance
4	775	35.2	28.0	0.0	13.1	3.87	0.01	0.02	4.80	0.03	0.02	1.31	0.73	0.03	89.1
5	1371	27.6	30.6	0.95	13.2	14.4	0.61	0.11	6.78	0.02	0.15	1.90	0.88	0.33	99.9
6	1355	28.4	27.6	0.87	17.2	10.0	0.55	0.13	5.50	0.08	0.30	1.80	1.00	0.31	94.8
8	626	68.3	10.0	0.0	6.7	1.85	0.0	0.0	7.35	0.0	0.0	1.04	0.16	0.0	97.0
9	664	63.0	17.5	0.0	7.3	2.72	0.0	0.0	3.05	0.03	0.0	1.5	0.13	0.06	96.6
10	864	34.9	20.1	0.02	13.9	4.45	0.07	0.07	3.65	0.06	0.12	2.0	1.1	0.22	82.7
11	882	33.6	16.1	0.20	19.0	5.97	0.08	0.08	4.57	0.09	0.28	2.0	1.3	0.23	87.4
12	1011	33.0	33.9	0.33	14.3	7.83	0.23	0.11	5.46	0.06	0.30	1.18	1.72	0.26	102.4
14	883	33.3	23.9	0.19	13.7	11.8	0.15	0.09	6.20	0.13	0.31	1.41	1.67	0.22	95.5
16	1344	26.1	16.4	0.95	12.3	14.7	0.40	0.12	3.96	0.16	0.38	1.35	1.42	0.29	80.0
17	1381	25.5	35.0	0.68	10.3	11.9	0.30	0.08	5.56	0.02	0.17	4.7	0.74	0.33	94.5
19	1110	33.3	24.3	0.58	13.8	8.2	0.31	0.12	4.90	0.04	0.18	--	0.92	0.31	90.7
20	1128	32.4	22.3	0.64	13.9	10.4	0.36	0.13	4.10	0.08	0.30	1.5	1.30	0.03	89.5
21	1120	32.5	24.3	0.67	8.2	9.32	0.40	0.12	3.90	0.04	0.30	2.4	1.13	0.28	91.1
22	1178	33.6	17.9	0.61	11.4	10.8	0.39	0.14	3.83	0.13	0.25	1.3	1.05	0.22	82.8
24	1149	31.9	26.0	0.72	11.2	10.7	0.40	0.11	5.83	0.13	0.30	0.93	0.95	0.18	90.2
25	1195	31.2	29.3	0.74	12.7	12.6	0.39	0.12	9.60	0.08	0.31	0.97	1.17	0.22	100.0
26	1253	30.7	23.8	0.71	12.0	12.6	0.36	0.11	4.56	0.12	0.27	1.10	0.94	0.31	89.3
27	1310	28.0	21.6	0.82	12.4	15.8	0.40	0.11	6.64	0.04	0.30	5.7	0.91	0.22	92.1
28	972	33.6	26.3	0.47	13.7	7.40	0.18	0.10	8.90	0.13	0.24	--	1.14	0.03	97.4
30	800	34.3	13.8	0.05	14.1	4.70	0.07	0.08	6.15	0.30	0.29	1.7	1.88	0.25	85.4
31	1157	28.5	20.9	0.85	13.2	17.2	0.39	0.10	6.62	0.10	0.27	1.3	0.84	0.28	95.7
32	1165	28.7	21.3	0.81	12.8	13.9	0.41	0.10	5.74	0.03	0.29	1.35	0.85	0.25	91.0
33	840	32.1	18.6	0.34	13.9	6.74	0.07	0.07	6.45	0.05	0.38	1.4	1.24	0.27	88.0
34	1284	25.4	21.5	0.74	11.9	16.1	0.33	0.09	4.40	0.05	0.28	1.1	0.98	0.20	84.0
35	687	35.5	17.2	0.0	11.1	4.0	0.0	0.0	6.0	0.02	0.08	1.5	0.67	0.10	90.5
36	692	37.0	21.2	0.01	15.1	4.1	0.01	0.01	7.1	0.09	0.13	1.2	0.75	0.20	88.5

APPENDIX E

(Char gasification)

Table E.1   Experiments H-38 and H-39 substantiate possibility
            of secondary reactions

H-38
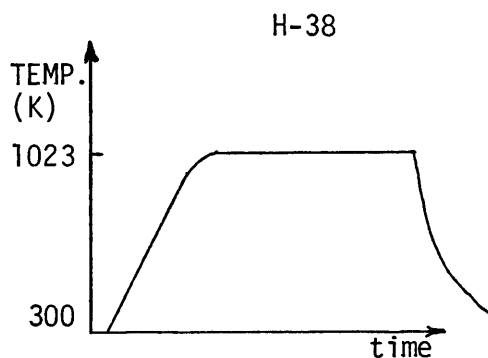
(Heatup to 1023K; held at
1023K for 20 seconds)

H-39
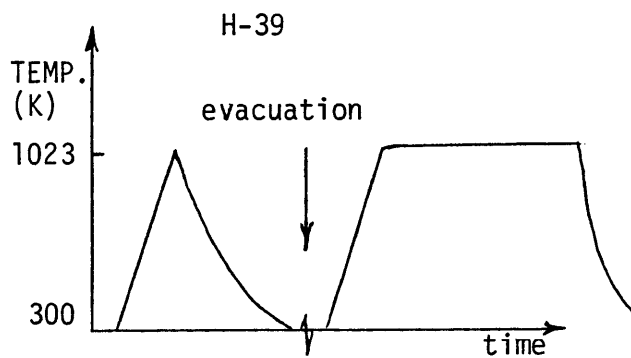
(Peak run to 1023K: STEP 1. Evacuate
reactor to remove CO_2 to reduce
opportunity for char gasification,
then repressurize with helium. Then
holding time run at 1023K for 19
seconds: STEP 2)

	H-38	H-39
CHAR YIELD	29.5 wt. %	28.1 wt. %
EXPECTED CHAR YIELD*	32.5 wt. %	32.5 wt. %
CO YIELD	15.7 wt. %	STEP 1: unknown STEP 2: 2.75 wt. %
EXPECTED CO YIELD*	7.6 wt. %	7.6 wt. %
CO_2 YIELD	15.0 wt. %	STEP 1: unknown STEP 2: 0.20 wt. %
EXPECTED CO_2 YIELD*	13.9 wt. %	13.9 wt. %

* Yield expected from peak temperature run at 1023K.

144

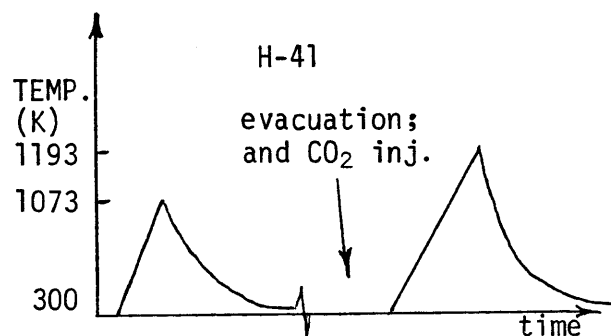Table E.2   Experiments H-40 and H-41 locate the temperature
interval in which secondary reactions assume importance.

H-40

TEMP.
(K)
1193
1073

300

time

H-41

TEMP.
(K)
1193
1073

300

evacuation;
and CO_2 inj.

time
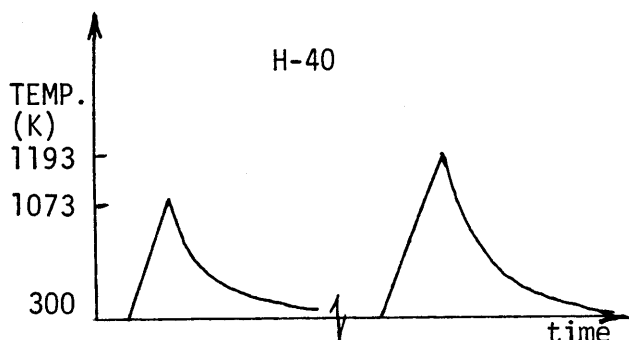
(Peak run at 1073K : STEP 1,
followed by peak run at 1193K :
STEP 2)

(Peak run to 1073K : STEP 1. Evacuate
reactor; repressurize with helium
and 4 cc-atm CO_2, followed by peak
run to 1193K : STEP 2)

	H-40	H-41
CHAR YIELD	26.8 wt. %	25.2 wt. %
EXPECTED CHAR YIELD	26.5 wt. %	25.5 wt. %
CO YIELD	STEP 1: unknown STEP 2: 12.3 wt. %	STEP 1: unknown STEP 2: 2.3 mg †
EXPECTED CO YIELD	STEP 1: 8.0 wt. % STEP 2: 16. wt. %	STEP 1: 8.0 wt. % STEP 2: N/A *
CO_2 YIELD	STEP 1: unknown STEP 2: 15.8 wt. %	STEP 1: unknown STEP 2: 6.5 mg †
EXPECTED CO_2 YIELD	STEP 1: 13.9 wt. % STEP 2: 12.0 wt, %	STEP 1: 13.9 wt. % STEP 2: N/A *

† (4 cc-atm CO_2 injected = 7.9 mg)

* Not applicable

APPENDIX F

(Mass and energy balances)

Table F.1   Elemental, total mass, and energy balances for
            Sweet Gum Xylan pyrolysis

Component	Approx. ultimate yield (wt. %)	C	H	O	Heat of combustion (Btu/lb)*	% of wood energy in component
Xylan	-	40.7	5.7	48.0	7090	100.0
Char	18.1	57.5	4.0	23.4	9500	24.2
Tar	38.5	46.7	5.7	43.9	7825	42.5
CH_4	0.75	0.56	0.19	-	23860	3.0
CO	13.1	5.6	-	7.5	4340	8.0
C_2H_4	0.35	0.30	0.05	-	21630	1.0
C_2H_6	0.09	0.07	0.02	-	22300	0.3
HCHO	0.02	0.01	T	T	8190	T
C_3H_6	0.19	0.16	0.3	-	21000	0.6
CH_3OH	0.5	0.19	0.05	0.3	9770	0.7
CH_3CHO	0.81	0.44	0.07	0.3	11400	1.0
Ethanol	0.36	0.19	0.05	0.13	12780	0.6
Furan	0.5	0.3	0.05	0.14	13280	1.0
Acetic acid	1.0	0.5	0.08	0.45	6270	1.0
Misc. C.H.O.	1.0	0.5	0.08	0.45	18000	3.0
Total	93.7	40.3	4.3	44.0		87.0
Closure	93.7	99.0	76.0	92.0		90.0%

* Heats of combustion from "Handbook of Chemistry and Physics";
  those for xylan, char and tar computed from:

$$Q \ (Btu/lb) = 146 \ (C) + 569 \ (H) - 51.5 \ (O)$$ (Mason and Gandhi, 1980)

T = trace amounts